

SIGN MATRIX POLYTOPES

A Dissertation
Submitted to the Graduate Faculty
of the
North Dakota State University
of Agriculture and Applied Science

By

Sara Louise Solhjem

In Partial Fulfillment of the Requirements
for the Degree of
DOCTOR OF PHILOSOPHY

Major Department:
Mathematics

July 2018

Fargo, North Dakota

NORTH DAKOTA STATE UNIVERSITY

Graduate School

Title

SIGN MATRIX POLYTOPES

By

Sara Louise Solhjem

The supervisory committee certifies that this dissertation complies with North Dakota State University's regulations and meets the accepted standards for the degree of

DOCTOR OF PHILOSOPHY

SUPERVISORY COMMITTEE:

Dr. Jessica Striker

Chair

Dr. Josef Dorfmeister

Dr. Jason Boynton

Dr. Michael Christoffers

Approved:

July 2, 2018

Date

Dr. Benton Duncan

Department Chair

ABSTRACT

Motivated by the study of polytopes formed as the convex hull of permutation matrices and alternating sign matrices, several new families of polytopes are defined as convex hulls of sign matrices, which are certain $\{0, 1, -1\}$ -matrices in bijection with semistandard Young tableaux. This bijection is refined to include standard Young tableau of certain shapes. One such shape is counted by the Catalan numbers, and the convex hull of these standard Young tableaux form a Catalan polytope. This Catalan polytope is shown to be integrally equivalent to the order polytope of the triangular poset: therefore the Ehrhart polynomial and volume can be combinatorial interpreted. Various properties of all of these polytope families are investigated, including their inequality descriptions, vertices, facets, and face lattices, as well as connections to alternating sign matrix polytopes, and transportation polytopes.

ACKNOWLEDGEMENTS

I would first like to acknowledge my adviser, Dr. Jessica Striker. Without her advice, knowledge and guidance I would not be here writing this thesis. She is the one that planted this topic in my head and helped me learn to be a researcher. Jessica was willing to meet wherever we needed to meet and our kids have become friends in the process. She pushed me when I needed to be pushed and she inspired me to find other interesting topics to research as well. Thanks for all your hard work and dedication on helping me do my best.

Next I would like to acknowledge Dr. Josef Dorfmeister. Seppi was not my advisor, but he supported me like he was. He was always there if I needed advice, or someone to bounce ideas off. Thanks for all of the extra work you put in to help me grow as a person, mathematician, teacher and researcher.

Dr. Jason Boynton, was one of the first professors I had the privilege of taking classes from at NDSU. It was fitting that he was there for me at the end, also. It was a pleasure to work with Jessica, Seppi and Jason, the three professors that I have taken the most classes from – by far. The three of them together have always been there for me; when I needed advice, mathematical insight, or a hug. They all pushed me, guided me and molded me into who I am as a professor and mathematician. They are the reason I am researching in something that bridges the gap between Algebra, Topology and Combinatorics. Jessica, Seppi and Jason are the ones that mean the most to me from my years at NDSU. Thank you for being on my committee!

Thank you also to Dr. Michael Christoffers for agreeing to be on my committee and for the helpful feedback. It is always fun to see you at concerts and Moorhead events.

I would also like to acknowledge all of my colleagues, fellow mathematics graduate students at NDSU. You have been my support, my distraction and friends. Good luck in all you do!

I would also like to thank the developers of SageMath [30] software, especially the code related to polytopes and tableaux, which was helpful in my research, and the developers of Co-Calc [19] for making SageMath more accessible. I also would like to thank the developers of Ipe [10] software for the ability to make beautiful clean graphics.

DEDICATION

This thesis is dedicated to my family. You have been there for me over the many years I have been in school. Mark, you have been my biggest supporter. I know it has been hard on you, but you hardly show it. You give me space when I need it and big hugs the rest of the time. You have earned this too – feel free to call me Dr. Sweetie whenever you feel the need. Emily, Jonathan and Jacob, what do I say to my three favorite kids? I know having your mom be a student along with you has had its fun times and rough times. You have been so helpful around the house when I was busy working. You have all grown and matured while I have been in graduate school – it has been fun to watch. I hope I make you a little proud. I know that you all make me so very proud to be your Mother. Oh, how God has blessed me. I also want to thank my family. The support from my Mom, Dad, sister and brothers has been so special. It isn't easy being the little sister; this may be me trying to show you that I am not just a little sister :) Thanks for being a shoulder to cry on, and only a phone call or text away when I need it. Then there are my friends, too many to name – thanks for all your love, prayers and patience with our family! Thank you Lord, for blessing us all and helping us through this – we made it with your help and amazing grace.

TABLE OF CONTENTS

ABSTRACT	iii
ACKNOWLEDGEMENTS	iv
DEDICATION	v
LIST OF FIGURES	viii
1. INTRODUCTION AND BACKGROUND	1
1.1. Introduction	1
1.2. Background	1
1.3. Polytopes	2
1.3.1. Polygons	2
1.3.2. d -dimensional polytopes	4
1.3.3. Posets	7
1.3.4. The face lattice of a polytope	12
1.3.5. The Ehrhart polynomial	13
1.3.6. The Birkhoff polytope	13
1.3.7. The alternating sign matrix polytope	17
1.3.8. The order polytope	21
1.3.9. The transportation polytope	23
1.4. Young tableaux	23
1.4.1. Standard Young tableaux	24
1.4.2. Semistandard Young tableaux	26
1.4.3. Special shapes of tableaux	28
1.5. Catalan objects	29
1.6. Other topics	34
2. SIGN MATRIX POLYTOPES FROM YOUNG TABLEAUX	36

2.1.	Semistandard Young tableaux and sign matrices	36
2.2.	Definition and vertices of $P(\lambda, n)$	38
2.3.	Definition and vertices of $P(m, n)$	42
2.4.	Inequality descriptions	45
2.5.	Facet enumerations	51
2.6.	Face lattice descriptions	60
2.7.	Connections and related polytopes	68
2.8.	$P(v, \lambda, n)$ and transportation polytopes	70
3.	CATALAN AND ORDER POLYTOPES	74
3.1.	Standard Young tableaux and standard sign matrices	74
3.2.	Catalan sign matrices and polytopes	77
3.3.	Building blocks of CP_m and $\mathcal{O}(Q_m)$	80
3.3.1.	Properties of Q_m and $\mathcal{O}(Q_m)$	80
3.3.2.	Order polytope to Catalan polytope	82
3.3.3.	Catalan polytope to order polytope	93
3.4.	The Catalan polytope and order polytope connection	98
3.5.	Inequality description of CP_m	101
3.6.	Face lattice of CP_m	102
3.7.	Ehrhart polynomial and volume	103
4.	FUTURE WORK	105
4.1.	Tableaux polytopes	105
4.2.	Sign matrices	105
4.3.	Connection to Gelfand-Tsetlin polytopes	106
	REFERENCES	108

LIST OF FIGURES

<u>Figure</u>	<u>Page</u>
1.1. A non-convex polygon on the left, and a convex polygon on the right.	3
1.2. The convex hull of eleven points in \mathbb{R}^2 . Note that only five points are vertices.	4
1.3. The same pentagon from Figure 1.2 with the bounding inequalities.	4
1.4. A 2-dimensional triangle in 3-dimensional space.	6
1.5. A Hasse diagram of a six element poset.	8
1.6. Two lattices on six vertices.	9
1.7. The divisibility lattice for 60, which is part of the infinite divisibility lattice.	9
1.8. An example of a poset.	10
1.9. The poset Q_5 with two generator elements highlighted and the corresponding order ideal.	10
1.10. The fourteen order ideals in $J(Q_4)$. The larger red elements are the generators of each order ideal.	11
1.11. A poset on the left and a linear extension of it on the right.	11
1.12. A square pyramid and its associated face lattice.	13
1.13. Two perfect matchings of $K_{3,3}$ on top. The bottom is the union of the others.	17
1.14. The seven 3×3 alternating sign matrices. Notice the first six are also permutation matrices.	17
1.15. The complete flow grid for $n = 5$	19
1.16. A 5×5 alternating sign matrix and its corresponding simple flow grid.	20
1.17. An elementary flow grid containing three doubly directed regions, which corresponds by Theorem 1.3.51 to a 3-dimensional face of ASM_5	21
1.18. A Young diagram of shape $[6, 3, 3, 1]$ and a standard Young tableau of the same shape.	25
1.19. A Young diagram with a hook shown.	25
1.20. The Young diagram of $[6, 3, 3, 1]$ with the hook lengths of each box.	25
1.21. A semistandard Young tableau of shape $[6, 3, 3, 1]$	26
1.22. Young diagram A is a $[6, 1]$ hook, B is a $[3, 1^4]$ hook and C is a staircase shaped diagram.	28

1.23. An example of a planar graph with regions labeled. R_6 is the exterior region.	34
1.24. Example of a 6×12 matrix and its corresponding partial column sums matrix $\hat{C}(X)$. . .	35
2.1. Example of the bijection between $SSYT$ and sign matrices.	37
2.2. The $SSYT$ of shape $[3, 3, 1, 1, 1]$ and corresponding sign matrix from Example 2.1.6. . .	39
2.3. The graph \hat{X} from Definition 2.2.4, with dots on only the internal vertices.	40
2.4. The six graphs corresponding to the six sign matrices in $M([2, 2], 3)$; these matrices correspond to $SSYT$ of shape $[2, 2]$ with entries at most 3.	42
2.5. Four of the 26 partial sum graphs corresponding to the sign matrices that are vertices in $P(2, 3)$ but not in $P([2, 2], 3)$	44
2.6. Left: A matrix X in $P([3, 3, 1], 4)$; Right: An open circuit in \hat{X}	49
2.7. Left: A matrix X in $P([3, 3, 1], 4)$; Right: A closed circuit in \hat{X}	49
2.8. The decomposition of the matrix from Figure 2.6 as the convex combination of X^+ and X^- ; see Example 2.4.2.	50
2.9. $\Gamma_{(m,n)}$ decorated with symbols that represent the inequalities that do not determine facets of $P(m, n)$	53
2.10. $\Gamma_{(\lambda_1,n)}$ decorated with symbols that represent inequalities that do not determine facets of $P(\lambda, n)$	57
2.11. Examples of portions of $\Gamma_{(\lambda_1,n)}$ that represent inequalities removed based on the fixed row sums.	58
2.12. $\Gamma_{(\lambda_1,n)}$ decorated with symbols that represent inequalities removed in Case 4.	59
2.13. The complete partial sum graph $\bar{\Gamma}_{(3,5)}$	61
2.14. A set of components of $\bar{\Gamma}_{(2,2)}$	63
2.15. A dimension 5 face of $P(3, 5)$, where the five regions are numbered.	66
2.16. The shape-complete partial sum graph of $P([3, 3, 3, 1], 5)$	67
2.17. An 8-dimensional component of $P([4, 4, 4, 1, 1], 6)$	68
2.18. The cube of $P(1, 3)$ with the $P(\lambda, 3)$ polytopes for each partition shape λ in a 1×3 box are also indicated.	69
3.1. Example of the bijection between $SYT([4, 3, 1, 1])$ and $SSM([4, 3, 1, 1])$	75
3.2. An example of a row tableau and its corresponding standard sign matrix.	76
3.3. An example of a column tableau and its corresponding standard sign matrix.	76

3.4. Examples of the extreme cases of partial column sum matrices of $CSM(6)$ and their corresponding $f \in \mathcal{O}(Q_6)$	78
3.5. Examples of a middle case of a partial column sum matrix of $CSM(6)$ and the corresponding $f \in \mathcal{O}(Q_6)$	78
3.6. The 14 order ideals in $J(Q_4)$ and their corresponding vectors in $\mathcal{O}(Q_m)$	80
3.7. Q_m for $m = 3, 4, 5$, respectively.	81
3.8. An illustration of the inequalities for the order polytope $\mathcal{O}(Q_m)$	82
3.9. The graph $\Delta(Q_6)$ before and after specifying boundary vertex labels as in Definition 3.3.3.	82
3.10. A way to visualize Definition 3.3.4, explained in Example 3.3.5.	84
3.11. Example of the maps between an element of $\Delta(Q_6)$ and a matrix in $\xi(f)$ used in Examples 3.3.5 and 3.3.10.	85
3.12. Example of the differences between labels of $\Delta(Q_m)$ to get entries of $\hat{R}(X)$	89
3.13. The general version of $\hat{R}(X)$ for $m = 6$ using $f(a_{i,j})$ values, written without the f due to space constraints.	89
3.14. The general version of $\hat{C}(X)$ for $m = 6$ using $f(a_{i,j})$ values, written without the f due to space constraints.	94
3.15. The visual representation of rows A and B for a large t and $t = 2$ in the proof of Lemma 3.3.11.	96
3.16. The poset Q_3 with added $\hat{1}$ and $\hat{0}$ to obtain \hat{Q}_3	103
3.17. The face lattice for the poset in Figure 3.16.	103
4.1. The 8 tableaux in $SSYT([2, 1], 3)$	105
4.2. The inequalities of the Gelfand-Tsetlin pattern are shown.	106
4.3. Example of the bijection between the Gelfand-Tsetlin pattern on the left and the $SSYT$ on the right.	107

1. INTRODUCTION AND BACKGROUND

1.1. Introduction

Polytopes are multi-dimensional geometric objects that are the solution to a set of inequalities. Polytopes can be studied from their vertices or from their inequalities. In linear algebra or optimization, whenever we are presented with a situation that has some constraining inequalities, there is a space bounded by the inequalities which may be a finite space or infinite space. The task at hand is usually to find points inside this region that fit all of the constraints and also maximizes or minimizes something. For this research, the polytopes are formed from *sign matrices*, which are a special type of $\{-1,0,1\}$ -matrix introduced by Aval [2] for their bijection with *Young tableaux*. The combinatorial nature of tableaux and sign matrices form objects that are accessible to work with, thus creating polytopes with nice properties [31, 3, 5, 32]. Using techniques established in the study of the Birkhoff polytope [32] and alternating sign matrix polytope [31], several new polytope families are established from tableaux and sign matrices. These new polytope families are the subject of this study. Results include connections with the transportation, alternating sign matrix and order polytopes.

1.2. Background

The two main combinatorial objects used in this thesis will be introduced in this chapter. The first object is the polytope, which is the higher dimensional analog of a convex polygon. A polytope is a geometric structure that results from combining either points or inequalities in a certain way. The discussion about polytopes will include their definition and their structure. To see the structure in the faces of a polytope, posets and lattices will be introduced in Subsection 1.3.3. Some well-studied polytopes will be discussed in Subsections 1.3.6 to 1.3.9.

The second object, introduced in Section 1.4, is a tableau. A tableau is a basic and well-studied combinatorial object. The enumeration and properties of various tableaux are known and will be given. The discussion highlights some of the different types and shapes of tableaux. One such type of tableau is a Catalan object, enumerated by the Catalan numbers. The Catalan numbers will be discussed in Section 1.5 and many different Catalan objects will be shown. Also there is a short discussion of graphs and two properties of matrices.

1.3. Polytopes

Polytopes are geometric structures used to arrive at solutions to problems relating to optimization and linear programming. Polytopes with two variables are in 2-dimensions and called convex polygons; more variables create an n -dimensional polytope. In addition to polytopes, posets will be examined as an introduction to a face lattice of a polytope. The face lattice, as well as dimension and enumeration of facets and vertices, is discussed with regard to some well-studied polytopes: the Birkhoff polytope, alternating sign matrix polytope, order polytope, and transportation polytope. Some proof techniques were inspired by the research in [1, 5, 22, 25, 31, 32]

The discussion on polytopes follows Ziegler's *Lectures on Polytopes* [34] unless otherwise cited.

1.3.1. Polygons

A set of inequalities in two variables can be graphed on a 2-dimensional coordinate plane. The inequalities form a region, and the points where the lines intersect can be used to maximize or minimize an objective equation. Cost and profit are examples of quantities that could be maximized or minimized. If the region is completely enclosed by the inequalities, a *convex* polygon is formed. However, the region could be infinite. For this discussion, all regions are assumed to be enclosed, or finite, regions.

These finite regions are called *polygons*, and are defined as follows: a polygon is formed by coplanar segments (called *sides*) such that: 1. Each segment intersects exactly two other segments, one at each endpoint. 2. No two segments with a common endpoint are collinear [6]. Some polygons in \mathbb{R}^2 (or the xy -plane) are triangles, parallelograms and trapezoids. Circles and sectors of circles are not polygons, since curved sides are not allowed in a polygon. Polygons are most commonly thought of as *convex polygons*. A convex polygon is defined as a polygon such that no line containing a side of the polygon contains points in the interior of the polygon [6]. A more concrete definition of convex is now given.

Definition 1.3.1 ([34, p. 3]). A set of points $K \subseteq \mathbb{R}^d$ is *convex* if for any two points $\vec{x}, \vec{y} \in K$, the straight line segment $[\vec{x}, \vec{y}] = \{\lambda\vec{x} + (1 - \lambda)\vec{y} : 0 \leq \lambda \leq 1\}$ is contained in K .

Definition 1.3.2. The *convex hull* of a finite set of points $\{\vec{v}_1, \vec{v}_2, \dots, \vec{v}_k\} \subset \mathbb{R}^d$ is the smallest convex set containing all of the points. Therefore, every point in the convex hull can be written as

the convex combination of $\{\vec{v}_1, \vec{v}_2, \dots, \vec{v}_k\}$, which is given by the formula:

$$\sum_i^k \mu_i \vec{v}_i \text{ where all } \mu_i \geq 0, \text{ and } \sum_i^k \mu_i = 1 \text{ for } 1 \leq i \leq k.$$

A convex polygon is the convex hull of a finite set of points in \mathbb{R}^2 . Consider some cases with a small number of points. The convex hull of three non-collinear points results in a triangle. However, the convex hull of four non-collinear points in \mathbb{R}^2 results in either a triangle or a quadrilateral.

A convex polygon can be thought of as putting a rubber band around the outside of the set of points. The rubber band will touch only the sides and vertices while enclosing the polygon. The difference between a convex and non-convex polygon is illustrated in Figure 1.1.

A three-dimensional analog of a convex polygon is a polyhedron. A polyhedron example in \mathbb{R}^3 is a pyramid or prism. Convex figures like these and others in higher dimensions are *polytopes*, which are defined formally in Subsection 1.3.2. When discussing polytopes in d -dimensions, the notation d -polytope will be used. For example, a polygon is a 2-polytope and a prism is a 3-polytope.

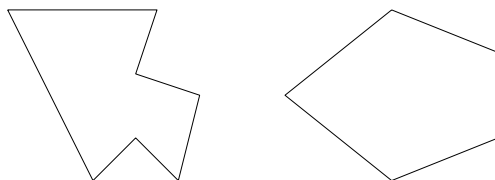


Figure 1.1. A non-convex polygon on the left, and a convex polygon on the right.

For an example of the convex combination, using the vertices in Figure 1.3, the point $\left(\frac{4}{3}, 2\right)$ is inside the polygon and can be written as:

$$\left(\frac{4}{3}, 2\right) = 0(0, 0) + \frac{1}{6}(3, 0) + \frac{1}{4}(3, 1) + \frac{1}{3}(1, 4) + \frac{1}{4}(-1, 2).$$

Notice that $0 + \frac{1}{6} + \frac{1}{4} + \frac{1}{3} + \frac{1}{4} = 1$ and all coefficients are nonnegative.

Note that a finite set of points is not necessarily the vertex set for the polygon; Figure 1.2 shows an example of such a case.

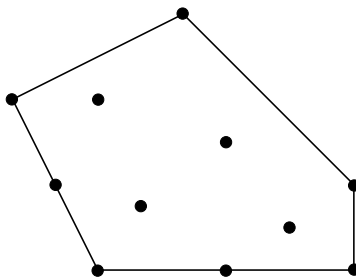


Figure 1.2. The convex hull of eleven points in \mathbb{R}^2 . Note that only five points are vertices.

When the vertices of a polygon are known, the convex hull is a very straightforward way to define a polygon. Starting with the vertices is not necessary however, as there is an equivalent way to define a polygon, stated below. The equivalence of the two definitions will be stated in Theorem 1.3.5.

Definition 1.3.3. A *polygon* in \mathbb{R}^2 is the bounded intersection of finitely many linear inequalities.

An example of a polygon described by bounded intersections is seen in Figure 1.3.

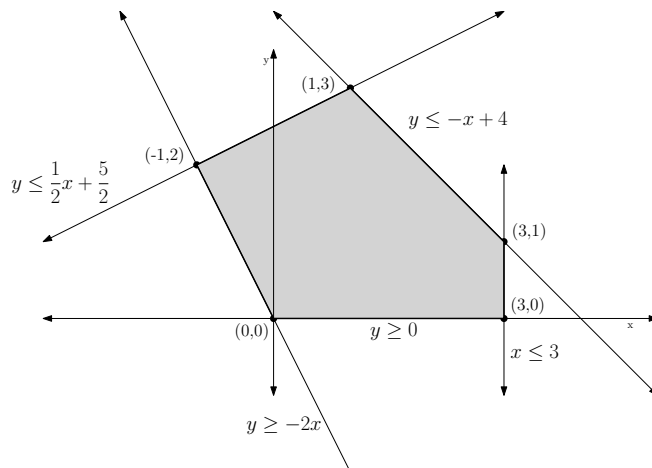


Figure 1.3. The same pentagon from Figure 1.2 with the bounding inequalities.

1.3.2. d -dimensional polytopes

Polygons in \mathbb{R}^2 , or 2-polytopes, can be generalized into higher dimensions. In this subsection, polytopes will be defined in full generality using two equivalent definitions. After they are defined, the parts of a polytope will also be defined. Finally, different types of characteristics that polytopes can possess will be discussed.

Definition 1.3.4. A subspace of dimension $d - 1$ in \mathbb{R}^d is called a *hyperplane*. *Halfspaces* are the geometric objects that are formed on either side of a hyperplane.

A hyperplane in 2-dimensions is a line and a hyperplane in 3-dimensions is a 2-dimensional plane.

It has been discussed that a polytope can be defined by a set of points and also by a set of inequalities (where the inequalities form a bounded, not infinite, region). The two ways to define a polytope are equivalent, as the following theorem confirms and will be used as the formal definition.

Theorem 1.3.5. *A subset $P \subseteq \mathbb{R}^d$ is the convex hull of a finite set of points*

$$P = \text{convex hull of } \{\vec{v}_1, \vec{v}_2, \dots, \vec{v}_k\} \text{ for } v_i \in \mathbb{R}^d \text{ for all } 1 \leq i \leq k$$

if and only if it is a bounded intersection of halfspaces

$$P = \{\vec{x} \in \mathbb{R}^d : A\vec{x} \leq \vec{z}\} \text{ for some } m \times d \text{ matrix } A, \vec{z} \in \mathbb{R}^m.$$

Consequently, the two ways to describe a polytope are equivalent definitions. However, obtaining both polytope definitions can be a challenge, even though both exist for every polytope. When specific polytopes are discussed in the following chapters, the proofs will start with the convex hull description to prove the inequality, or halfspace, description. Also, one definition of a polytope can be preferred to the other to more easily prove different properties of a polytope.

The discussion will now change from basic definitions to the parts of a polytope. Parts of a polytope can be categorized by dimension. After dimension is known, how the pieces of the polytope fit together will be discussed.

Definition 1.3.6. A *face* of a polytope is the intersection of the polytope with a hyperplane for which the polytope is entirely contained in one of the two halfspaces determined by the hyperplane.

Faces of the cube are vertices, edges and squares. However, the *empty face* and the entire cube itself are also faces. In a d -polytope, a *proper face* is any face of dimension less than d . Some faces of a polytope also have special names. A formal definition of vertices, edges and other faces is now given.

Definition 1.3.7. Given a polytope P of dimension d , the faces of P of dimensions 0, 1, $d - 2$, and $d - 1$ are called *vertices*, *edges*, *ridges*, and *facets*, respectively. In particular, the vertices are the minimal nonempty faces, and the facets are the maximal proper faces.

The facets of a polygon are the edges and the facets of a polyhedron are the 2-dimensional faces. For larger polytopes, the 0-dimensional faces are vertices, 1-dimensional faces are edges; however the rest of the faces are denoted by the dimension and not given a name until ridges and facets. Vertices and facets are of importance in Chapters 2 and 3.

Polytopes are not always full-dimensional, meaning all the variables involved are not necessarily needed. A smaller-dimensional polytope sitting in a higher-dimensional space is seen in Example 1.3.8.

Example 1.3.8. A simple example of a polytope not being full-dimensional is a 2-dimensional triangle sitting in 3-dimensional space, as in Figure 1.4.

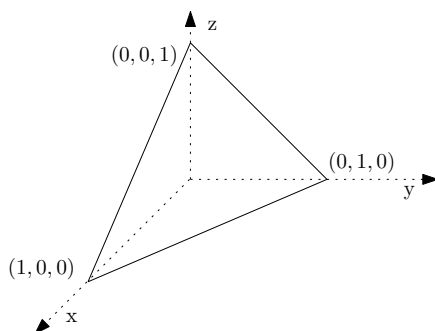


Figure 1.4. A 2-dimensional triangle in 3-dimensional space.

Polytopes can have different or specific properties that make them unique. The following are some commonly studied properties of polytopes.

- An *integral* polytope has integer values for all vertex coordinates.
- A *regular* polytope requires all vertices to be contained in the same number of edges.
- A *simplicial* polytope requires every facet to have the minimal number of vertices. This also means that all facets have the same number of vertices.

- A *simple* polytope requires every vertex to be contained in the minimal number of facets. This means that all vertices are contained in the same number of facets.

All polytopes have structure as to how the faces are connected. In the next two subsections, the structure between faces of a polytope is discussed.

1.3.3. Posets

Faces of a polytope have a natural partial order based on dimension of each face; this will be discussed in Subsection 1.3.4. So that this partial order of faces may be discussed, the definition and properties of a partially ordered set, or poset, are given. A Hasse diagram is introduced as a way a poset can be visualized. A specific type of poset is a lattice. Furthermore, within posets, the structure of order ideals will be discussed. This discussion can be referenced in Chapter 3 of Stanley's *Enumerative Combinatorics, Volume 1* [27], unless cited otherwise.

Definition 1.3.9. A *partially ordered set* (P, \leq) (or *poset*) is a set P together with a binary relation, denoted \leq , satisfying the following three properties on $s, t, u \in P$:

- For all $t \in P$, $t \leq t$ (reflexivity).
- If $s \leq t$ and $t \leq s$, then $s = t$ (antisymmetry).
- If $s \leq t$ and $t \leq u$, then $s \leq u$ (transitivity).

In this thesis, a poset will be denoted by the set P , as the relation is understood to be \leq . A poset can be visualized with a diagram. For a diagram to be meaningful, it needs to show how the elements of a poset relate to each other. This relationship is given in the following definition. Additionally, the notation $a < b$ will be used to indicate $a \leq b$ and $a \neq b$.

Definition 1.3.10. *Cover relations* for a poset (P, \leq) are as follows: if $s, t \in P$, then it is said that t *covers* s or s is *covered by* t if $s \leq t$ and no element $u \in P$ satisfies $s < u < t$.

Definition 1.3.11. The *Hasse diagram* of a finite poset P is the graph whose vertices are the elements of P , whose edges are the cover relations, and such that if $s \leq t$ then t is drawn above s .

An example of a Hasse diagram is given in Figure 1.5 for the six elements $\{A, B, C, D, E, F\}$. The figure illustrates the previous definitions; for example, notice $D < C < F < A$. Notice further, E and C cannot be compared, B covers both E and C , and also C is covered by both F and B .

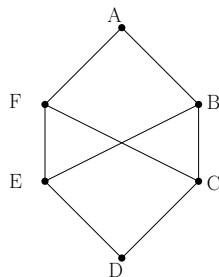


Figure 1.5. A Hasse diagram of a six element poset.

A special type of poset called a lattice will be defined next. Characteristics of a lattice will also be given.

- Definition 1.3.12.**
- The *join* (or *least upper bound*) of s and t is an upper bound u of s and t such that every upper bound v of s and t satisfies $v \geq u$. The join of s and t is denoted $s \vee t$.
 - The *meet* (or *greatest lower bound*) of s and t is a lower bound u of s and t such that every lower bound v of s and t satisfies $v \leq u$. The meet of s and t is denoted $s \wedge t$.

Definition 1.3.13. A poset P is a *lattice* if every pair of elements $s, t \in P$ has a join and a meet.

Example 1.3.14 will show why the poset of Figure 1.5 is not a lattice and why the posets in Figure 1.6 are lattices.

Example 1.3.14. Two examples of lattices are in Figure 1.6. There is a meet and a join for each pair of elements in each poset. In the poset on the left, $3 \wedge 5 = 6$ and $3 \vee 5 = 2$, and in the poset on the right, $b \wedge f = d$ and $b \vee f = a$. However, in Figure 1.5, notice the least upper bounds of E and C are both F and B . Similarly, greatest lower bounds of F and B are both E and C . Therefore, the poset in Figure 1.5 is not a lattice.

A poset can be either finite or infinite. Similarly, a poset may or may not have a unique maximum or minimum element. The definition of this unique maximum or minimum is below.

Definition 1.3.15. A finite poset P has a $\hat{0}$ if there exists an element $\hat{0} \in P$ such that $t \geq \hat{0}$ for all $t \in P$. Similarly, P has a $\hat{1}$ if there exists $\hat{1} \in P$ such that $t \leq \hat{1}$ for all $t \in P$.

In Figure 1.6, both lattices are finite and have unique maximum and minimum elements. The $\hat{0}$ elements are the 6 and d , whereas the $\hat{1}$ elements are the 1 and a . Figure 1.8 gives an example of a poset with no unique minimal element.

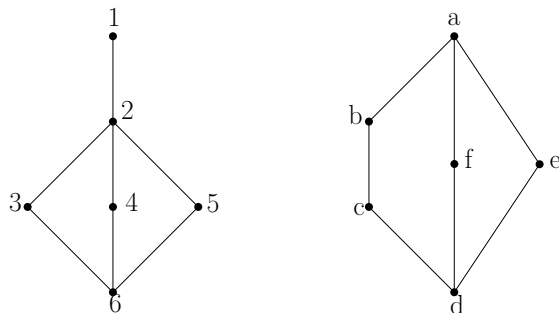


Figure 1.6. Two lattices on six vertices.

An example of an infinite lattice is the divisibility lattice. The divisibility lattice has as elements all positive integers. The cover relations are defined as follows: b covers a if a is a factor of b . Figure 1.7 shows part of the infinite divisibility lattice for factors of 60. The $\hat{0}$ element is 1; above 1 are the primes. Notice that the greatest common factors are the meets and the least common multiples are the joins.

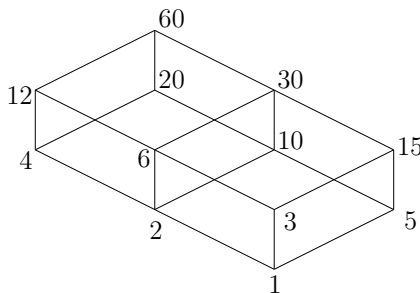


Figure 1.7. The divisibility lattice for 60, which is part of the infinite divisibility lattice.

Next there are a few definitions that will be needed to discuss special lattices related to polytopes.

Definition 1.3.16. A *chain* is a poset in which any two elements are comparable. A subset C of a poset P is called a *chain* if C is a chain when regarded as a subposet of P . The *length* of a finite chain is one less than the number of elements in the chain. The *rank* of a finite poset P is the length of the maximal chain. If all maximal chains of P are the same, then the rank of elements in the poset are as follows: if s is a minimal element, then the rank of s is zero, and if t covers s , then the rank of t is the rank of s plus 1.

Thus in the poset in Figure 1.8, the elements a, b, c, d have rank 0, the elements e, f, g have rank 1 and h has rank 2.

The discussion will now shift to a special subset of a poset.

Definition 1.3.17. An *order ideal* of a poset P is a subset I of P such that if $t \in I$ and $s \leq t$, then $s \in I$. Let $J(P)$ denote the set of order ideals of P .

Example 1.3.18. For examples of order ideals, consider the poset in Figure 1.8. If e is in an order ideal I , then $a, b \in I$. If $f \in I$, then $b \in I$. If $a, b \in I$ nothing else is required. Finally, if $h \in I$, then all poset elements are in I .

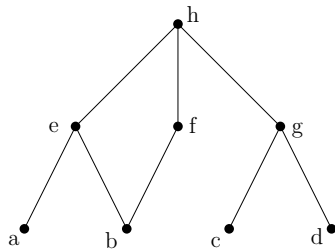


Figure 1.8. An example of a poset.

Next, a special poset is defined. The set of order ideals of this poset have nice properties.

Definition 1.3.19. Define a poset Q_τ that is in the shape of an equilateral triangle with top point the maximum element and $\tau - 1$ minimal elements.

An example of Q_5 with generators of an order ideal highlighted and the resulting order ideal is shown in Figure 1.9. The example of $J(Q_4)$, the set of all order ideals of Q_4 is in Figure 1.10.

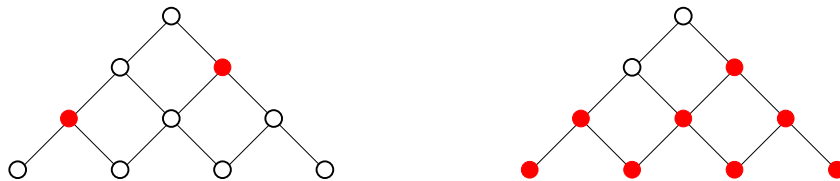


Figure 1.9. The poset Q_5 with two generator elements highlighted and the corresponding order ideal.

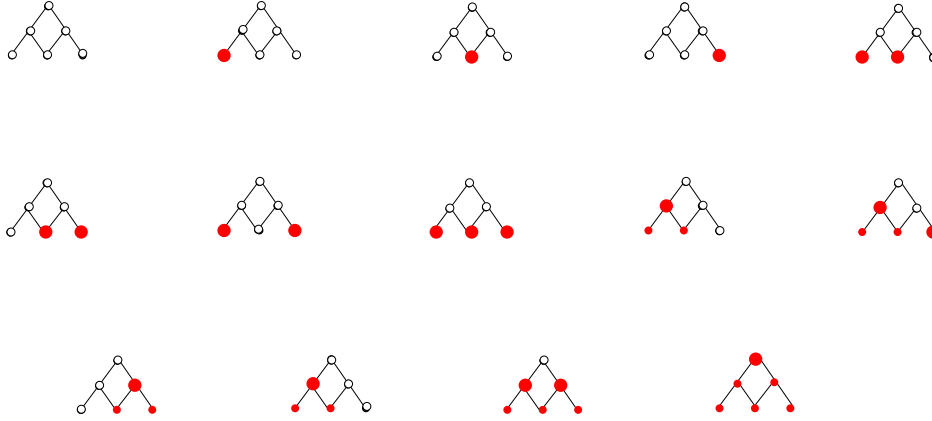


Figure 1.10. The fourteen order ideals in $J(Q_4)$. The larger red elements are the generators of each order ideal.

Definition 1.3.20. A *linear extension* of a poset P is a bijective function $f : P \rightarrow \{1, \dots, n\}$ where the number of elements in P is n , such that if $p_1 < p_2$ in P then $f(p_1) < f(p_2)$. The number of linear extensions of P is denoted $e(P)$.

An example of a linear extension is shown in Figure 1.11. Notice that the elements of the poset receive numbered labels and these labels preserve the partial ordering.

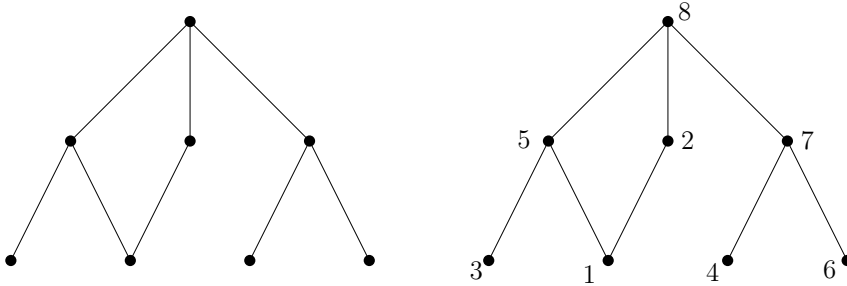
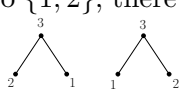


Figure 1.11. A poset on the left and a linear extension of it on the right.

Definition 1.3.21. Let P be a finite n -element poset and t a positive integer. Define $\Omega(P, t)$ to be the number of order-preserving maps $\eta : P \rightarrow \{1, \dots, t\}$; i.e., if $x \leq y$ in P then $\eta(x) \leq \eta(y)$. Then $\Omega(P, t)$ is a polynomial function of t of degree n , called the *order polynomial* of P .

Theorem 1.3.22. The leading coefficient of $\Omega(P, t)$ is $\frac{e(P)}{n!}$.

Example 1.3.23. Consider the triangular poset on three elements . This poset has order polynomial: $\frac{1}{3}t^3 + \frac{1}{2}t^2 + \frac{1}{6}t$.

When $t = 1$ the result is 1, since there is only one map into $\{1\}$. When $t = 2$, the map is from P into $\{1, 2\}$, there are 5 possibilities and there are 5 order ideals. Notice there are two linear extensions  and $n! = 3! = 6$ so $\frac{e(P)}{n!} = \frac{2}{6} = \frac{1}{3}$, the leading coefficient.

Definition 1.3.24. Two posets P and Q are *isomorphic* if there exists an *order-preserving bijection* $\phi: P \rightarrow Q$ whose inverse is order-preserving; that is,

$$s \leq t \in P \iff \phi(s) \leq \phi(t) \in Q.$$

1.3.4. The face lattice of a polytope

The concepts of faces, posets and lattices have been discussed. Putting these concepts together motivates the discussion of the face lattice of a polytope. The face lattice incorporates how the faces of a polytope are connected. The Hasse diagram shows this structure visually.

Definition 1.3.25 ([34, p. 57]). The *face lattice* of a convex polytope P is the poset of all faces of P , partially ordered by inclusion.

The face lattice of a polytope naturally has the needed inclusion relationship. The inclusion in a polytope is as follows: a vertex is part of an edge, if two vertices form an edge there is only one edge between them and so on. The dimension of each face dictates the rank in the lattice. The empty set has rank 0, the vertices have rank 1, the edges have rank 2 and so on. The dimension of a face is one less than the rank in the face lattice poset. The face lattice of a square pyramid is shown in Example 1.3.26.

Example 1.3.26. Given the 3-polytope square pyramid on the left in Figure 1.12, the Hasse diagram of its face lattice is on the right. Notice the empty set is the $\hat{0}$ at the bottom, then the vertices, next the edges, then the 3-dimensional faces, and finally the entire pyramid is the $\hat{1}$ at the top.

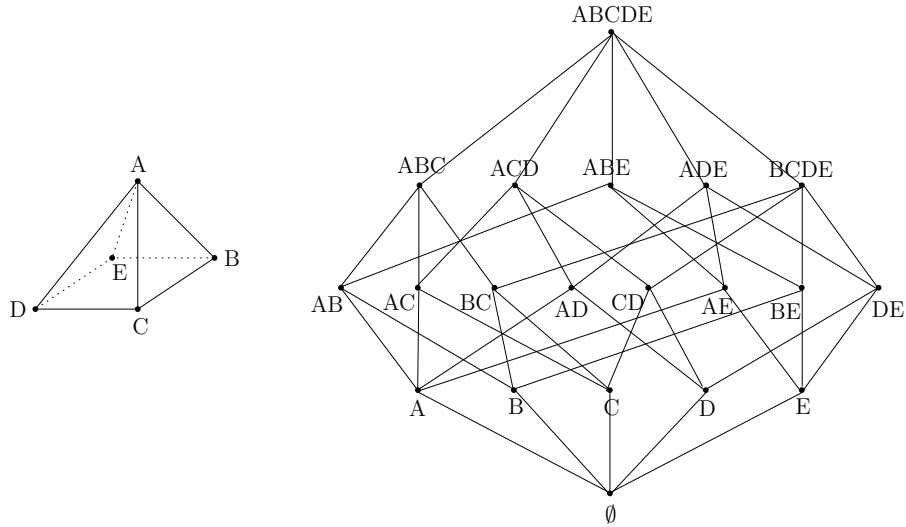


Figure 1.12. A square pyramid and its associated face lattice.

1.3.5. The Ehrhart polynomial

Next the Ehrhart polynomial of a polytope is discussed. A property of the Ehrhart polynomial is that the volume of the polytope is given as part of the polynomial. To define the Ehrhart polynomial, let \mathcal{P} be a d -dimensional integral convex polytope in \mathbb{R}^n . This subsection will reference Stanley's paper [25].

Definition 1.3.27. If t is a positive integer, define $i(\mathcal{P}, t)$ to be the cardinality of $(t\mathcal{P} \cap \mathbb{Z}^n)$.

In other words, $i(\mathcal{P}, t)$ is the number of integer points in the t th dilate of the \mathcal{P} .

Theorem 1.3.28. $i(\mathcal{P}, t)$ is a polynomial function of t of degree d , called the Ehrhart polynomial of \mathcal{P} . When $d = n$ the leading coefficient of $i(\mathcal{P}, t)$ is the volume $V(\mathcal{P})$ of \mathcal{P} . The normalized volume is the leading coefficient of $i(\mathcal{P}, t)$ multiplied by $n!$.

The following subsections discuss several special classes of polytopes.

1.3.6. The Birkhoff polytope

One of the classical and well-studied polytopes is the Birkhoff polytope, which is the convex hull of permutation matrices. The Birkhoff polytope along with the proof of its inequality description were an inspiration for work in Subsection 1.3.7 and Chapters 2 and 3. To discuss this special polytope, a definition from algebra is needed.

Definition 1.3.29 ([13, p. 29]). Let Ω be any nonempty set. The *symmetric group on the set Ω* under the action of composition, denoted \mathfrak{S}_Ω , is the set of all bijections from Ω to itself (otherwise known as the set of all *permutations* of Ω). If $\Omega = \{1, 2, 3, \dots, n\}$, denote \mathfrak{S}_Ω as \mathfrak{S}_n .

For the purpose of this thesis a group is not vital in the definition of a permutation, as a permutation on a finite set can be thought of as the rearranging of the elements in the set. The following definition shows permutations with a matrix representation.

Definition 1.3.30 ([27, p. 41]). If $w \in \mathfrak{S}_n$, then define the $n \times n$ matrix P_w , with rows and columns indexed by $\{1, 2, \dots, n\}$, as follows:

$$(P_w)_{ij} = \begin{cases} 1, & \text{if } w(i) = j \\ 0, & \text{otherwise.} \end{cases}$$

The matrix P_w is called the *permutation matrix* corresponding to w .

Permutation matrices are examples of *doubly stochastic* matrices, which means that all entries are non-negative and both the columns and rows sum to 1. The six 3×3 permutation matrices are shown in Figure 1.14 and some of the 4×4 doubly stochastic matrices are shown in Example 1.3.31.

Example 1.3.31. Two of the twenty-four 4×4 permutation matrices are on the left and a doubly stochastic matrix that is not a permutation matrix is on the right. Notice permutation matrices have one 1 in each row and in each column, with the other entries 0.

$$\begin{pmatrix} 0 & 0 & 1 & 0 \\ 0 & 1 & 0 & 0 \\ 0 & 0 & 0 & 1 \\ 1 & 0 & 0 & 0 \end{pmatrix} \quad \begin{pmatrix} 0 & 0 & 0 & 1 \\ 0 & 1 & 0 & 0 \\ 1 & 0 & 0 & 0 \\ 0 & 0 & 1 & 0 \end{pmatrix} \quad \begin{pmatrix} \frac{5}{12} & \frac{1}{3} & \frac{1}{4} & 0 \\ 0 & \frac{1}{4} & \frac{1}{6} & \frac{7}{12} \\ \frac{1}{4} & \frac{1}{6} & \frac{7}{12} & 0 \\ \frac{1}{3} & \frac{1}{4} & 0 & \frac{5}{12} \end{pmatrix}.$$

$n \times n$ matrices can be seen as vectors in \mathbb{R}^{n^2} . Take the vector to be the first row taken in order, then the second row taken in order and so on. There are n^2 entries in each matrix, thus n^2 entries in the vector and so the vectors are in \mathbb{R}^{n^2} . Therefore, the dimension of a permutation matrix is n^2 .

Definition 1.3.32 ([34, p. 20]). The *Birkhoff Polytope*, B_n , is the convex hull of all $n \times n$ permutation matrices, considered as vectors in \mathbb{R}^{n^2} .

The Birkhoff polytope has several other names. The Birkhoff Polytope was named after Garrett Birkhoff, who first defined it [5]. Another name is the *assignment polytope*; since there is one 1 in each row and column, a permutation matrix can be thought of as the rows and columns being assigned to one another. Permutation matrices are doubly stochastic matrices, thus the name *polytope of doubly stochastic matrices* is also used.

Example 1.3.33. Every point inside the $n = 3$ Birkhoff polytope, B_3 , is given by the following convex combination, for some set of μ_i .

$$\mu_1 \begin{pmatrix} 1 & 0 & 0 \\ 0 & 1 & 0 \\ 0 & 0 & 1 \end{pmatrix} + \mu_2 \begin{pmatrix} 1 & 0 & 0 \\ 0 & 0 & 1 \\ 0 & 1 & 0 \end{pmatrix} + \mu_3 \begin{pmatrix} 0 & 1 & 0 \\ 1 & 0 & 0 \\ 0 & 0 & 1 \end{pmatrix} + \mu_4 \begin{pmatrix} 0 & 1 & 0 \\ 0 & 0 & 1 \\ 1 & 0 & 0 \end{pmatrix} + \mu_5 \begin{pmatrix} 0 & 0 & 1 \\ 1 & 0 & 0 \\ 0 & 1 & 0 \end{pmatrix} + \mu_6 \begin{pmatrix} 0 & 0 & 1 \\ 0 & 1 & 0 \\ 1 & 0 & 0 \end{pmatrix}$$

where $\sum_{i=1}^6 \mu_i = 1$ and $\mu_i \geq 0$ for all i .

It is known that the permutation matrices are the vertices of B_n , thus there are $n!$ vertices. It is also known that the dimension is $(n - 1)^2$ and there are n^2 facets [5]. Notice that the dimension is not n^2 , which would be full-dimensional. The vectors of the polytope live in \mathbb{R}^{n^2} ; this is the *ambient dimension*. However, sometimes there are entries of the matrix that are determined, so the dimension of the polytope is less than the ambient dimension. Doubly stochastic matrices have determined entries, as the rows and columns need to add to 1. The Birkhoff polytope, therefore, has dimension $(n - 1)^2$.

An inequality description of the Birkhoff polytope will be discussed now.

Theorem 1.3.34 ([5, 32]). *The Birkhoff polytope B_n consists of all $n \times n$ real matrices $X = (X_{ij})$ such that:*

$$\begin{aligned} X_{ij} &\geq 0 & 1 \leq i, j \leq n, \\ \sum_{k=1}^n X_{ik} &= 1 & 1 \leq i \leq n, \\ \sum_{k=1}^n X_{kj} &= 1 & 1 \leq j \leq n. \end{aligned}$$

This result was proven independently by Birkhoff [5] and von Neumann [32]. The inequality proofs in Theorems 2.4.1 and 2.4.3 are modeled after the technique used by von Neumann to prove the inequality description of the Birkhoff polytope.

A permutation can be shown as a perfect matching in a bipartite graph. Discussed next will be the definition of bipartite graphs and perfect matchings. Then the relationship between the Birkhoff polytope and perfect matchings of bipartite graphs will be stated.

Definition 1.3.35. A *bipartite graph* on $2n$ vertices is a graph that can be drawn with two rows of n vertices in each row. The only allowed edges are between points on opposite rows. A *complete bipartite graph* is a bipartite graph with all possible edges, denoted $K_{n,n}$. A *perfect matching* of a graph is a subset of the edges such that each vertex is contained in exactly one edge.

Some examples of bipartite graphs can be found in Example 1.3.37. Given two graphs on the same vertex set, let the *union* of those graphs be the graph on the vertex set whose edge set is the union of the two edge sets. Graphs constructed as the union of perfect matchings are examples of *elementary graphs*, which means every edge is in some perfect matching.

Now the theorem that connects the Birkhoff polytope to the complete bipartite graph is stated.

Theorem 1.3.36 ([4, 7]). *The lattice of elementary subgraphs of $K_{n,n}$ ordered by inclusion, is in bijection with the face lattice of the Birkhoff polytope. Thus, the number of cycles in an elementary graph gives the dimension of the corresponding Birkhoff polytope face.*

Example 1.3.37. In Figure 1.13, the top two bipartite graphs are perfect matchings of $K_{3,3}$ and represent the permutations 132 and 312. Think of the top row as where the line starts and the bottom row where it ends. Notice in the left graph, the 1 goes to 1, the 2 goes to 3 and the 3 goes to 2, thus this represents the permutation 132. The bottom graph is the union of the top two, and thus is an elementary graph. Notice that there is one cycle in the bottom graph; this represents a dimension 1 face, or edge, of the Birkhoff polytope.

Remark 1.3.38. It is interesting to note that within the Birkhoff polytope the only integer points are the permutation matrices; there are no other points within the polytope that have all integer coordinates. Such integer points are called *lattice points*. In other words, the Birkhoff polytope contains no non-vertex lattice points. A similar result will be proved in Proposition 2.7.5.

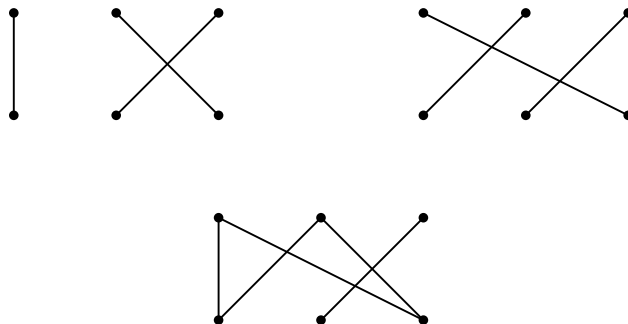


Figure 1.13. Two perfect matchings of $K_{3,3}$ on top. The bottom is the union of the others.

1.3.7. The alternating sign matrix polytope

Another well-studied polytope is the alternating sign matrix polytope. The alternating sign matrix polytope contains the Birkhoff polytope. This discussion of the alternating sign matrix polytope will follow Striker’s work [31], unless otherwise stated.

Definition 1.3.39 ([23]). An *alternating sign matrix* is a square matrix with entries in $\{-1, 0, 1\}$ such that the rows and columns each sum to one and the nonzero entries along any row or column alternate in sign. Let $A(n)$ denote the set of $n \times n$ alternating sign matrices.

$$\begin{pmatrix} 1 & 0 & 0 \\ 0 & 1 & 0 \\ 0 & 0 & 1 \end{pmatrix}, \begin{pmatrix} 1 & 0 & 0 \\ 0 & 0 & 1 \\ 0 & 1 & 0 \end{pmatrix}, \begin{pmatrix} 0 & 1 & 0 \\ 1 & 0 & 0 \\ 0 & 0 & 1 \end{pmatrix}, \\ \begin{pmatrix} 0 & 1 & 0 \\ 0 & 0 & 1 \\ 1 & 0 & 0 \end{pmatrix}, \begin{pmatrix} 0 & 0 & 1 \\ 1 & 0 & 0 \\ 0 & 1 & 0 \end{pmatrix}, \begin{pmatrix} 0 & 0 & 1 \\ 0 & 1 & 0 \\ 1 & 0 & 0 \end{pmatrix}, \begin{pmatrix} 0 & 1 & 0 \\ 1 & -1 & 1 \\ 0 & 1 & 0 \end{pmatrix}.$$

Figure 1.14. The seven 3×3 alternating sign matrices. Notice the first six are also permutation matrices.

There are seven 3×3 alternating sign matrices; all are shown in Figure 1.14. Notice that six of the matrices are the 3×3 permutation matrices; a permutation matrix is always an alternating sign matrix. This is why the Birkhoff polytope is contained in the alternating sign matrix polytope.

Theorem 1.3.40 ([21, 33]). *The total number of $n \times n$ alternating sign matrices is given by the expression:*

$$\prod_{j=0}^{n-1} \frac{(3j+1)!}{(n+j)!}.$$

This enumeration of alternating sign matrices was first conjectured by Mills, Robbins, and Rumsey [23]. Several years later it was proved by Zeilberger [33] with a shorter proof following by Kuperberg [21]. This shorter proof used a bijection between alternating sign matrices and configurations of the statistical physics model of square ice with domain wall boundary conditions.

Alternating sign matrices have also been studied as polytopes [3, 31]. The rest of this subsection discusses a family of polytopes formed from alternating sign matrices.

Definition 1.3.41. The n th alternating sign matrix polytope, denoted ASM_n , is the convex hull in \mathbb{R}^{n^2} of the $n \times n$ alternating sign matrices.

It has been proved that ASM_n has the alternating sign matrices as the vertices and has dimension $(n-1)^2$ [3, 31]. Also the inequality description is known to be the following.

Theorem 1.3.42 ([3, 31]). *The convex hull of $n \times n$ alternating sign matrices consists of all $n \times n$ real matrices $X = \{X_{ij}\}$ such that:*

$$\begin{aligned} 0 \leq \sum_{i'=1}^i X_{ij} &\leq 1 && 1 \leq i \leq n, 1 \leq j \leq n \\ 0 \leq \sum_{j'=1}^j X_{ij} &\leq 1 && 1 \leq j \leq n, 1 \leq i \leq n. \\ \sum_{i=1}^n X_{ij} &= 1 && 1 \leq j \leq n. \\ \sum_{j=1}^n X_{ij} &= 1 && 1 \leq i \leq n. \end{aligned}$$

Now the number of facets is discussed.

Theorem 1.3.43. *ASM_n has $4[(n-2)^2 + 1]$ facets, for $n \geq 3$.*

The proofs of the previous two theorems use certain graphs called *flow grids*. Flow grids are also used to prove some interesting results about the face lattice of ASM_n . These will be defined and discussed next.

Definition 1.3.44. Consider a directed graph with $n^2 + 4n$ vertices: n^2 *internal* vertices (i, j) and $4n$ *boundary* vertices $(i, 0), (0, j), (i, n + 1),$ and $(n + 1, j)$ where $i, j = 1, \dots, n$. These vertices are naturally depicted in a grid in which vertex (i, j) appears in row i and column j . Define the *complete flow grid* C_n to be the directed graph on these vertices with edge set $\{((i, j), (i, j \pm 1)), ((i, j), (i \pm 1, j)) \mid i, j = 1, \dots, n\}$.

Thus C_n has directed edges pointing in both directions, called *doubly directed*, between neighboring internal vertices and also directed edges from internal vertices to neighboring boundary vertices. In other words, the directed edges all point out to the boundary vertices and they go both directions in the interior of the graph. A complete flow grid is shown in Figure 1.15.

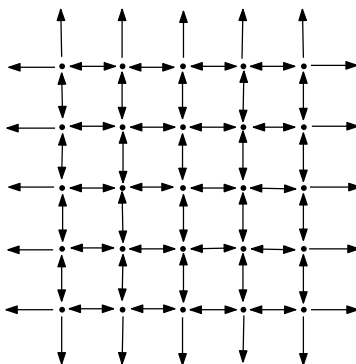


Figure 1.15. The complete flow grid for $n = 5$.

Definition 1.3.45. A *simple flow grid* of order n is a subgraph of C_n consisting of all the vertices of C_n , and in which four edges are incident to each internal vertex: either all four edges directed inward, all four edges directed outward, or both horizontal edges pointing in the same direction and both vertical edges pointing in the same direction.

An example of a simple flow grid and its corresponding alternating sign matrix from the bijection in the following proposition are both shown in Figure 1.16.

Proposition 1.3.46. *There exists an explicit bijection between simple flow grids of order n and $n \times n$ alternating sign matrices.*

A short explanation of the proof is as follows. A vertex configuration of four edges directed outward is called a *source*, the configuration of four edges directed inward is called a *sink*. Each

internal vertex of the simple flow grid corresponds to an entry in the matrix. If there is a source, the corresponding entry is a 1 and a sink corresponds to a -1 . Everything else is a 0. Starting with an alternating sign matrix, a simple flow grid is constructed as follows. All of the boundary vertices have a directed edge pointing to them, by definition. For the internal vertices, if there was a 1 in the matrix the corresponding vertex is a source and, similarly, a -1 corresponds to a sink. Once the sinks and sources are drawn, the rest of the directed edges “continue” in the direction they are already going and will end at a boundary vertex or a sink. Figure 1.16 has an example of an alternating sign matrix and its corresponding simple flow grid.

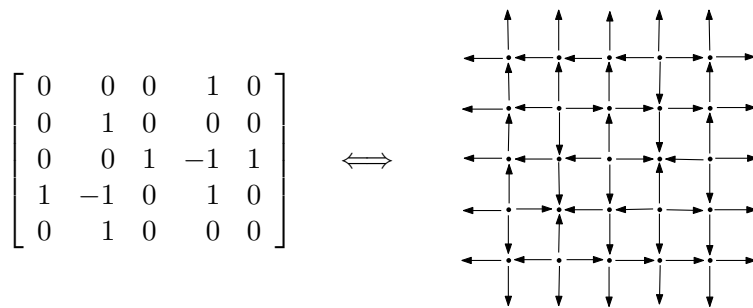


Figure 1.16. A 5×5 alternating sign matrix and its corresponding simple flow grid.

Definition 1.3.47. For any face F of ASM_n define the grid corresponding to the face, $g(F)$, to be the union over all the vertices of F of the simple flow grids corresponding to the vertices.

Definition 1.3.48. An *elementary flow grid* G is a subgraph of the complete flow grid C_n such that the edge set of G is the union of the edge sets of simple flow grids.

Definition 1.3.49. A *doubly directed region* of an elementary flow grid G is a connected collection of cells in G completely bounded by double directed edges (edges with arrows in both directions) but containing no double directed edges in the interior.

The union in Definition 1.3.48 is the same as in the discussion about perfect matchings in Example 1.3.37. The edge arrows only pointing in one direction can now point in both directions, giving the doubly directed edges of the graph. Figure 1.17 shows an example of doubly directed regions on an elementary flow grid.

Now recall the definition of a face lattice given in Definition 1.3.25. The face lattice of the Birkhoff polytope was described in Theorem 1.3.36. These ideas were extended to help study the face lattice of ASM_n .

Theorem 1.3.50. *The face lattice of ASM_n is isomorphic to the lattice of all $n \times n$ elementary flow grids ordered by inclusion.*

Theorem 1.3.51. *The dimension of a face F of ASM_n is the number of doubly directed regions in the corresponding elementary flow grid $g(F)$. In particular, the edges of ASM_n are represented by elementary flow grids containing exactly one cycle of double directed edges.*

Figure 1.17 shows an example of three regions of an elementary flow grid corresponding to a 3-dimensional face of ASM_n , as discussed in the previous theorem.

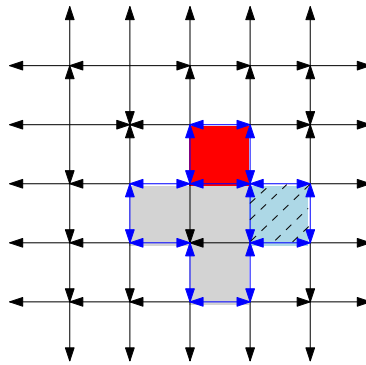


Figure 1.17. An elementary flow grid containing three doubly directed regions, which corresponds by Theorem 1.3.51 to a 3-dimensional face of ASM_5 .

1.3.8. The order polytope

The order polytope is a polytope defined from a poset and is one of the few polytopes where the Ehrhart polynomial is known, thus the volume is known as well. The study of the order polytope had been scattered throughout combinatorial literature until Stanley [25] summarized all the relevant properties in 1986. This paper will be a reference for the following discussion.

Definition 1.3.52. Given a poset P with elements $\{a_1, a_2, \dots, a_n\}$, the *order polytope*, $\mathcal{O}(P)$ is the set of all functions $f : P \rightarrow \mathbb{R}$ which satisfy the following conditions:

$$0 \leq f(a_i) \leq 1, \quad \text{for all } i \quad (1.1)$$

$$f(a_i) \leq f(a_j), \quad \text{if } a_j \text{ covers } a_i \text{ in } P. \quad (1.2)$$

Proposition 1.3.53. *The vertices of $\mathcal{O}(P)$ are the set $J(P)$, the order ideals of P .*

Stanley also gives the polytope $\hat{\mathcal{O}}(P)$, which defines a combinatorially equivalent polytope to $\mathcal{O}(P)$.

Definition 1.3.54. Obtain \hat{P} from P by adjoining a maximal element $\hat{1}$ and a minimal element $\hat{0}$. Define a polytope $\hat{\mathcal{O}}(P)$ to be the set of functions $g : \hat{P} \rightarrow \mathbb{R}$ satisfying $g(\hat{0}) = 0$, $g(\hat{1}) = 1$, and $g(x) \leq g(y)$, if $x \leq y$ in \hat{P} .

(1.1) is independent from (1.2), so together they define the facets of $\mathcal{O}(P)$. Since the polytopes $\mathcal{O}(P)$ and $\hat{\mathcal{O}}(P)$ are combinatorially equivalent, the facets are related.

Proposition 1.3.55. *A facet of $\mathcal{O}(P)$ consists of those $f \in \mathcal{O}(P)$ satisfying exactly one of the following conditions:*

$$f(x) = 0, \quad \text{for some minimal } x \in P, \quad (1.3)$$

$$f(x) = 1, \quad \text{for some maximal } x \in P, \quad (1.4)$$

$$f(x) = f(y), \quad \text{for some } y \text{ covering } x \text{ in } P. \quad (1.5)$$

A facet of $\hat{\mathcal{O}}(P)$ consists of those $g \in \hat{\mathcal{O}}(P)$ satisfying $g(x) = g(y)$ for some fixed pair (x, y) for which y covers x in \hat{P} .

From these definitions some nice results are obtained.

Theorem 1.3.56. *Suppose P is a poset with a maximal elements, b minimal elements and c cover relations. The number of facets of either $\hat{\mathcal{O}}(P)$ or $\mathcal{O}(P)$ is $a + b + c$.*

Next recall the Ehrhart polynomial from Theorem 1.3.28 and consider the Ehrhart polynomial of $\mathcal{O}(P)$. Further recall that the leading coefficient of the Ehrhart polynomial gives the volume of the polytope. Also, recall the definition of the order polynomial $\Omega(P, t)$ from Definition 1.3.21.

Theorem 1.3.57. *The Ehrhart polynomial of $\mathcal{O}(P)$ is given by*

$$i(\mathcal{O}(P), t) = \Omega(P, t + 1).$$

Corollary 1.3.58. *The normalized volume of $\mathcal{O}(P)$ is given by*

$$V(\mathcal{O}(P)) = e(P).$$

1.3.9. The transportation polytope

The polytope discussed in this subsection is the *transportation polytope*. The transportation polytope connects to the social sciences. An example of a polytope in this setting is as follows; consider moving n objects from a set of out-going facilities, S , to a set of in-coming facilities, C . A matrix can be used to organize and represent the information with S along the top and C along the side. Let each column vector stand for the amounts going out of each S_j and each row vector stands for the amounts coming into each C_i . Therefore in the matrix X , let X_{ij} be the amount of objects coming from S_j and going to C_i . This matrix has nonnegative entries and with fixed row and column integer sums.

Definition 1.3.59 ([11]). Fix two integers $p, q \in \mathbb{Z}_{>0}$ and two vectors $\vec{y} \in \mathbb{R}_{\geq 0}^p$ and $\vec{z} \in \mathbb{R}_{\geq 0}^q$. The *transportation polytope* $P_{(y,z)}$ is the convex polytope defined in the pq variables $X_{ij} \in \mathbb{R}_{\geq 0}$, $1 \leq i \leq p, 1 \leq j \leq q$, satisfying the $p + q$ equations:

$$\sum_{j'=1}^q X_{ij'} = y_i \text{ for all } 1 \leq i \leq p \tag{1.6}$$

$$\sum_{i'=1}^p X_{i'j} = z_j \text{ for all } 1 \leq j \leq q. \tag{1.7}$$

The relationship between transportation polytopes and sign matrix polytopes is discussed in Section 2.8.

1.4. Young tableaux

This section will discuss the second main element in this research, semistandard Young tableaux. *Young tableaux* are well-loved objects for their nice combinatorial properties, including beautiful enumerative formulas, and nontrivial connections to Lie algebras, representation theory,

and statistical physics [8, 15, 20]. Two main types of Young tableaux will be discussed: *standard Young tableaux* and *semistandard Young tableaux*. These two types of tableaux are the objects that are used to create polytopes in Chapters 2 and 3. Information from this section is referenced from *Young Tableaux* by Fulton [15] unless stated otherwise.

Definition 1.4.1. A *partition* is a weakly decreasing sequence of positive integers $\lambda = [\lambda_1, \lambda_2, \dots, \lambda_k]$. The positive integers λ_i are called the *parts* of the partition and k is the *length* of the partition.

Definition 1.4.2. A *Young diagram* is a finite collection of boxes, or cells, arranged in left-justified rows, with a weakly decreasing number of boxes in each row. The shape of a Young diagram is denoted λ .

The definition above is the English notation; see Figure 1.18 for an example. The English notation will be used in this thesis, however there are other notations that are commonly used. The French notation for a Young diagram is lower left justified, whereas the Russian notation takes the French diagram and rotates it 45 degrees counter-clockwise; this puts the upper left box (of the English diagram) at the bottom. Again, the English notation is to be assumed hereafter.

1.4.1. Standard Young tableaux

A Young diagram can be filled with numbers; one such filling and the resulting tableaux are discussed in this subsection. In addition to defining these tableaux, their enumeration will also be discussed.

Definition 1.4.3. A *standard Young tableau*, denoted *SYT*, is defined as a filling of a Young diagram with the numbers 1 through n . There are n boxes, each used exactly once and such that the numbers in the rows and the columns are strictly increasing when starting at the left or top, respectively.

An example of a standard Young tableau is shown in Figure 1.18.

When working with *SYT*, referring to a specific shape of the tableau is useful. The set of *SYT* of shape λ is denoted $SYT(\lambda)$. The enumeration of $SYT(\lambda)$ is given using the *hook length formula*. Next some elements needed to find this enumeration are given.

Definition 1.4.4. A *hook* in a Young diagram is the collection of boxes obtained by taking a specific box of the diagram along with all of the boxes to the right and below this box.

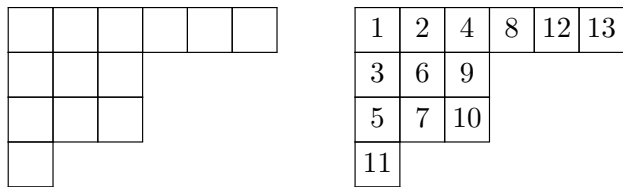


Figure 1.18. A Young diagram of shape $[6, 3, 3, 1]$ and a standard Young tableau of the same shape.

See Figure 1.19 for an example of a hook in a Young diagram. When referring to a specific hook, a specific box of the diagram is being referenced also. That box is usually called u .

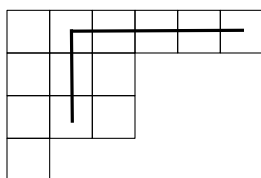


Figure 1.19. A Young diagram with a hook shown.

Now the hook length of a box in a Young diagram is discussed.

Definition 1.4.5. The *hook length* of a box u in a Young diagram λ is the number of boxes contained in the hook established from u , denoted $h(u)$.

Each box of a Young diagram has its own hook length. This is shown in Figure 1.20. Frame, Robinson and Thrall used hook length in their enumeration of standard Young tableaux.

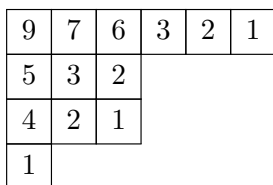


Figure 1.20. The Young diagram of $[6,3,3,1]$ with the hook lengths of each box.

Theorem 1.4.6 ([14]). *Let λ be a partition with n boxes. The number of tableaux in $SYT(\lambda)$, denoted by f^λ , is given by the hook length formula: $f^\lambda = \frac{n!}{\prod_{u \in \lambda} h(u)}$.*

Example 1.4.7. The number of tableaux in $SYT([6, 3, 3, 1])$ uses the hook lengths in Figure 1.20 and is as follows: $f^{[6,3,3,1]} = \frac{13!}{9 \cdot 7 \cdot 6 \cdot 3 \cdot 2 \cdot 1 \cdot 5 \cdot 3 \cdot 2 \cdot 4 \cdot 2 \cdot 1 \cdot 1} = 11440$.

Young diagrams may be filled in different ways to create other types of tableaux. Standard Young tableaux is one such type and they are used in Chapter 3. The next definition describes another way to fill a Young diagram with numbers and will be used in Chapter 2.

1.4.2. Semistandard Young tableaux

Semistandard Young tableaux are other fillings of a Young diagram. These new tableaux will be defined and enumerated in the following discussion.

Definition 1.4.8. A *semistandard Young tableau (SSYT)* is a filling of a Young diagram with positive integers such that the rows are weakly increasing and the columns are strictly increasing.

An example of a semistandard Young tableau is seen in Figure 1.21.

1	1	2	4	5	7
2	2	3			
3	4	5			
6					

Figure 1.21. A semistandard Young tableau of shape $[6, 3, 3, 1]$.

The following refinement is studied in Chapter 2 and places more restrictions on the tableaux.

Definition 1.4.9. Let $SSYT(m, n)$ denote the set of *semistandard Young tableaux with at most m columns and entries at most n* .

In 1983, Gordon enumerated $SSYT(m, n)$ as follows.

Theorem 1.4.10 ([17]). *The number of SSYT with at most m columns and entries at most n is:*

$$\prod_{1 \leq i \leq j \leq n} \frac{m + i + j - 1}{i + j - 1}.$$

Example 1.4.11. This example shows how the formula for enumerating $SSYT(m, n)$ is used.

$$SSYT(3, 2) = \binom{3+1+1-1}{1+1-1} \binom{3+1+2-1}{1+2-1} \binom{3+2+2-1}{2+2-1} = \binom{4}{1} \binom{5}{2} \binom{6}{3} = 20$$

Therefore, there are 20 different semistandard Young tableau with first row of length at most 3 and entries at most 2. These tableau come from semistandard Young tableau of shapes:

[3], [3, 1], [3, 2], [3, 3], [2], [2, 1], [2, 2], [1], \emptyset . There can be at most two rows in the tableau since the entries may be at most 2.

As with *SYT*, at times it is necessary to refer to the shape of the tableau. Notation using the shape of the tableaux is now discussed.

Definition 1.4.12. Let $SSYT(\lambda, n)$ denote the set of *semistandard Young tableaux of partition shape λ and entries at most n* .

For example, the tableau in Figure 1.21 is in both $SSYT(6, n)$ and $SSYT([6, 3, 3, 1], n)$ for any $n \geq 7$.

Stanley's enumeration of $SSYT(\lambda, n)$ is discussed in the following definition and theorem.

Definition 1.4.13. The *content*, $c(u)$, is given by $c(u) = j - i$ for every $u = (i, j)$ in a Young diagram.

Example 1.4.14. The content of each box in a Young diagram of shape [6, 3, 3, 1] is given below. Notice that $u = (3, 2)$ represents the box in the third row and second column from the upper left.

0	1	2	3	4	5
-1	0	1			
-2	-1	0			
-3					

Theorem 1.4.15 ([26, p. 403]). *The number of $SSYT$ of shape λ with entries at most n is given by the hook-content formula:*

$$\prod_{u \in \lambda} \frac{n + c(u)}{h(u)}$$

where $c(u)$ is the content of the $SSYT$ and $h(u)$ is the hook length of u .

Example 1.4.16. The hook content formula is applied to enumerate $SSYT$ of shape [6,3,3,1] with entries at most 7:

$$\begin{aligned} & \left(\frac{7+0}{9}\right) \left(\frac{7+1}{7}\right) \left(\frac{7+2}{6}\right) \left(\frac{7+3}{3}\right) \left(\frac{7+4}{2}\right) \left(\frac{7+5}{1}\right) \left(\frac{7+(-1)}{5}\right) \left(\frac{7+0}{3}\right) \\ & \left(\frac{7+1}{2}\right) \left(\frac{7+(-2)}{4}\right) \left(\frac{7+(-1)}{2}\right) \left(\frac{7+0}{1}\right) \left(\frac{7+(-3)}{1}\right) = 344960. \end{aligned}$$

Therefore, there are 344960 semistandard Young tableau of shape $[6, 3, 3, 1]$ that have entries at most 7.

Notice that in Theorem 1.4.15 a shape of tableau is needed. Conversely, in Theorem 1.4.10 all tableau that fit in a certain size box are considered. Example 1.4.11 shows that there are many shapes that make up $SSYT(m, n)$.

1.4.3. Special shapes of tableaux

There are many special shapes of tableaux that are studied for various reasons. Some of these special shapes will be discussed in the following subsection. These special tableaux show other ways that tableaux can be used in combinatorics, and some will be further discussed in later chapters.

Definition 1.4.17. A *hook-shaped* Young diagram is a Young diagram with only one row and one column (of length $k - 1$), denoted $[\lambda_1, 1^{k-1}]$.

Recall that λ_1 is the length of the first row of a Young diagram. Two examples of hook shapes are given in Figure 1.22, *A* and *B*. Hook shaped tableaux tend to have nice properties. $SSYT$ of hook shape will be discussed in Chapter 2 and SYT of hook shape will be discussed in Chapter 3.

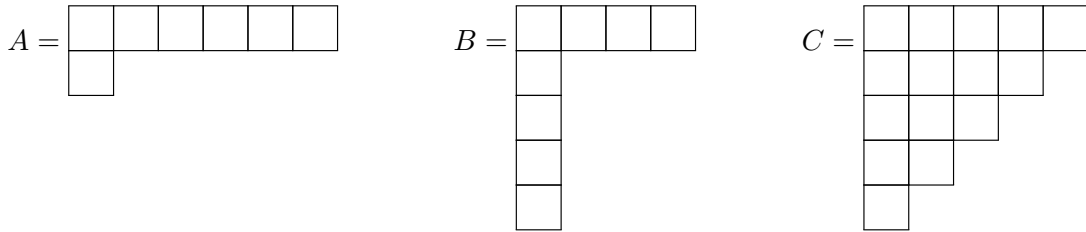


Figure 1.22. Young diagram *A* is a $[6, 1]$ hook, *B* is a $[3, 1^4]$ hook and *C* is a staircase shaped diagram.

Definition 1.4.18. A *staircase-shaped* Young diagram is a Young diagram where the row lengths decrease by one with every row. Thus the shapes of these Young diagrams are $[n, n - 1, \dots, 2, 1]$.

The example of a staircase shaped Young diagram is $[5,4,3,2,1]$, in Figure 1.22 *C*. When the maximum entry is also the number of rows of the tableau, then the hook content formula gives the enumeration of these special *SSYT* as $2^{\binom{n}{2}}$. Staircase shaped semistandard Young tableaux with the extra condition that each diagonal is strictly increasing from upper right to lower left are in bijection with alternating sign matrices [23]. Examples of enumerating tableaux of these shapes is given in Example 1.4.19.

Example 1.4.19. First the enumerations of hook shaped tableaux for both a *SYT* (Theorem 1.4.6) and *SSYT* (Theorem 1.4.15) are given to compare.

Using the $[6, 1]$ hook from Figure 1.22 the number of *SYT* $([6, 1])$ is:

$$f^{[6,1]} = \frac{7!}{1 * 2 * 3 * 4 * 5 * 7 * 1} = 6.$$

The number of *SSYT* $([6, 1], 7)$ of the same shape is:

$$\frac{(7+0)(7+1)(7+2)(7+3)(7+4)(7+5)(7-1)}{1 * 2 * 3 * 4 * 5 * 7 * 1} = \frac{7 * 8 * 9 * 10 * 11 * 12 * 6}{1 * 2 * 3 * 4 * 5 * 7 * 1} = 4752.$$

The enumeration for *SSYT* of staircase shape was given; now the enumeration of *SYT* of staircase shape is given.

$$f^{[n,n-1,\dots,3,2,1]} = \frac{\left(\frac{(n+1)(n)}{2}\right)!}{1^n * 3^{n-1} * 5^{n-2} * \dots * (2n-3)^3 * (2n-1)^1}$$

1.5. Catalan objects

It is well-known that two row rectangular standard Young tableaux are counted by the Catalan numbers, and therefore they are a Catalan object [27, p.259]. A polytope made from these Catalan objects will be the focus of Chapter 3. Catalan objects will be defined and enumerated in the following discussion, in addition to several examples of Catalan objects. Stanley's book *Catalan Numbers* [28] is the reference for this subsection unless stated otherwise.

Definition 1.5.1. The n th Catalan number C_n is:

$$C_n = \frac{1}{n+1} \binom{2n}{n} = \frac{(2n)!}{(n+1)!n!}.$$

Any countable collection of sets such that the n th set is enumerated by C_n is called a collection of *Catalan objects*.

Catalan numbers count many objects in combinatorics. Stanley's book *Catalan numbers* [28] lists 214 different known objects that are counted by these numbers, and are thus Catalan objects. The following theorem contains several common Catalan objects.

Theorem 1.5.2. *The Catalan number C_n counts the following:*

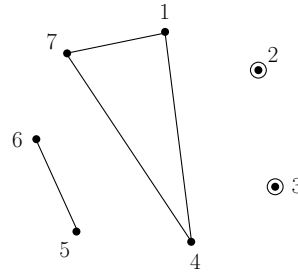
- i. Plane binary trees with $n + 1$ endpoints (or $2n + 1$ vertices).*
- ii. Sequences $i_1 i_2 \cdots i_{2n}$ of 1's and -1 's with $i_1 + i_2 + \cdots + i_j \geq 0$ for all j . These are called ballot sequences.*
- iii. Arrangements of n left parentheses '(' and n right parentheses ')' so that all the parentheses match. These are called binary parenthesizations.*
- iv. Paths P in the (x, y) plane from $(0, 0)$ to $(2n, 0)$, with steps $(1, 1)$ and $(1, -1)$, that never pass below the x -axis. Such paths are called Dyck paths.*
- v. Dissections of a convex $(n + 2)$ -gon into n triangles by drawing $n - 1$ diagonals, no two of which intersect in their interior. Such dissections are called triangulations of an $(n + 2)$ -gon (with no new vertices).*
- vi. Partitions of a set with n elements such that all the elements in the set are separated into non-empty groups, called blocks, where every element is included in one and only one block and such that the blocks are non-crossing. These are called non-crossing set partitions on n points.*
- vii. Graphs with $2n$ nodes that are connected into pairs by n edges in such a way that no two of them intersect. Such graphs are called non-crossing matchings.*
- viii. Standard Young tableaux of shape $[n, n]$.*
- ix. Order ideals of the triangular poset Q_n .*

The bijections between these nine Catalan objects are demonstrated and briefly explained in Example 1.5.3. However, this is not a proof of the bijections, just examples of them.

Example 1.5.3. Here are several Catalan objects that are in bijection with each other, (note in our examples, $n = 7$). The objects are numbered according to their number in the theorem, and the idea of the bijections is briefly described from one Catalan object to the next (denoted, e.g., *vi to vii*, for each transition). Notice the examples are organized so that the picture of one object is shown, then the description of getting from this first object to the next object, with the second object displayed after the transition.

The first Catalan object discussed is the non-crossing set partition.

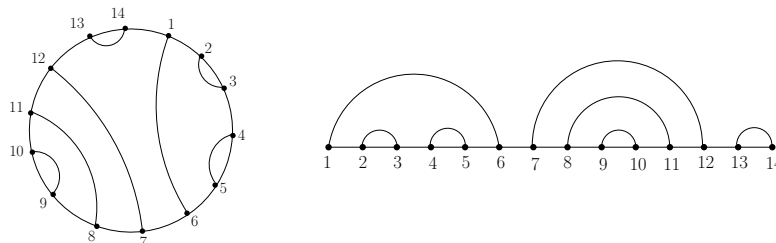
vi. Non-crossing set partition: 147|2|3|56, or pictorially



The non-crossing set partition can be seen as a partitioned number sequence or pictorially as follows. Start with n numbered nodes in a circle, in this case there are seven nodes numbered in order clockwise around the circle. Then for each section of the partition, the nodes of the corresponding number are connected in order. Note that none of the connections cross.

vi to vii: For each vertex in the circle of the non-crossing set partition, separate it into two vertices. Renumber around the circle (make a note which vertices came from which original number). For this example, the 1 from the non-crossing set partition becomes the 1 and 14 in the non-crossing matching. Now repeat the connections as they were before, while keeping in mind the original numbering. Thus a single vertex becomes two vertices and the split vertices will each have a connection. One line becomes two lines and so on. Notice there are no crossings of the new lines either. There are two ways to draw a non-crossing matching. To get from the circle to the line example of non-crossing matchings, cut the circle between 1 and 14 and lay it straight.

vii. Non-crossing matching, drawn two ways:



vii. to iii.: Starting with the second non-crossing matching, move in order from left to right. When there is a start of an arc, write “ (”, when there is an end of an arc, write “) ”.

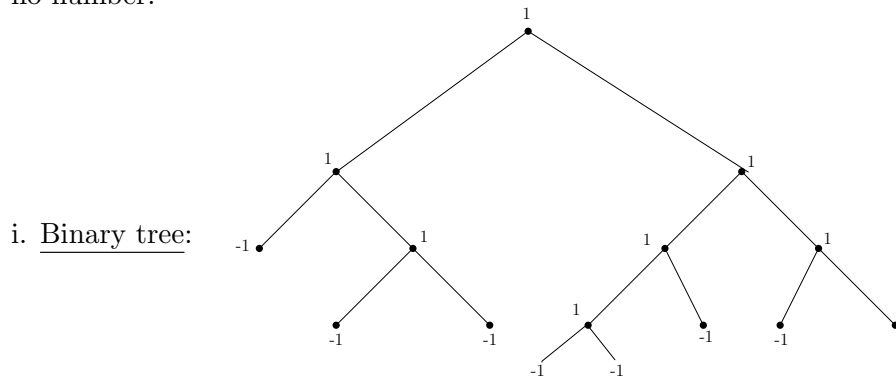
iii. Binary parenthesization: (() ()) ((())) ()

iii. to ii.: Replace “(” in the binary parenthesization by a 1 and “)” by a -1.

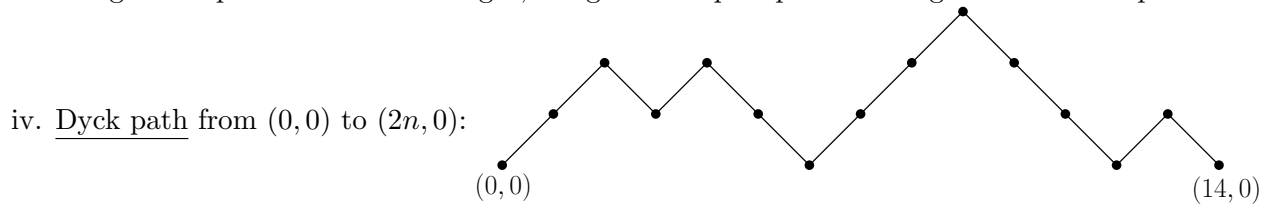
ii. Ballot sequence: 1 1 -1 1 -1 -1 1 1 1 -1 -1 -1 1 -1

i. to ii.: First some terminology for binary trees will be discussed. A binary tree begins at the top with a 1. Then the *branches* which extended both to the right and left are called *children*. A branch separates into children at a *node* and if there is an ending place, that is a *leaf*.

Starting with a binary tree and going to a ballot sequence will be discussed. Start at the top and think about an ant “walking” around the outside, counter-clockwise. The ballot sequence is found when noting new numbers as they are encountered the first time, however the last leaf gets no number.



ii. to iv.: Here, start again with the ballot sequence. The Dyck path starts at $(0, 0)$; following the sequence from left to right, a 1 gives an up-step and a -1 gives a down-step.

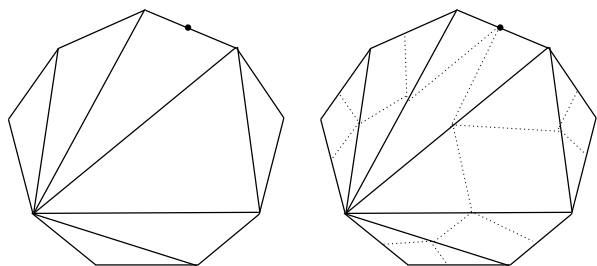


iv. to viii.: In the Dyck path, number each step from left to right. Make a Young diagram with two rows each the length of half the number of steps in the Dyck path. Working from left to right across the Dyck path, if the step is up, that number is written in the first available top box (also working from left to right). If on the Dyck path there is a down-step, the number is written in the next available bottom box.

viii. Two row rectangular standard Young tableau:

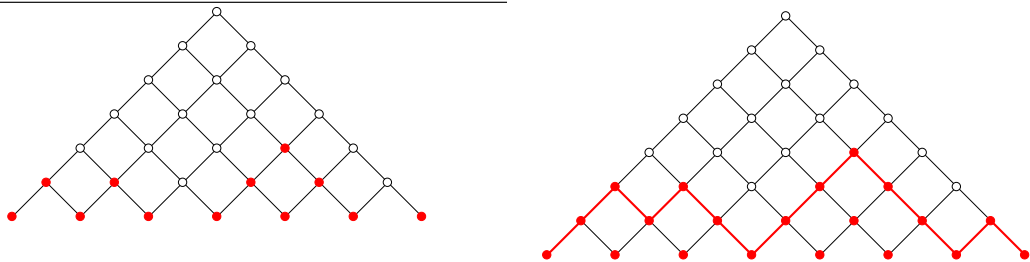
1	2	4	7	8	9	13
3	5	6	10	11	12	14

vi. Triangulation of an $(n + 2)$ -gon:



vi. to i. Start with a triangulation on an $(n + 2)$ -gon. In this case the triangulation is of a 9-gon. In the pictures, the triangulation is on the left and the triangulation with the binary tree in the 9-gon is on the right. On the n -gon, start with a point on a fixed edge. From this point, connect a line to all adjacent diagonals. At this connection point in the diagonals, a node is placed. Then two branches will connect to the next diagonals. Continue to make nodes and branches until an edge of the n -gon is reached. When finished, all diagonals will have a node and every polygon edge (besides the top of the tree with the starting edge) will have an ending leaf. Thus it is a binary tree inside the n -gon, like the one on the right.

ix. Order ideals on the triangular poset, Q_{n+1} :



ix. to iv. This example starts with an order ideal of Q_8 . The elements of the order ideal are red dots in the picture above. Now add another row of dots at the bottom of the order ideal, these will all be included in the order ideal by construction. If the lower left dot is $(0, 0)$ connect the upper elements in the order ideal with a line that starts at $(0, 0)$ and ends at $(2(7), 0)$. Notice there are 14 steps and this line always stays above the x -axis. Thus this line is a Dyck path.

This is just a glimpse at how all of these Catalan objects are in bijection with each other and with all of the 214 Catalan objects that have been documented so far. The vertices of the polytope discussed in Chapter 3 can be added to this list of Catalan objects.

1.6. Other topics

This subsection contains a few other topics related to either matrices or graphs. The background on graphs will be used in Section 2.6 and the material on matrices will be used in both Chapters 2 and 3.

Definition 1.6.1 ([9]). A graph G is called a *planar graph* if G can be drawn in the plane without any two of its edges crossing.

Definition 1.6.2 ([9]). When those points in the plane that correspond to the vertices and edges of a planar graph G are removed from the plane, the resulting connected pieces of the plane are the *regions* of G . One of the regions is unbounded and is called the *exterior region* of G .

Remark 1.6.3. The above definition of region is valid even when a graph is disconnected. For a disconnected graph, the regions depend on the planar embedding. The graphs considered in this thesis are given with a specific planar embedding, so this will not cause ambiguity.

A planar graph and its regions are shown in Figure 1.23.

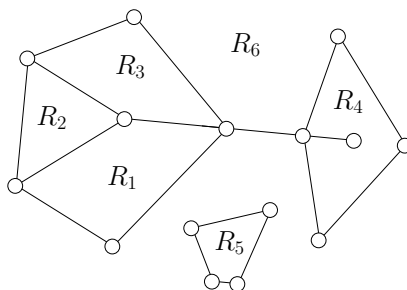


Figure 1.23. An example of a planar graph with regions labeled. R_6 is the exterior region.

Now the discussion turns to matrices. Most properties of matrices used in this research are basic properties, so only a few items will be discussed here. Partial column sums and partial row sums of a matrix are defined first. These matrices will be used in Sections 3.3 and 3.4. Note that this is notation used in this research and is not standard notation for partial sum matrices.

Definition 1.6.4. Let $\hat{C}(X)$ be the *partial column sum matrix* of an $m \times n$ matrix X , defined as

$$c_{i,j} = \sum_{i'=1}^i X_{i',j} \quad (1 \leq i \leq m, 1 \leq j \leq n).$$

An example of a matrix and its partial column sum matrix is given in Figure 1.24.

$$\begin{bmatrix} 0 & 0 & 0 & 0 & 0 & .2 & 0 & 0 & .7 & .1 & 0 & 1 \\ 0 & 0 & 0 & 0 & .5 & -.1 & 0 & .4 & -.7 & -.1 & 1 & -1 \\ 0 & 0 & 0 & .5 & -.4 & -.1 & .4 & -.4 & .1 & .9 & -1 & 0 \\ 0 & 0 & .9 & -.4 & -.1 & .4 & -.4 & .4 & .1 & -.9 & 0 & 0 \\ 0 & .9 & -.8 & -.1 & .4 & -.4 & .4 & -.2 & -.2 & 0 & 0 & 0 \\ 1 & -.8 & -.1 & .4 & -.4 & .3 & -.2 & -.2 & 0 & 0 & 0 & 0 \end{bmatrix} \quad \begin{bmatrix} 0 & 0 & 0 & 0 & 0 & .2 & 0 & 0 & .7 & .1 & 0 & 1 \\ 0 & 0 & 0 & 0 & .5 & .1 & 0 & .4 & 0 & 0 & 1 & 0 \\ 0 & 0 & 0 & .5 & .1 & 0 & .4 & 0 & .1 & .9 & 0 & 0 \\ 0 & 0 & .9 & .1 & 0 & .4 & 0 & .4 & .2 & 0 & 0 & 0 \\ 0 & .9 & .1 & 0 & .4 & 0 & .4 & .2 & 0 & 0 & 0 & 0 \\ 1 & .1 & 0 & .4 & 0 & .3 & .2 & 0 & 0 & 0 & 0 & 0 \end{bmatrix}$$

Figure 1.24. Example of a 6×12 matrix and its corresponding partial column sums matrix $\hat{C}(X)$.

Definition 1.6.5. Let $\hat{R}(X)$ be the *partial row sum matrix* of an $m \times n$ matrix X , defined as

$$r_{i,j} = \sum_{j'=1}^j X_{i,j'} \quad (1 \leq i \leq m, \quad 1 \leq j \leq n).$$

Remark 1.6.6. Any $m \times n$ matrix X can be recovered from $\hat{C}(X)$ or $\hat{R}(X)$ as follows.

$$\hat{C}^{-1} \text{ is given by } X_{i,j} = \begin{cases} c_{i,j} - c_{i-1,j} & 2 \leq i \leq m, \quad 1 \leq j \leq n \\ c_{i,j} & i = 1, \quad 1 \leq j \leq n \end{cases}$$

$$\hat{R}^{-1} \text{ is given by } X_{i,j} = \begin{cases} r_{i,j} - r_{i,j-1} & 1 \leq i \leq m, \quad 2 \leq j \leq n \\ r_{i,j} & 1 \leq i \leq m, \quad j = 1 \end{cases}$$

2. SIGN MATRIX POLYTOPES FROM YOUNG TABLEAUX¹

This chapter discusses polytopes formed by different semistandard Young tableaux and defines a new set of matrices called sign matrices. A bijection between sign matrices and semistandard Young tableaux will be discussed. In Theorem 2.1.5 this bijection is refined to a bijection between semistandard Young tableaux with a given shape and sign matrices with prescribed row sums. The two polytope families discussed are the convex hulls of certain sign matrices. Sections 2.2 to 2.6 will define the two polytope families and discuss their dimension, vertices, inequalities, facet enumerations and face lattice descriptions. Section 2.7 discusses the connection of the two polytope families to each other and to the alternating sign matrix polytope. Section 2.8 investigates the connection of these polytope families to the transportation polytope. This chapter is based on work from [24].

2.1. Semistandard Young tableaux and sign matrices

In this section, the definition of semistandard Young tableaux is recalled and sign matrices are defined. Then a bijection between them is discussed, due to Aval. This bijection is refined in Theorem 2.1.5 to a bijection between semistandard Young tableaux with a given shape and sign matrices with prescribed row sums.

Recall that a semistandard Young tableau is a filling of a Young diagram such that the rows are weakly increasing and the columns are strictly increasing. More information about these tableaux can be found in Section 1.4. The next definition uses partitions, which were introduced in Definition 1.4.1.

Definition 2.1.1. The *frequency representation* of a partition λ is the sequence $[a_1, a_2, \dots, a_{\lambda_1}]$ where a_i equals the number of parts of λ equal to i .

Example 2.1.2. The partition $\lambda = [6, 3, 3, 1]$ has frequency representation $[1, 0, 2, 0, 0, 1]$ and $k = 4$. An example of the Young diagram with this partition shape is pictured on the left in Figure 1.18.

Aval [2] defined a new set of objects, called sign matrices, which will be the building blocks of the polytopes that will be our main objects of study.

¹The material in this chapter was co-authored by Sara Solhjem and Dr. Jessica Striker. Solhjem had primary responsibility for all computations involved in this research and resulting theorem statements. Solhjem and Striker worked collaboratively to prove most of the theorems in this chapter. Solhjem was the primary drafter of this chapter; both Solhjem and Striker revised and proofread this chapter.

Definition 2.1.3 ([2]). A *sign matrix* is a matrix $M = (M_{ij})$ with entries in $\{-1, 0, 1\}$ such that:

$$\sum_{i'=1}^i M_{i'j} \in \{0, 1\}, \quad \text{for all } i, j. \quad (2.1)$$

$$\sum_{j'=1}^j M_{ij'} \geq 0, \quad \text{for all } i, j. \quad (2.2)$$

In words, the column partial sums from the top of a sign matrix equal either 0 or 1 and the partial sums of the rows from the left are non-negative.

Aval showed that $m \times n$ sign matrices are in bijection with SSYT with at most m columns and largest entry at most n [2, Proposition 1]. Defined now is the set of sign matrices shown in Theorem 2.1.5 to be in bijection with $SSYT(\lambda, n)$; this is a refinement of Aval's bijection. See Figure 2.1 for an example of this bijection.

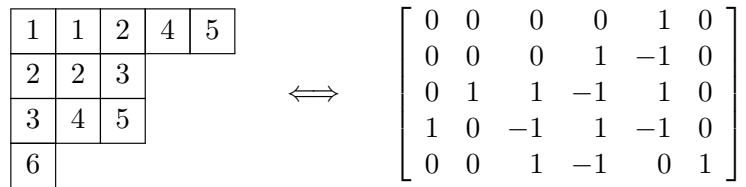


Figure 2.1. Example of the bijection between $SSYT$ and sign matrices.

Definition 2.1.4. Fix a partition λ with frequency representation $[a_1, a_2, \dots, a_{\lambda_1}]$ and fix $n \in \mathbb{N}$. Let $M(\lambda, n)$ be the set of $\lambda_1 \times n$ sign matrices $M = (M_{ij})$ such that:

$$\sum_{j=1}^n M_{ij} = a_{\lambda_1-i+1}, \quad \text{for all } 1 \leq i \leq \lambda_1. \quad (2.3)$$

Call $M(\lambda, n)$ the set of *sign matrices of shape λ and content at most n* .

Theorem 2.1.5. $M(\lambda, n)$ is in explicit bijection with $SSYT(\lambda, n)$.

Proof. We first outline the bijection of Aval [2] between $SSYT$ and sign matrices. Given an $m \times n$ sign matrix M , construct a tableau $\Phi(M) = T \in SSYT(m, n)$ such that the entries in the i th row of M determine the $(m - i + 1)$ st column (from the left) of T . In the i th row of M , note which columns have a partial sum (from the top) of one. Record the numbers of the matrix columns in

which this occurs, in increasing order from top down, to form column $m - i + 1$ of T . Since we record the entries in increasing order for each column of T and each entry only occurs once in a column, the columns of T are strictly increasing. The rows of T are weakly increasing, since by (2.2) the partial sums of the rows of M are non-negative. Thus, T is a *SSYT*. The length of the first row of T is m and the entries of T are at most n , since M is an $m \times n$ matrix. Thus Φ maps into $SSYT(m, n)$.

Aval proved in [2] that Φ is an invertible map that gives a bijection between $SSYT(m, n)$ and $m \times n$ sign matrices. We refine this to a bijection between $SSYT(\lambda, n)$ and $M(\lambda, n)$ by keeping track of the row sums of M and the shape of T . Given a tableau, $T \in SSYT(\lambda, n)$, we show that $\Phi^{-1}(T) = M \in M(\lambda, n)$. By [2], it is known that M is a sign matrix, so we only need to show it satisfies the condition (2.3). Consider the frequency representation $[a_1, a_2, a_3, \dots, a_{\lambda_1}]$ of the partition λ . Consider columns $\lambda_1 - i$ and $\lambda_1 - i + 1$ of T . If a number, ℓ , appears in both columns $\lambda_1 - i + 1$ and $\lambda_1 - i + 2$ of T , then $M_{i\ell} = 0$. So we can ignore when a number is repeated in adjacent columns of T , since it corresponds to a zero in M , which does not contribute to the row sum. Suppose ℓ appears in column $\lambda_1 - i + 2$ of T but not column $\lambda_1 - i + 1$. Then $M_{i\ell} = -1$. Suppose ℓ appears in column $\lambda_1 - i + 1$ of T but not column $\lambda_1 - i + 2$. Then $M_{i\ell} = 1$. So the total row sum $\sum_{j'=1}^n M_{ij'}$ equals the number of entries that appear in column $\lambda_1 - i + 1$ of T but not column $\lambda_1 - i + 2$ minus the number of entries that appear in column $\lambda_1 - i + 2$ but not column $\lambda_1 - i + 1$. This is exactly the length of column $\lambda_1 - i + 1$ minus the length of column $\lambda_1 - i + 2$, which is given by $a_{\lambda_1 - i + 1}$. \square

See Figure 2.2 and Example 2.1.6.

Example 2.1.6. In Figure 2.2, a semistandard Young tableau T of shape $[3, 3, 1, 1, 1]$ is given and the corresponding sign matrix M formed by the bijection discussed in Theorem 2.1.5. To see that M satisfies (2.3), note that the total row sums of M are 2, 0 and 3, while the frequency representation of the partition $[3, 3, 1, 1, 1]$ is $[3, 0, 2]$.

2.2. Definition and vertices of $P(\lambda, n)$

In this section, we define the first of the two polytopes that we are studying and prove some of its properties.

1	2	3
2	3	6
4		
5		
6		

 \iff

$$\begin{bmatrix} 0 & 0 & 1 & 0 & 0 & 1 \\ 0 & 1 & 0 & 0 & 0 & -1 \\ 1 & 0 & -1 & 1 & 1 & 1 \end{bmatrix}$$

Figure 2.2. The SSYT of shape $[3, 3, 1, 1, 1]$ and corresponding sign matrix from Example 2.1.6.

Definition 2.2.1. Let $P(\lambda, n)$ be the polytope defined as the convex hull, as vectors in $\mathbb{R}^{\lambda_1 n}$, of all the matrices in $M(\lambda, n)$. Call this the *sign matrix polytope of shape λ* .

We now investigate the structure of this polytope, starting with its dimension.

Proposition 2.2.2. *The dimension of $P(\lambda, n)$ is $\lambda_1(n - 1)$ if $1 \leq k < n$. When $k = n$, the dimension is $(\lambda_1 - \lambda_n)(n - 1)$.*

Proof. Since each matrix in $M(\lambda, n)$ is $\lambda_1 \times n$, the ambient dimension is $\lambda_1 n$. However, when constructing the sign matrix corresponding to a tableau of shape λ , as in Theorem 2.1.5, the last column is determined by the shape λ via the prescribed row sums (2.3) of Definition 2.1.4. This is the only restriction on the dimension when $1 \leq k < n$, reducing the free entries in the matrix by one column. Thus, the dimension is $\lambda_1(n - 1)$.

When $k = n$ the dimension depends on the number of columns of length n in λ ; this is given by λ_n . A column of length n in a SSYT with entries at most n is forced to be filled with the numbers $1, 2, \dots, n$. So the matrix rows corresponding to these columns are determined, and thus do not contribute to the dimension. Thus the dimension is $(\lambda_1 - \lambda_n)(n - 1)$. \square

From now on, it is assumed $k < n$. We now define a graph associated to any matrix. The graph will be useful in upcoming theorems; see Figure 2.3.

Definition 2.2.3. We define the $m \times n$ *grid graph* $\Gamma_{(m,n)}$ as follows. The vertex set is $V(m, n) := \{(i, j) : 1 \leq i \leq m + 1, 1 \leq j \leq n + 1\}$. We separate the vertices into two categories. We say the *internal vertices* are $\{(i, j) \text{ for } 1 \leq i \leq m, 1 \leq j \leq n\}$ and the *boundary vertices* are

$\{(m+1, j) \text{ and } (i, n+1) \text{ for } 1 \leq i \leq m, 1 \leq j \leq n\}$. The edge set is

$$E(m, n) := \begin{cases} (i, j) \text{ to } (i+1, j) & 1 \leq i \leq m, 1 \leq j \leq n \\ (i, j) \text{ to } (i, j+1) & 1 \leq i \leq m, 1 \leq j \leq n. \end{cases}$$

We draw the graph with i 's increasing to the right and j 's increasing down, to correspond with matrix indexing.

Definition 2.2.4. Given an $m \times n$ matrix X , define a graph, \hat{X} , which is a labeling of the edges of $\Gamma_{(m,n)}$ from Definition 2.2.3. The horizontal edges from (i, j) to $(i, j+1)$ are each labeled by the corresponding row partial sum $r_{ij} = \sum_{j'=1}^j X_{ij'}$ ($1 \leq i \leq m, 1 \leq j \leq n$). Likewise, the vertical edges

from (i, j) to $(i+1, j)$ are each labeled by the corresponding column partial sum $c_{ij} = \sum_{i'=1}^i X_{i'j}$ ($1 \leq i \leq m, 1 \leq j \leq n$). In many of the figures, the interior vertices are labeled with their corresponding matrix entry \mathbf{X}_{ij} ($1 \leq i \leq m, 1 \leq j \leq n$).

Remark 2.2.5. Note that given either the row or column partial sum labels of \hat{X} , one can uniquely recover the matrix X . See Remark 1.6.6.

See Figures 2.3 and 2.4.

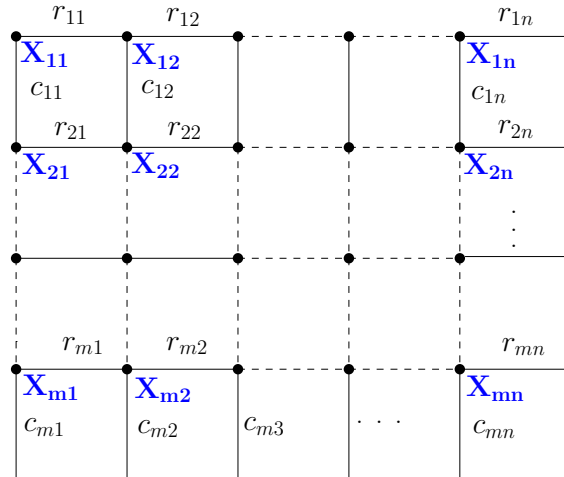


Figure 2.3. The graph \hat{X} from Definition 2.2.4, with dots on only the internal vertices.

The above notation will be used in proving the next theorem, which identifies the vertices of $P(\lambda, n)$.

Theorem 2.2.6. *The vertices of $P(\lambda, n)$ are the sign matrices $M(\lambda, n)$.*

Proof. Fix a sign matrix $M \in M(\lambda, n)$. In order to show that M is a vertex of $P(\lambda, n)$, we need to find a hyperplane with M on one side and all the other sign matrices in $M(\lambda, n)$ on the other side. Then since $P(\lambda, n)$ is the convex hull of $M(\lambda, n)$, M will necessarily be a vertex.

Let c_{ij} denote the column partial sums of M , as in Definition 2.2.4. Define $C_M := \{(i, j) \mid c_{ij} = 1\}$. Note that C_M is unique for each M , since the column partial sums can only be 0 or 1, and by Remark 2.2.5, we can recover M from the c_{ij} . Also note that $|C_M| = |\lambda|$, that is, the number of partial column sums that equal one in M equals the number of boxes in λ .

Define a hyperplane in $\mathbb{R}^{\lambda_1 n}$ as follows, on coordinates X_{ij} corresponding to positions in a $\lambda_1 \times n$ matrix:

$$H_M(X) := \sum_{(i,j) \in C_M} \sum_{i'=1}^i X_{i'j} = |\lambda| - \frac{1}{2}. \quad (2.4)$$

If $X = M$, then $H_M(X) = H_M(M) = |\lambda|$, since $|C_M| = |\lambda|$. Given a hyperplane formed in this manner, we may recover the matrix from which it is formed, thus H_M is unique for each M .

By definition, every matrix in $M(\lambda, n)$ has $|\lambda|$ partial column sums that equal 1. Let $M' \neq M$ be another matrix in $M(\lambda, n)$. It must be that there is an (i, j) where $c_{ij} = 1$ in M and $c_{ij} = 0$ in M' . $H_M(M')$ will be smaller than $H_M(M)$ by one for every time this occurs. For any (i, j) such that $c_{ij} = 0$ in M and $c_{ij} = 1$ in M' , $(i, j) \notin C_M$, so this partial sum does not contribute to H_M .

Therefore, $H_M(M) = |\lambda| > |\lambda| - \frac{1}{2}$ while $H_M(M') < |\lambda| - \frac{1}{2}$. Thus the sign matrices of $M(\lambda, n)$ are the vertices of $P(\lambda, n)$. \square

Example 2.2.7. Figure 2.4 gives the six graphs corresponding to the six sign matrices in $M(\lambda, 3)$ for $\lambda = [2, 2]$; these matrices correspond to *SSYT* of shape $[2, 2]$ with entries at most 3. Let M_e be the sign matrix corresponding to the graph in Figure 2.4(e). The equation for the hyperplane, H_{M_e} , described in Theorem 2.2.6, is $H_{M_e}(X) = X_{11} + (X_{11} + X_{21}) + X_{13} + (X_{12} + X_{22}) = 2X_{11} + X_{12} + X_{13} + X_{21} + X_{22} = |\lambda| - \frac{1}{2} = 3.5$. Now we substitute the entries of each matrix in $M([2, 2], 3)$ into this equation to show (e) is the only matrix on one side of this hyperplane.

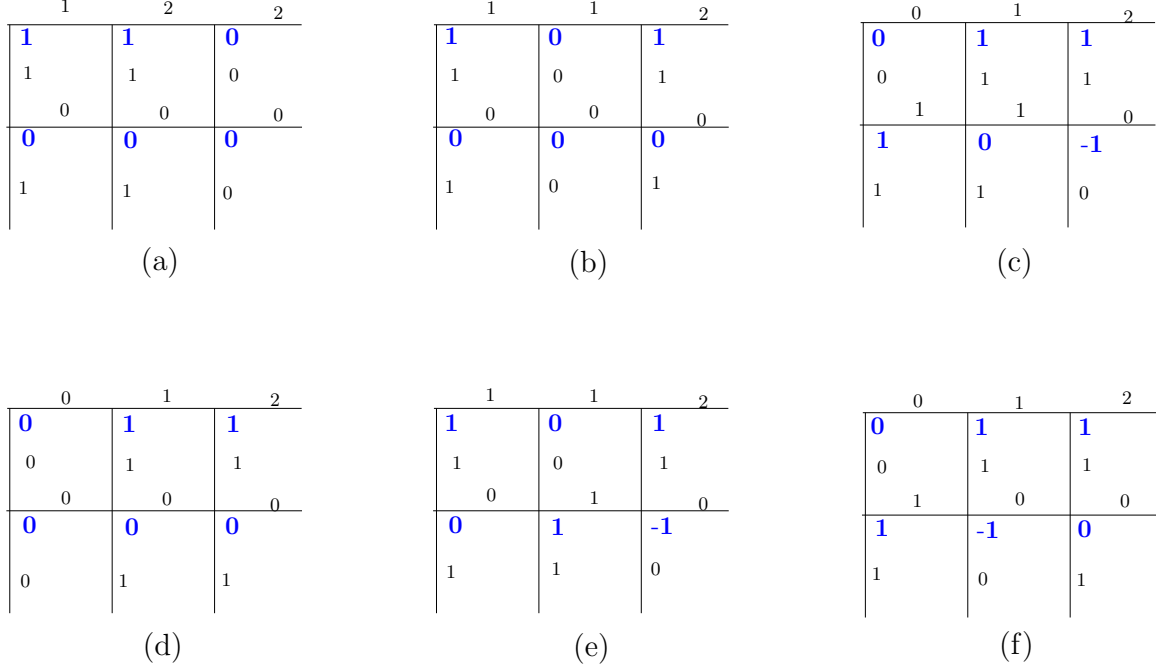


Figure 2.4. The six graphs corresponding to the six sign matrices in $M([2, 2], 3)$; these matrices correspond to $SSYT$ of shape $[2, 2]$ with entries at most 3.

- (a): $X_{11} = 1, X_{12} = 1, X_{13} = 0, X_{21} = 0, X_{22} = 0 \rightarrow H_{M_e}(M_a) = 2 + 1 + 0 + 0 + 0 = 3$;
(b): $X_{11} = 1, X_{12} = 0, X_{13} = 1, X_{21} = 0, X_{22} = 0 \rightarrow H_{M_e}(M_b) = 2 + 0 + 1 + 0 + 0 = 3$;
(c): $X_{11} = 0, X_{12} = 1, X_{13} = 1, X_{21} = 1, X_{22} = 0 \rightarrow H_{M_e}(M_c) = 0 + 1 + 1 + 1 + 0 = 3$;
(d): $X_{11} = 0, X_{12} = 1, X_{13} = 1, X_{21} = 0, X_{22} = 0 \rightarrow H_{M_e}(M_d) = 0 + 1 + 1 + 0 + 0 = 2$;
(e): $X_{11} = 1, X_{12} = 0, X_{13} = 1, X_{21} = 0, X_{22} = 1 \rightarrow H_{M_e}(M_e) = 2 + 0 + 1 + 0 + 1 = 4$;
(f): $X_{11} = 0, X_{12} = 1, X_{13} = 1, X_{21} = 1, X_{22} = -1 \rightarrow H_{M_e}(M_f) = 0 + 1 + 1 + 1 + (-1) = 2$.

Note that M_e is on one side of $2X_{11} + X_{13} + X_{21} + X_{22} = 3.5$ and the other five matrices in $M([2, 2], 3)$ are on the other side.

2.3. Definition and vertices of $P(m, n)$

Another family of polytopes will now be defined and studied, constructed using all $m \times n$ sign matrices.

Definition 2.3.1. Let $P(m, n)$ be the polytope defined as the convex hull of all $m \times n$ sign matrices. Call this the (m, n) sign matrix polytope.

Proposition 2.3.2. The dimension of $P(m, n)$ is mn for all $m > 1$.

Proof. Since every entry is essential, all mn of the entries contribute to the dimension. \square

Theorem 2.3.3. *The vertices of $P(m, n)$ are the sign matrices of size $m \times n$.*

Proof. Fix an $m \times n$ sign matrix M . In order to show that M is a vertex of $P(m, n)$, we need to find a hyperplane in \mathbb{R}^{mn} with M on one side and all the other $m \times n$ sign matrices on the other side. Then since $P(m, n)$ is the convex hull of all $m \times n$ sign matrices, M would necessarily be a vertex.

Let $c_{ij} = \sum_{i'=1}^i X_{i'j}$ in M , as in Definition 2.2.4. Recall from the proof of Theorem 2.2.6 the notation $C_M = \{(i, j) \mid c_{ij} = 1 \text{ in } M\}$ and $H_M(X) = \sum_{(i,j) \in C_M} \sum_{i'=1}^i X_{i'j}$.

Define a hyperplane in \mathbb{R}^{mn} as follows, on coordinates X_{ij} corresponding to positions in an $m \times n$ matrix.

$$K_M(X) := H_M(X) - \sum_{(i,j) \notin C_M} \sum_{i'=1}^i X_{i'j} = |C_M| - \frac{1}{2}. \quad (2.5)$$

Note that C_M is unique for each sign matrix M since we may recover any sign matrix from its column partial sums (see Remark 2.2.5). Therefore $K_M(X)$ is unique for each matrix M .

We wish to show the hyperplane $K_M(X) = |C_M| - \frac{1}{2}$ has M on one side and all the other $m \times n$ sign matrices on the other. Note that if $X = M$, then $K_M(X) = K_M(M) = |C_M|$. So we wish to show that given any $M' \in M(m, n)$ such that $M' \neq M$, $K_M(M') < |C_M| - \frac{1}{2}$.

We have two cases:

Case 1: There is a (i, j) entry $c_{ij} = 0$ in M and $c_{ij} = 1$ in M' . In this case, $(i, j) \notin C_M$. So in $K_M(M')$, this partial sum gets subtracted making $K_M(M')$ one smaller than $K_M(M)$ for every such (i, j) .

Case 2: There is a (i, j) entry $c_{ij} = 1$ in M and $c_{ij} = 0$ in M' . In this case, $(i, j) \in C_M$. So this partial sum contributed one to $H_M(M)$, whereas in $H_M(M')$ there is a contribution of zero. Therefore $H_M(M)$ is one greater than $H_M(M')$ so that $K_M(M)$ is one greater than $K_M(M')$ for every such (i, j) .

Since M and M' must differ in at least one column partial sum, $|C_M| = K_M(M) \geq K_M(M') + 1$ so that $K_M(M') < |C_M| - \frac{1}{2}$ for all $m \times n$ sign matrices M' . Thus the $m \times n$ sign matrices are the vertices of $P(m, n)$. \square

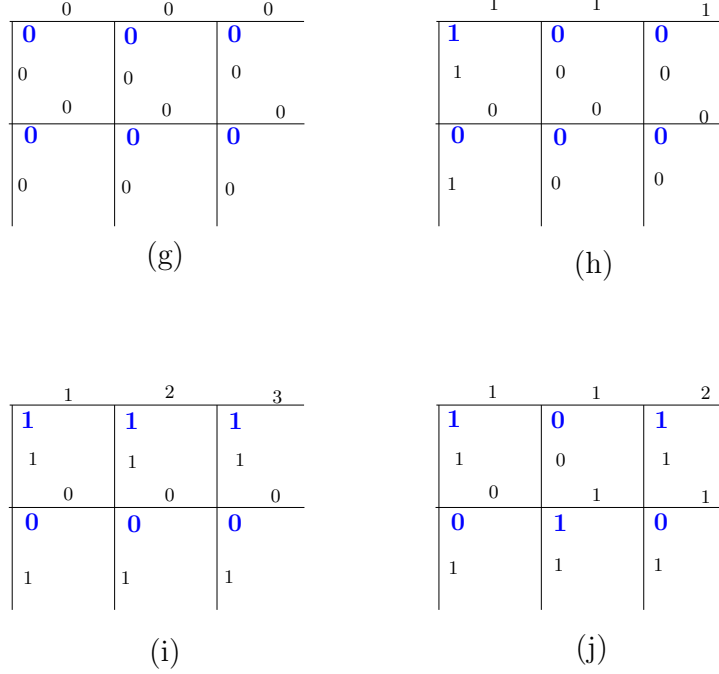


Figure 2.5. Four of the 26 partial sum graphs corresponding to the sign matrices that are vertices in $P(2, 3)$ but not in $P([2, 2], 3)$.

Example 2.3.4. Let M_h be the sign matrix corresponding to the graph in Figure 2.5(h). So $H_{M_h}(X) = 2X_{11} + X_{12}$, and therefore $H_{M_h}(M_a) = H_{M_h}(M_b) = H_{M_h}(M_c) = H_{M_h}(M_h) = H_{M_h}(M_i) = H_{M_h}(M_j) = 3$. This shows that the hyperplane of Theorem 2.2.6 does not separate M from all the other $m \times n$ sign matrices. But using Theorem 2.3.3, we find the needed hyperplane to be $K_{M_h}(X) = X_{11} + (X_{11} + X_{21}) - X_{12} + (X_{12} + X_{22}) - X_{13} - (X_{13} + X_{23}) = 2X_{11} + X_{21} - 2X_{12} - X_{22} - 2X_{13} - X_{23} = |C_M| - \frac{1}{2} = 3 - \frac{1}{2} = 2.5$. One may calculate the following: $K_{M_h}(M_a) = K_{M_h}(M_b) = K_{M_h}(M_c) = 0$; $K_{M_h}(M_h) = 3$; $K_{M_h}(M_i) = K_{M_h}(M_j) = -1$. This illustrates how the hyperplane $K_M(X) = |C_M| - \frac{1}{2}$ separates M from the other $m \times n$ sign matrices, even though $H_M(X) = |C_M| - \frac{1}{2}$ fails to.

In the following remark, we give some properties and non-properties of $P(m, n)$ and $P(\lambda, n)$. Definitions of these properties can be found at the end of Subsection 1.3.2.

Remark 2.3.5. Both $P(\lambda, n)$ and $P(m, n)$ are *integral polytopes*, as all vertices have integer values. Neither $P(\lambda, n)$ nor $P(m, n)$ are *regular polytopes*. For example, some of the vertices in $P(2, 2)$ from Figure 2.14 are adjacent to 4 edges, while others are adjacent to 5 or 6 edges. These polytopes are not *simplicial*, since the facets of these polytopes have varying numbers of vertices. For example,

the facets of $P(2, 2)$ have between 4 and 7 vertices. These polytopes are not *simple*; the vertices corresponding to δ_5 and δ_6 in Figure 2.14 are contained in 20 and 14 facets, respectively.

2.4. Inequality descriptions

In analogy with the Birkhoff polytope [5, 32] and the alternating sign matrix polytope [3, 31], we find an inequality description of $P(\lambda, n)$.

Theorem 2.4.1. $P(\lambda, n)$ consists of all $\lambda_1 \times n$ real matrices $X = (X_{ij})$ such that:

$$0 \leq \sum_{i'=1}^i X_{i'j} \leq 1, \quad \text{for all } 1 \leq i \leq \lambda_1, 1 \leq j \leq n \quad (2.6)$$

$$0 \leq \sum_{j'=1}^j X_{ij'}, \quad \text{for all } 1 \leq i \leq \lambda_1, 1 \leq j \leq n \quad (2.7)$$

$$\sum_{j'=1}^n X_{ij'} = a_{\lambda_1-i+1}, \quad \text{for all } 1 \leq i \leq \lambda_1. \quad (2.8)$$

Proof. This proof builds on techniques developed by Von Neumann in his proof of the inequality description of the Birkhoff polytope [32]. First we need to show that any $X \in P(\lambda, n)$ satisfies (2.6) – (2.8). Suppose $X \in P(\lambda, n)$, thus $X = \sum_{\gamma} \mu_{\gamma} M_{\gamma}$ where $\sum_{\gamma} \mu_{\gamma} = 1$ and the $M_{\gamma} \in M(\lambda, n)$. Since we have a convex combination of sign matrices, by Definition 2.1.3 we obtain (2.6) and (2.7) immediately. (2.8) follows from (2.3) in the definition of $M(\lambda, n)$ (Definition 2.1.4). Thus $P(\lambda, n)$ fits the inequality description.

Let X be a real-valued $\lambda_1 \times n$ matrix satisfying (2.6), (2.7), and (2.8). We wish to show that X can be written as a convex combination of sign matrices in $M(\lambda, n)$, so that it is in $P(\lambda, n)$. Consider the corresponding graph \hat{X} of Definition 2.2.4. Let $r_{i0} = 0 = c_{0j}$ for all i, j . Then for all $1 \leq i \leq \lambda_1, 1 \leq j \leq n$, we have $X_{ij} = r_{ij} - r_{i,j-1} = c_{ij} - c_{i-1,j}$. Thus,

$$r_{ij} + c_{i-1,j} = c_{ij} + r_{i,j-1}. \quad (2.9)$$

If X has no non-integer partial sums, then X is a $\lambda_1 \times n$ sign matrix, since (2.6), (2.7), and (2.8) reduce to Definitions 2.1.3 and 2.1.4.

So we assume X has at least one non-integer partial sum r_{ij} or c_{ij} . We may furthermore assume X has at least one non-integer column partial sum, since if all column partial sums of X

were integers, $X_{ij} = c_{ij} - c_{i-1,j}$ would imply the X_{ij} would be integers, thus all row partial sums would also be integers.

We construct an *open* or *closed circuit* in \hat{X} whose edges are labeled by non-integer partial sums. We say a *closed circuit* is a simple cycle in \hat{X} , that is, it begins and ends at the same vertex with no repetitions of vertices, other than the repetition of the starting and ending vertex. We say an *open circuit* is a simple path in \hat{X} that begins and ends at different boundary vertices along the bottom of the graph, that is, it begins at a vertex $(\lambda_1 + 1, j)$ and ends at vertex $(\lambda_1 + 1, j_0)$ for some $j_0 \neq j$.

We create such a circuit by first constructing a path in \hat{X} as follows. If there exists j such that $0 < c_{\lambda_1 j} < 1$, we start the path at bottom boundary vertex $(\lambda_1 + 1, j)$. If there is no such j , we find some c_{ij} such that $0 < c_{ij} < 1$ and start at the vertex corresponding to X_{ij} . By (2.9), at least one of $c_{i\pm 1, j}, r_{i, j\pm 1}$ is also a non-integer. Therefore, we may form a path by moving through \hat{X} vertically and horizontally along edges labeled by non-integer partial sums.

Now \hat{X} is of finite size and all the boundary partial sums on the left, right, and top are integers (since for all i and j , $r_{i0} = c_{0j} = 0$ and $r_{in} = a_{\lambda_1 - i + 1}$). So the path eventually reaches one of the following: (1) a vertex already in the path, or (2) a vertex $(\lambda_1 + 1, j_0)$. In Case (2), this means $c_{\lambda_1 j_0}$ is not an integer. But the total sum of the matrix is $\sum_{i=1}^{\lambda_1} r_{in} = \sum_{i=1}^{\lambda_1} a_{\lambda_1 - i + 1}$. Each $a_{\lambda_1 - i + 1}$ is an integer, so the total sum of all matrix entries is an integer. Since $c_{\lambda_1 j_0}$ is not an integer, there must be some other column sum $c_{\lambda_1 j}$ that is also not an integer. By construction, the path began at a bottom boundary vertex $(\lambda_1 + 1, j)$ with $c_{\lambda_1 j}$ not an integer, for some $j \neq j_0$. So this process yields an open circuit whose edge labels are all non-integer. In Case (1), the constructed path consists of a simple closed loop and possibly a simple path connected to the closed loop at some vertex $X_{i_0 j_0}$. We delete this path, and keep the closed loop. This process yields a closed circuit in \hat{X} whose edge labels are all non-integer. See Figures 2.6 and 2.7 for examples.

Let the following denote a circuit constructed as above, where the circled c and r values denote the edge labels as we traverse the circuit, and the boxed X_{ij} 's denote the matrix entries corresponding to the vertices on the corners of the circuit where the path changes from vertical to horizontal or vice versa. (Note how the boxes and circles appear in Figures 2.6 and 2.7.)

$$\left(\textcircled{c_0}, \dots, \textcircled{c'_0}, \boxed{X_{i_1, j_0}}, \textcircled{r_1}, \dots, \textcircled{r'_1}, \boxed{X_{i_1, j_1}}, \textcircled{c_1}, \dots, \textcircled{c'_1}, \boxed{X_{i_2, j_1}}, \textcircled{r_2}, \dots \right)$$

Using this circuit, we are able to write X as the convex combination of two new matrices, call them X^+ and X^- , that each have at least one more partial sum equal to its maximum or minimum possible value.

Construct a matrix X^+ by setting

$$X_{i_\alpha, j_\beta}^+ = \begin{cases} X_{i_\alpha, j_\beta} + \ell^+ & \text{if } \alpha + \beta \text{ is odd} \\ X_{i_\alpha, j_\beta} - \ell^+ & \text{if } \alpha + \beta \text{ is even} \end{cases}$$

and setting all other entries equal to the corresponding entry of X . That is, construct X^+ by alternately adding and subtracting a number ℓ^+ from each entry in X that corresponds to a corner in the circuit and leaving all other matrix entries unchanged. ℓ^+ is chosen to be the maximum possible value that preserves (2.6), (2.7), and (2.8) when added and subtracted from the corners as indicated above. That is, ℓ^+ equals the minimum value of the union of the following sets:

$$\begin{aligned} & \{c_{ij} \mid \text{the edge labeled by } c_{ij} \text{ is below a circuit corner } X_{i_\alpha, j_\beta} \text{ with } \alpha + \beta \text{ even}\}, \\ & \{1 - c_{ij} \mid \text{the edge labeled by } c_{ij} \text{ is below a circuit corner } X_{i_\alpha, j_\beta} \text{ with } \alpha + \beta \text{ odd}\}, \\ & \{r_{ij} \mid \text{the edge labeled by } r_{ij} \text{ is to the right of a circuit corner } X_{i_\alpha, j_\beta} \text{ with } \alpha + \beta \text{ even}\}. \end{aligned}$$

Note $\ell^+ > 0$ since all the partial sums in the circuit are non-integer.

Construct a matrix X^- by setting

$$X_{i_\alpha, j_\beta}^- = \begin{cases} X_{i_\alpha, j_\beta} - \ell^- & \text{if } \alpha + \beta \text{ is odd} \\ X_{i_\alpha, j_\beta} + \ell^- & \text{if } \alpha + \beta \text{ is even.} \end{cases}$$

and setting all other entries equal to the corresponding entry of X . That is, construct X^- by alternately subtracting and adding a number ℓ^- from each entry in X that corresponds to a corner in the circuit and leaving all other matrix entries unchanged. ℓ^- is chosen to be the maximum

possible value that preserves (2.6), (2.7), and (2.8) when subtracted and added from the corners as indicated above. That is, ℓ^- equals the minimum value of the union of the following sets:

$$\begin{aligned} &\{c_{ij} \mid \text{the edge labeled by } c_{ij} \text{ is below a circuit corner } X_{i\alpha j\beta} \text{ with } \alpha + \beta \text{ odd}\}, \\ &\{1 - c_{ij} \mid \text{the edge labeled by } c_{ij} \text{ is below a circuit corner } X_{i\alpha j\beta} \text{ with } \alpha + \beta \text{ even}\}, \\ &\{r_{ij} \mid \text{the edge labeled by } r_{ij} \text{ is to the right of a circuit corner } X_{i\alpha j\beta} \text{ with } \alpha + \beta \text{ odd}\}. \end{aligned}$$

Note $\ell^- > 0$ since all the partial sums in the circuit are non-integer.

Now in the case of either an open or closed circuit, there will be an even number of corners in the circuit. Note that for open circuits, each row has an even number of corners and there will be two columns with an odd number of corners, namely the columns where the path begins and ends. Whenever there is an even number of circuit corners in a row or column, this means that the same number is alternately added to and subtracted from the corners, thus the total row or column sum is not changed. Whenever there is an odd number of circuit corners in a column, this means that the total column sum will change, however it will stay between 0 and 1. Thus our constructions of X^+ and X^- above are well-defined.

Both X^+ and X^- satisfy (2.6)–(2.8) by construction. Also by construction,

$$X = \frac{\ell^-}{\ell^+ + \ell^-} X^+ + \frac{\ell^+}{\ell^+ + \ell^-} X^-$$

and $\frac{\ell^-}{\ell^+ + \ell^-} + \frac{\ell^+}{\ell^+ + \ell^-} = 1$. This is shown as follows: First notice that if $X_{i,j}$ is unchanged in X^+ it is also unchanged in X^- . Thus in this case,

$$\frac{\ell^-}{\ell^+ + \ell^-} X_{i,j}^+ + \frac{\ell^+}{\ell^+ + \ell^-} X_{i,j}^- = \left(\frac{\ell^-}{\ell^+ + \ell^-} + \frac{\ell^+}{\ell^+ + \ell^-} \right) X_{i,j} = \left(\frac{\ell^+ + \ell^-}{\ell^+ + \ell^-} \right) X_{i,j} = X_{i,j}.$$

If $X_{i,j}$ is changed to $X_{i,j} + \ell^+$ in X^+ , then in X^- , $X_{i,j}$ becomes $X_{i,j} - \ell^-$. Thus in this case,

$$\frac{\ell^- (X_{i,j} + \ell^+)}{\ell^+ + \ell^-} + \frac{\ell^+ (X_{i,j} - \ell^-)}{\ell^+ + \ell^-} = \frac{\ell^- X_{i,j} + \ell^- \ell^+ + \ell^+ X_{i,j} - \ell^+ \ell^-}{\ell^+ + \ell^-} = \frac{(\ell^+ + \ell^-) X_{i,j}}{\ell^+ + \ell^-} = X_{i,j}.$$

Again, if $X_{i,j}$ is changed to $X_{i,j} - \ell^+$ in X^+ , then in X^- , $X_{i,j}$ becomes $X_{i,j} + \ell^-$. Thus in this case,

$$\frac{\ell^-(X_{i,j} - \ell^+)}{\ell^+ + \ell^-} + \frac{\ell^+(X_{i,j} + \ell^-)}{\ell^+ + \ell^-} = \frac{\ell^- X_{i,j} - \ell^- \ell^+ + \ell^+ X_{i,j} + \ell^+ \ell^-}{\ell^+ + \ell^-} = \frac{(\ell^+ + \ell^-) X_{i,j}}{\ell^+ + \ell^-} = X_{i,j}.$$

So X is a convex combination of the two matrices X^+ and X^- that still satisfy the inequalities and are each at least one step closer to being sign matrices, since they each have at least one more partial sum attaining its maximum or minimum bound. Hence, by iterating this process, X can be written as a convex combination of sign matrices in $M(\lambda, n)$. \square

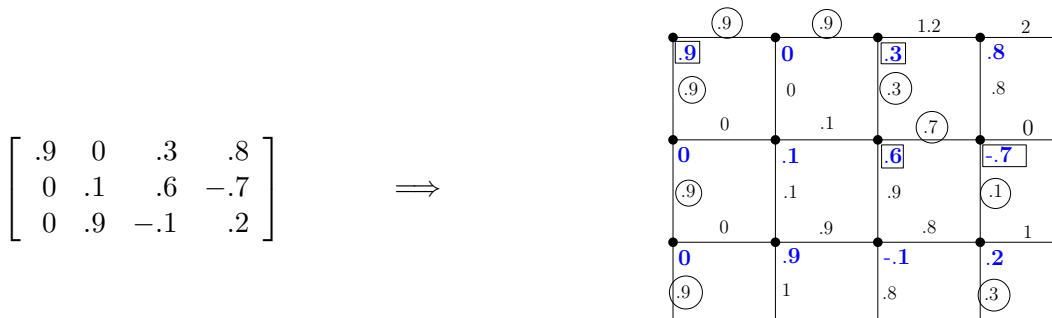


Figure 2.6. Left: A matrix X in $P([3, 3, 1], 4)$; Right: An open circuit in \hat{X} .

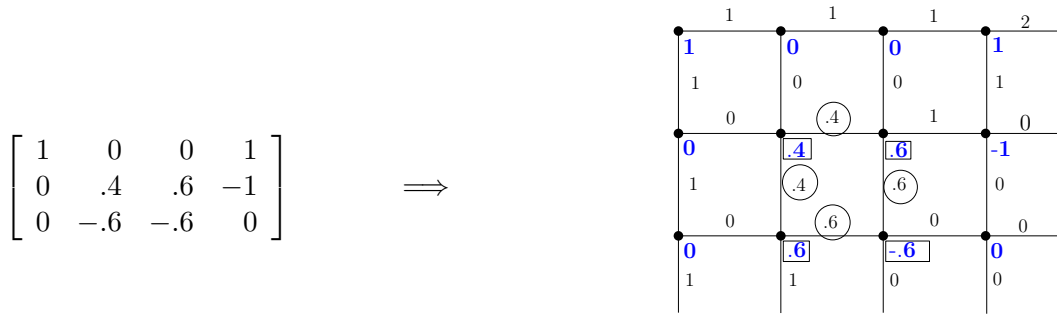


Figure 2.7. Left: A matrix X in $P([3, 3, 1], 4)$; Right: A closed circuit in \hat{X} .

Example 2.4.2. We use the open circuit in Figure 2.6 to show how to find X^+ , X^- , ℓ^+ and ℓ^- . The circuit is $\left((.9), (.9), (.9), (.9), (.9), (.9), (.3), (.3), (.6), (.7), (-.7), (.1), (.3) \right)$, where the circled and bold entries are the partial column sums and the circled non-bold entries are the row partial

$$\begin{bmatrix} .9 & 0 & .3 & .8 \\ 0 & .1 & .6 & -.7 \\ 0 & .9 & -.1 & .2 \end{bmatrix} = \frac{.7}{.1+.7} \begin{bmatrix} 1 & 0 & .2 & .8 \\ 0 & .1 & .7 & -.8 \\ 0 & .9 & -.1 & .2 \end{bmatrix} + \frac{.1}{.1+.7} \begin{bmatrix} .2 & 0 & 1 & .8 \\ 0 & .1 & -.1 & 0 \\ 0 & .9 & -.1 & .2 \end{bmatrix}$$

Figure 2.8. The decomposition of the matrix from Figure 2.6 as the convex combination of X^+ and X^- ; see Example 2.4.2.

sums of the circuit. The matrix entries at the corners of the circuit are boxed for emphasis. To construct X^+ , we label the corner entries alternately plus and minus, so the plus value goes on the .9 and .6 corners and the minus on the .3 and -.7 corners. Looking at the partial sums, we see that ℓ^+ will be the minimum of $\{.3, .1, .3\} \cup \{1 - .9, 1 - .9, 1 - .9\} \cup \emptyset$. Thus $\ell^+ = .1$, so .1 will be added to plus corners and subtracted from minus corners with X^+ as the result. We now switch the plus and minus corners. ℓ^- will be the minimum of $\{.9, .9, .9\} \cup \{1 - .3, 1 - .1, 1 - .3\} \cup \{.9, .9, .7\}$ so $\ell^- = .7$. So then .7 is added to the plus corners and subtracted from the minus corners to get X^- . Thus we may write the matrix as the convex combination of the matrices X^+ and X^- as in Figure 2.8.

We now find an inequality description of $P(m, n)$.

Theorem 2.4.3. $P(m, n)$ consists of all $m \times n$ real matrices $X = \{X_{ij}\}$ such that:

$$0 \leq \sum_{i'=1}^i X_{i'j} \leq 1 \quad \text{for all } 1 \leq i \leq m, 1 \leq j \leq n. \quad (2.10)$$

$$0 \leq \sum_{j'=1}^j X_{ij'} \quad \text{for all } 1 \leq i \leq m, 1 \leq j \leq n. \quad (2.11)$$

Proof. The proof follows the proof of Theorem 2.4.1, with a few differences. The open circuits are no longer restricted to start and end at the bottom of the matrix; they may also start and end at vertices $(i, n + 1)$ and $(i_0, n + 1)$ ($i \neq i_0$) on the right border of $\Gamma_{(m,n)}$, or they may start at the bottom at vertex $(m + 1, j)$ and end on the right at vertex $(i, n + 1)$. Therefore the evenness of corners is not needed here, since unlike in Theorem 2.4.1, there is no analogue of Equation (2.8) that specifies the row sums. With these less restrictive exceptions, the matrices X^- and X^+ will be found in the same way as in the proof of Theorem 2.4.1. \square

2.5. Facet enumerations

In this section, we use the inequality descriptions of the previous section to enumerate the facets in $P(m, n)$ and $P(\lambda, n)$. Note this is not as straightforward as counting the inequalities in the theorems of the previous section, as these inequality descriptions are not minimal.

Theorem 2.5.1. $P(m, n)$ has $3mn - n - 2(m - 1)$ facets.

Proof. We have three defining inequalities in the inequality description of Theorem 2.4.3 for each entry X_{ij} of $X \in P(m, n)$: $0 \leq \sum_{i'=1}^i X_{i'j}$, $\sum_{i=1}^i X_{i'j} \leq 1$, and $0 \leq \sum_{j'=1}^j X_{ij'}$. Therefore there are at most $3mn$ facets, each made by turning one of the inequalities to an equality. We now determine which of these inequalities give *unique* facets.

Notice first that $0 \leq X_{1j}$ (from the column partial sums) is always present. This implies that the partial sums of the first row are all nonnegative, since each entry in the first row must be nonnegative. Thus the inequalities $0 \leq \sum_{j=1}^j X_{1j'}$ for $1 \leq j \leq n$ are all unnecessary; and there are n inequalities of this form.

We have already counted $0 \leq X_{11}$ in the column partial sums. From the partial row sums, we have that $0 \leq X_{21}$. But in the partial column sum we have $0 \leq X_{11} + X_{12}$; this is implied by $0 \leq X_{11}$ and $0 \leq X_{21}$. Similarly, the partial column sums $0 \leq \sum_{i'=1}^i X_{i'1}$ for $2 \leq i \leq m$ are all implied by the partial row sums $0 \leq X_{i'1}$. There are $m - 1$ inequalities of this form.

Note that $\sum_{i'=1}^m X_{i'1} \leq 1$. Furthermore, note that $0 \leq X_{m1}$ from the row partial sums. Therefore we have that $\sum_{i'=1}^{m-1} X_{i'1} \leq 1 - X_{m1} \leq 1$. Similarly, the $m - 1$ inequalities in the form of $\sum_{i'=1}^i X_{i'1} \leq 1$ for $1 \leq i < m$ are all implied by the partial row sums $0 \leq X_{i'1}$.

Therefore we have the number of facets to be at most $3mn - n - 2(m - 1)$. (See Figure 2.9 for an illustration of the discarded inequalities.) We claim this upper bound is the facet count. That is, a facet can be defined as all $X \in P(m, n)$ which satisfy exactly one of the following:

$$r_{ij} = \sum_{j'=1}^j X_{ij'} = 0, \quad 2 \leq i \leq m \text{ and } 1 \leq j \leq n \quad (2.12)$$

$$c_{ij} = \sum_{i'=1}^i X_{i'j} = 0, \quad 1 \leq i \leq m \text{ and } 2 \leq j \leq n \quad (2.13)$$

$$c_{ij} = \sum_{i'=1}^i X_{i'j} = 1, \quad 1 \leq i \leq m \text{ and } 2 \leq j \leq n \quad (2.14)$$

$$r_{11} = c_{11} = X_{11} = 0 \quad (2.15)$$

$$c_{m1} = \sum_{i'=1}^m X_{i'1} = 1. \quad (2.16)$$

Note each equality fixes exactly one entry, thus lowering the dimension by one. Let two generic equalities of the form (2.12)-(2.16) be denoted as $\alpha_{ij} = \gamma$ and $\beta_{de} = \delta$ for $\alpha, \beta \in \{r, c\}$ and $\gamma, \delta \in \{0, 1\}$, where the choice of r or c for each of α and β indicates whether the equality involves a row partial sum r_{ij} or column partial sum c_{ij} , and the indices (i, j) and (d, e) must be in the corresponding ranges indicated by (2.12)-(2.16). To finish the proof, we construct an $m \times n$ sign matrix M , such that M satisfies $\alpha_{ij} = \gamma$ and not $\beta_{de} = \delta$. We work with \hat{M} rather than M itself, recalling the bijection between M and \hat{M} . Recall from Definition 2.2.4, \hat{M} is a graph whose horizontal edges are labeled by the partial row sums of M and whose vertical edges are labeled by the partial column sums of M . Since all of the equalities in (2.12)-(2.16) are given by setting a c_{ij} equal to 0 or 1 or a r_{ij} equal to 0, set the edge label of \hat{M} corresponding to α_{ij} equal to γ and the edge label corresponding to the equality β_{de} equal to $1 - \delta$. Now we transform \hat{M} back to M and if we can fill in the rest of the matrix so it is a sign matrix, the proof will be complete. In the cases below, we construct such a sign matrix M satisfying equality α and not equality β .

Case 1: $\alpha_{ij} = 0$ and $\beta_{de} = 1$. So in \hat{M} , $\beta_{de} = 0$. It suffices to set M equal to the zero matrix.

Case 2: $\alpha_{ij} = 0$ and $\beta_{de} = 0$. So in \hat{M} , $\beta_{de} = 1$. If $i \neq d$ and $j \neq e$, let $M_{de} = 1$ and the rest of the entries equal to zero.

Suppose $\alpha = \beta = c$. If $j \neq e$, let $M_{de} = 1$ and the rest of the entries equal to zero. If $j = e$ and $i < d$, let $M_{de} = 1$ and the rest of the entries equal to zero. If $j = e$ and $i > d$, let $M_{de} = 1$, $M_{d+1,e} = -1$, $M_{d+1,e-1} = 1$, and the rest of the entries equal to zero. (Note $e \geq 2$ since $\beta = c$.)

Suppose $\alpha = \beta = r$. If $i \neq d$, let $M_{de} = 1$ and the rest of the entries equal to zero. If $i = d$ and $j < e$, let $M_{de} = 1$ and the rest of the entries equal to zero. If $i = d$ and $j > e$, let $M_{de} = 1$,

$M_{d,e+1} = -1$, $M_{d-1,e+1} = 1$, and the rest of the entries equal to zero. Note since $\beta = r$, $d \geq 2$, so $d - 1 \geq 1$.

If $\alpha = r$ and $\beta = c$, let $M_{1e} = 1$ and the rest of the entries equal to zero. (Note since $\alpha = r$, $i \geq 2$.)

If $\alpha = c$ and $\beta = r$, let $M_{d1} = 1$ and the rest of the entries equal to zero. (Note since $\alpha = c$, $j \geq 2$.)

Case 3: $\alpha_{ij} = 1$ and $\beta_{de} = 1$. So in \hat{M} , $\beta_{de} = 0$. Note only column partial sums are set equal to 1 in the above list of equalities, so $\alpha = c$ and $\beta = c$. If $j \neq e$, set $M_{ij} = 1$ and the rest of the entries of M equal to zero. If $j = e$ and $i < d$, set $M_{ij} = M_{i+1,j-1} = 1$ and $M_{i+1,j} = -1$ and all other entries equal to zero. Note $j - 1 \geq 1$ since (2.14) requires that $2 \leq j \leq n$. If $j = e$ and $i > d$, set $M_{ij} = 1$ and the rest of the entries of M equal to zero.

Case 4: $\alpha_{ij} = 1$ and $\beta_{de} = 0$. So in \hat{M} , $\beta_{de} = 1$. Note $\alpha = c$, so $j \geq 2$. If $j \neq e$, let $M_{ij} = M_{de} = 1$ and the rest of the entries zero. If $j = e$ and $\beta = c$, let $M_{1j} = 1$ and the rest of the entries equal to zero. If $j = e$ and $\beta = r$, if $i \neq d$, let $M_{ij} = 1$ and $M_{d1} = 1$ (we noted above that $j \geq 2$, so these ones are not in the same column) and the rest of the entries equal to zero. If $j = e$, $\beta = r$, and $i = d$, set $M_{ij} = 1$ and the rest of the entries equal to zero.

Thus we may always complete to a sign matrix. M is constructed to satisfy $\alpha_{ij} = \gamma$ but not $\beta_{ij} = \delta$, thus each of the equalities in (2.12)-(2.16) gives rise to a unique facet. \square

We now state a theorem on the number of facets of $P(\lambda, n)$. We then give simpler formulas as corollaries in the special cases of two-row shapes, rectangles, and hooks.

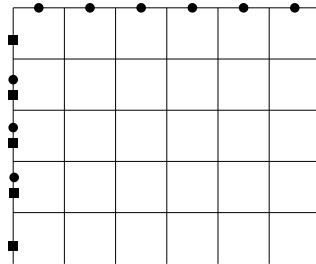


Figure 2.9. $\Gamma_{(m,n)}$ decorated with symbols that represent the inequalities that do not determine facets of $P(m, n)$. Squares represent partial column sums of the form $\sum X_{ij} \leq 1$ and dots represent partial row or column sums of the form $\sum X_{ij} \geq 0$.

Theorem 2.5.2. *The number of facets of $P(\lambda, n)$ is:*

$$3n\lambda_1 - n - 3(\lambda_1 - 1) - (n - 2)(\lambda_1 - \lambda_2 + \lambda_{n-1}) - (k - a_{\lambda_1}) - 2(\lambda_1 - D(\lambda)) - C(\lambda) \quad (2.17)$$

where $D(\lambda)$ is the number of distinct part sizes of λ (each part size counts once, even though there may be multiple parts of a given size), we take $\lambda_i = 0$ if $k < i$, and $C(\lambda)$ equals the following:

$$C(\lambda) = \begin{cases} 2 & \text{if } k = 1, \\ 1 & \text{if } 1 < k < n - 1 \text{ and } \lambda_1 \neq \lambda_2, \\ 0 & \text{if } 1 < k < n - 1 \text{ and } \lambda_1 = \lambda_2, \\ 2 & \text{if } k = n - 1 \text{ and either } \lambda_1 \neq \lambda_2 \text{ or } \lambda = \lambda_1^k, \\ 1 & \text{if } k = n - 1, \lambda_1 = \lambda_2, \text{ and } \lambda \neq \lambda_1^k. \end{cases}$$

Proof. By Theorem 2.5.1, since $P(\lambda, n)$ satisfies all the inequalities satisfied by $P(m, n)$ for $m = \lambda_1$, we have at most $3n\lambda_1 - n - 2(\lambda_1 - 1)$ facets, given by the equalities (2.12)–(2.16). See Figure 2.9.

But note equalities of the form (2.12) with $j = n$ no longer give facets, since by (2.8) the total sum of each matrix row is fixed. There are $\lambda_1 - 1$ such inequalities, so we now have at most $3\lambda_1 n - n - 3(\lambda_1 - 1)$ facets. See Figure 2.10.

To prove our count in (2.17), we determine which of the remaining equalities in (2.12)–(2.16) are unnecessary. We discuss each remaining term of (2.17) below. Let $X \in P(\lambda, n)$.

1. $-(n - 2)(\lambda_1 - \lambda_2 + \lambda_{n-1})$: First, suppose $\lambda_1 \neq \lambda_2$, otherwise $(n - 2)(\lambda_1 - \lambda_2) = 0$. Since $\lambda_1 \neq \lambda_2$, the first row of X sums to 1 and the next $\lambda_1 - \lambda_2 - 1$ rows sum to 0. So the first i rows all together sum to 1 for any $1 \leq i \leq \lambda_1 - \lambda_2$. That is, for any fixed $i \in [1, \lambda_1 - \lambda_2]$, $\sum_{i'=1}^i \sum_{j'=1}^n X_{i'j'} = 1$. Also, by (2.6), $\sum_{i'=1}^i X_{i'j} \geq 0$, and by (2.7), $\sum_{j'=1}^j X_{ij'} \geq 0$. So we have the following sum:

$$1 = \sum_{i'=1}^i \sum_{j'=1}^n X_{i'j'} = \underbrace{\sum_{i'=1}^i \sum_{j'=1}^{j-1} X_{i'j'}}_{\geq 0} + \underbrace{\sum_{j'=j}^n \sum_{i'=1}^i X_{i'j'}}_{\geq 0}.$$

Since we have all positive terms summing to 1, none of these terms may exceed 1. Therefore,

$$\sum_{i'=1}^i X_{i'j} \leq 1 \text{ for all } 1 \leq i \leq \lambda_1 - \lambda_2, 1 \leq j \leq n.$$

Thus the partial sums of the form $\sum_{i'=1}^i X_{i'j} \leq 1$ for $1 \leq i \leq \lambda_1 - \lambda_2$, $1 \leq j \leq n$ are unnecessary. We have already disregarded these inequalities for $j = 1$, $1 \leq i \leq n-1$ in Theorem 2.5.1. Now consider $j = 1$, $i = n$ in Case 4, to count the partial column sums in the n th column in Case 3. Thus, for this term we count the $(n-2)(\lambda_1 - \lambda_2)$ unnecessary inequalities $\sum_{i'=1}^i X_{i'j} \leq 1$ for $1 \leq i \leq \lambda_1 - \lambda_2$, $2 \leq j \leq n-1$.

Now suppose $k = n-1$ so that $\lambda_{n-1} \neq 0$, otherwise $(n-2)\lambda_{n-1} = 0$. Since $\lambda_{n-1} \neq 0$, the last λ_{n-1} rows of X sum to 0. That is, for any fixed $i \in [\lambda_1 - \lambda_{n-1} + 1, \lambda_1]$, $\sum_{i'=i+1}^{\lambda_1} \sum_{j'=1}^n X_{i'j'} = 0$.

Also, by (2.8), $\sum_{i'=1}^{\lambda_1} \sum_{j'=1}^n X_{i'j'} = \sum_{i'=1}^{\lambda_1} a_{\lambda_1-i+1} = k = n-1$, since λ has $n-1$ parts. Also, by

(2.6), $\sum_{i'=1}^i X_{i'j} \leq 0$. So we have the following sum:

$$n-1 = \sum_{j'=1}^n \sum_{i'=1}^{\lambda_1} X_{i'j'} = \underbrace{\sum_{j'=1}^n \sum_{i'=1}^i X_{i'j'}}_{\leq 1} + \underbrace{\sum_{j'=1}^n \sum_{i'=i+1}^{\lambda_1} X_{i'j'}}_{=0}$$

Since we have n terms $\sum_{i'=1}^i X_{i'j'}$ summing to $n-1$, each at most 1, none of these terms may be negative. Therefore, $\sum_{i'=1}^i X_{i'j} \geq 0$ for all $\lambda_1 - \lambda_{n-1} + 1 \leq i \leq \lambda_1$, $1 \leq j \leq n$.

Thus the partial sums of the form $\sum_{i'=1}^i X_{i'j} \geq 0$ for $\lambda_1 - \lambda_{n-1} + 1 \leq i \leq \lambda_1$, $1 \leq j \leq n$ are unnecessary. We have already disregarded these inequalities for $j = 1$, $2 \leq i \leq n$ in Theorem 2.5.1. Now the partial column sums in the n th column will be counted in Case 3. Thus, for this term we count the $(n-2)\lambda_{n-1}$ unnecessary inequalities $\sum_{i'=1}^i X_{i'j} \leq 1$ for $\lambda_1 - \lambda_{n-1} + 1 \leq i \leq \lambda_1$, $2 \leq j \leq n-1$. See Figure 2.10.

2. $-(k - a_{\lambda_1})$: Let $i > 1$. By (2.8), $\sum_{j'=1}^n X_{ij'} = a_{\lambda_1-i+1}$. Now $0 \leq \sum_{i'=1}^{i-1} X_{in}$ and $\sum_{i'=1}^i X_{in} \leq 1$

imply $X_{in} \leq 1$, so we have $\sum_{j'=1}^{n-1} X_{ij'} \geq a_{\lambda_1-i+1} - 1$. This implies the inequality $\sum_{j'=1}^{n-1} X_{ij'} \geq 0$

whenever $a_{\lambda_1-i+1} > 0$. Similarly, $\sum_{j'=1}^{n-z} X_{ij'} \geq a_{\lambda_1-i+1} - z$ for all $1 \leq z \leq a_{\lambda_1-i+1}$ since the last

z entries in that row sum to at most z (since entries can be no more than 1, by the column partial sums). Thus, the a_{λ_1-i+1} inequalities $\sum_{j'=1}^{n-z} X_{ij'} \geq 0$, $1 \leq z \leq a_{\lambda_1-i+1}$, are unnecessary.

By reindexing, this is equivalent to $\sum_{j'=1}^j X_{ij'} \geq 0$, $n - a_{\lambda_1-i+1} \leq j \leq n - 1$.

We already discarded all the row partial sum inequalities in the first row in Theorem 2.5.1, so we do not count those here. Thus a_{λ_1} is not included. So we have $\sum_{i'=1}^{\lambda_1-1} a_{i'}$ unnecessary partial sum inequalities. This equals the total number of parts of λ minus the number of parts with part size λ_1 , that is, $k - a_{\lambda_1}$. See Figure 2.11.

3. $-2(\lambda_1 - D(\lambda))$: Suppose $a_{\lambda_1-i+1} = 0$ so that the total sum of row i of X equals 0. Then the last entry X_{in} may not be greater than 0, since this would contradict $\sum_{j'=1}^{n-1} X_{ij'} \geq 0$. So the

inequality $\sum_{i'=1}^i X_{i'n} \leq 1$ is unnecessary. Also, since the total sum of row i of X equals 0, we

have then $X_{in} = -\sum_{j=1}^{n-1} X_{ij}$. In addition, $\sum_{i'=1}^i X_{i'n} \geq 0$. We substitute the previous equality

into this inequality to obtain $\sum_{i'=1}^{i-1} X_{i'n} - \sum_{j=1}^{n-1} X_{ij} \geq 0$. We know $\sum_{j=1}^{n-1} X_{ij} \geq 0$, so this implies

$$\sum_{i'=1}^{i-1} X_{i'n} \geq 0.$$

So for each $a_{\lambda_1-i+1} = 0$ we have two unnecessary inequalities: $\sum_{i'=1}^i X_{i'n} \leq 1$ and $\sum_{i'=1}^{i-1} X_{i'n} \geq 0$.

The number of row sums equal to zero is given by the number of integers ℓ with $1 \leq \ell \leq \lambda_1$ such that $a_\ell = 0$. This count equals $\lambda_1 - D(\lambda)$, where $D(\lambda)$ equals the number of distinct part sizes of λ . Thus, we have $2(\lambda_1 - D(\lambda))$ unnecessary inequalities. See Figure 2.11.

4. $-C(\lambda)$: We now have a few more border inequalities to discard, depending on λ . We take each case in turn. See Figure 2.12.

- (a) When $\lambda_1 \neq \lambda_2$, we may also discard the inequality $X_{1n} \leq 1$, as this is a partial sum of the form $\sum_{i'=1}^i X_{i'n} \leq 1$ for $1 \leq i \leq \lambda_1 - \lambda_2$, which by reasoning in Case 1 may be discarded. The other inequalities of that form have already been counted in Case 3, thus we have

one additional unnecessary inequality whenever $\lambda_1 \neq \lambda_2$. Note, since $\lambda_2 = 0 \neq \lambda_1$ for $k = 1$, this inequality is also discarded in the case $k = 1$.

- (b) When $k = 1$, since $\sum_{j'=1}^n X_{1j'} = 1$ and $\sum_{j'=1}^n X_{ij'} = 0$ for all $2 \leq i \leq \lambda_1$, we have that the

sum of all the entries in the matrix is 1. This, together with the inequalities $\sum_{i'=1}^{\lambda_1} X_{i'j} \geq 0$,

$2 \leq j \leq n$, implies $\sum_{i'=1}^{\lambda_1} X_{i'1} \leq 1$. So we have one additional unnecessary inequality when $k = 1$.

- (c) When $1 < k = n - 1$, by the reasoning in the $k = n - 1$ case of Case 1 we may discard the inequality $\sum_{i'=1}^{\lambda_1} X_{i'n} \geq 0$. If $k = 1, n = 2$, we may not discard this inequality, since in this case we have already discarded the inequality in (4b).

- (d) Suppose $k = n - 1$ and λ is a rectangle, so $\lambda_{n-1} = \lambda_1$. In this case, we may also discard the inequality $X_{11} \geq 0$; this is a partial sum of the form $\sum_{i'=1}^i X_{i'1} \geq 0$ for $\lambda_1 - \lambda_{n-1} + 1 \leq i \leq \lambda_1$ which by the reasoning in Case 1 may be discarded. The other inequalities of that form have already been counted in Case 3, thus we have one additional unnecessary inequality whenever $\lambda_1 = \lambda_1^{n-1}$ and $k > 1$. If $k = 1, n = 2$, we may not discard this inequality, since we have already discarded the inequality in (4a).

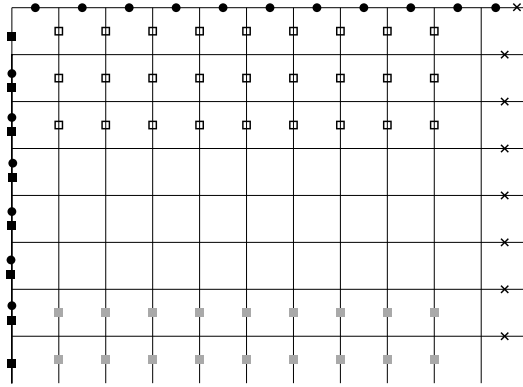


Figure 2.10. $\Gamma_{(\lambda_1, n)}$ decorated with symbols that represent inequalities that do not determine facets of $P(\lambda, n)$. Squares represent partial column sums of the form $\sum X_{ij} \leq 1$ and dots represent partial row or column sums of the form $\sum X_{ij} \geq 0$. The filled-in shapes represent inequalities that were already removed in the facet proof for $P(m, n)$. The crosses represent the fixed row sums in $P(\lambda, n)$. The open squares and gray squares represent inequalities that are removed in Case 1.

Thus the total number of facets is at most (2.17). We claim this upper bound is the facet count. That is, a facet can be defined as all $X \in P(\lambda, n)$ which satisfy exactly one of the following:

$$r_{ij} = \sum_{j'=1}^j X_{ij'} = 0, \quad 2 \leq i \leq \lambda_1 \text{ and } 1 \leq j \leq n - a_{\lambda_1-i+1} - 1 \quad (2.18)$$

$$c_{ij} = \sum_{i'=1}^i X_{i'j} = 0, \quad 1 \leq i \leq \lambda_1 \text{ and } 2 \leq j \leq n - 1 \quad (2.19)$$

$$c_{in} = \sum_{i'=1}^i X_{i'n} = 0, \quad (i = \lambda_1 \text{ and } k < n - 1) \text{ or } (1 \leq i \leq \lambda_1 - 1 \text{ and } a_{\lambda_1-i} > 0) \quad (2.20)$$

$$c_{ij} = \sum_{i'=1}^i X_{i'j} = 1, \quad \lambda_1 - \lambda_2 + 1 \leq i \leq \lambda_1 \text{ and } 2 \leq j \leq n - 1 \quad (2.21)$$

$$c_{in} = \sum_{i'=1}^i X_{i'n} = 1, \quad \lambda_1 - \lambda_2 + 1 \leq i \leq \lambda_1 \text{ and } a_{\lambda_1-i+1} > 0 \quad (2.22)$$

$$r_{11} = c_{11} = X_{11} = 0 \quad \text{if } \lambda = \lambda_1^{n-1} \text{ and } k > 1 \quad (2.23)$$

$$c_{\lambda_1 1} = \sum_{i'=1}^{\lambda_1} X_{i'1} = 1 \quad \text{if } k = 1. \quad (2.24)$$

Note each equality fixes exactly one matrix entry, lowering the dimension by one. By an argument similar to that given in Theorem 2.5.1, given any two equalities above, we may construct a sign matrix in $M(\lambda, n)$ that satisfies one but not the other. \square



Figure 2.11. Examples of portions of $\Gamma_{(\lambda_1, n)}$ that represent inequalities removed based on the fixed row sums. The left diagram shows removed inequalities discussed in Case 2, $a_{\lambda_1-i+1} > 0$. The right diagram shows removed inequalities discussed in Case 3, $a_{\lambda_1-i+1} = 0$.

Corollary 2.5.3. *The number of facets of $P([\lambda_1, \lambda_2], n)$ when $\lambda_1 \neq \lambda_2$ is as follows:*

- $3n\lambda_1 - n - 5(\lambda_1 - 1) - (n - 2)(\lambda_1 - \lambda_2)$, when $n > 3$;
- $3n\lambda_1 - n - 5(\lambda_1 - 1) - (n - 2)\lambda_2 - 1$, when $n = 3$.

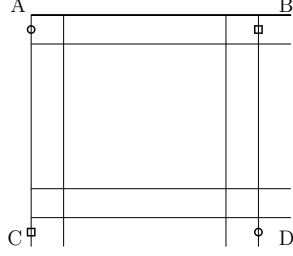


Figure 2.12. $\Gamma_{(\lambda_1, n)}$ decorated with symbols that represent inequalities removed in Case 4. A is discussed in (4d), B is discussed in (4a), C is discussed in (4b), and D is discussed in (4c).

Proof. Suppose $\lambda_1 \neq \lambda_2$ and $n > 3$. Then $a_{\lambda_1} = 1$, $D(\lambda) = 2$, and $C(\lambda) = 1$ from 4a. Thus since $k = 2$, the formula of Theorem 2.5.2 specializes to $3n\lambda_1 - n - 3(\lambda_1 - 1) - (n - 2)(\lambda_1 - \lambda_2) - (2 - 1) - 2(\lambda_1 - 2) - 1$, which reduces to the above formula. Now suppose $\lambda_1 \neq \lambda_2$ and $n = 3$. In this case $\lambda_{n-1} = \lambda_2$ and $C(\lambda) = 2$ but the rest of the values remain the same. Thus, the formula of Theorem 2.5.2 specializes to the above. \square

In the above corollary, we required $\lambda_1 \neq \lambda_2$. The case $\lambda = [\lambda_1, \lambda_1]$ is a special case of the next corollary, which enumerates the facets when λ is a rectangle.

Corollary 2.5.4. *The number of facets of $P(\lambda_1^k, n)$ is as follows:*

- 0, when $k = n$;
- $2n\lambda_1 - n - 3(\lambda_1 - 1)$, when $k = n - 1$;
- $3n\lambda_1 - n - 5(\lambda_1 - 1)$, when $1 < k < n - 1$;
- $2n\lambda_1 - n - 3(\lambda_1 - 1)$, when $k = 1$.

Proof. Suppose $k = n$. By Proposition 2.2.2, since $k = n$ we have that the dimension of $P(\lambda_1^k) = (\lambda_1 - \lambda_n)(n - 1) = (\lambda_1 - \lambda_1)(n - 1) = 0$. Since the polytope is zero dimensional, there are no facets.

Suppose $k = n - 1$. We then have the following: $\lambda_1 = \lambda_2$, $\lambda_{n-1} = \lambda_1$, $a_{\lambda_1} = k = n - 1$, $D(\lambda) = 1$, and $C(\lambda) = 2$. Therefore by Theorem 2.5.2 the number of facets is $3n\lambda_1 - n - 3(\lambda_1 - 1) - (n - 1)(0 + \lambda_1) - 0 - 2(\lambda_1 - 1) - 2$ which reduces to the formula above.

For $1 < k < n - 1$, by Theorem 2.5.2 the number of facets is $3n\lambda_1 - n - 3(\lambda_1 - 1) - (n - 2)(\lambda_1 - \lambda_2 + \lambda_{n-1}) - (k - a_{\lambda_1}) - 2(\lambda_1 - D(\lambda)) - C(\lambda)$. Since $\lambda_1 = \lambda_2$ and $\lambda_{n-1} = 0$, the 4th term

equals 0. The 5th term equals 0 since $a_{\lambda_1} = k$. Note $D(\lambda_1^k) = 1$, so the 6th term equals $2(\lambda_1 - 1)$. $C(\lambda) = 0$, so the resulting count follows.

When $k = 1$, by Theorem 2.5.2 the number of facets is $3n\lambda_1 - n - 3(\lambda_1 - 1) - (n - 2)(\lambda_1 - \lambda_2 + \lambda_{n-1}) - (k - a_{\lambda_1}) - 2(\lambda_1 - D(\lambda)) - C(\lambda) = 3n\lambda_1 - n - 3(\lambda_1 - 1) - (n - 2)(\lambda_1 - 0 + 0) - (1 - 1) - 2(\lambda_1 - 1) - 2$, since $a_{\lambda_1} = D(\lambda) = 1$ and $\lambda_2 = 0$. The resulting count follows. \square

Finally, we have the following corollary in the case that λ is hook-shaped.

Corollary 2.5.5. *The number of facets of $P([\lambda_1, 1^{k-1}], n)$ is as follows:*

- $2n(\lambda_1 - 1) - n - 3(\lambda_1 - 2)$, when $k = n$;
- $2n\lambda_1 - 2n - 3(\lambda_1 - 1) + 4$, when $k = n - 1$;
- $2n\lambda_1 - 3(\lambda_1 - 1) - k + 2$, when $1 < k < n - 1$.

Proof. When $k = n$, the first column of the tableau corresponding to any sign matrix in the polytope is fixed as $1, 2, \dots, n$, so this reduces to the case of rectangles of one row, that is, shape $[\lambda_1 - 1]$. So by Corollary 2.5.4, we have $2n(\lambda_1 - 1) - n - 3((\lambda_1 - 1) - 1) = 2n\lambda_1 - 3n - 3\lambda_1 + 6$ facets.

When $k = n - 1$, in formula in Theorem 2.5.2 we have that $\lambda_2 = 1$, $a_{\lambda_1} = 1$, $D(\lambda) = 2$ and $C(\lambda) = 2$. Therefore, by Theorem 2.5.2 the number of facets is $3n\lambda_1 - n - 3(\lambda_1 - 1) - (n - 2)(\lambda_1 - 1 + 1) - (n - 1 - 1) - 2(\lambda_1 - 2) - 2$, which when simplified yields the desired result.

When $1 < k < n - 1$, $a_{\lambda_1} = 1$, $D(\lambda) = 2$, and $\lambda_1 \neq \lambda_2$ so $C(\lambda) = 1$. So by Theorem 2.5.2 the number of facets is $3n\lambda_1 - n - 3(\lambda_1 - 1) - (n - 2)(\lambda_1 - 1) - (k - 1) - 2(\lambda_1 - 2) - 1$, which when simplified yields the desired result. \square

2.6. Face lattice descriptions

In this section, we determine the face lattice of the $P(m, n)$ and $P(\lambda, n)$ polytope families. We also show that given any two faces, we may determine the smallest dimensional face in which they are contained. The ideas for proving the face lattice were inspired by [31] and [1].

Recall the definition of face lattice from Definition 1.3.25.

Definition 2.6.1. We define the *complete partial sum graph* denoted $\bar{\Gamma}_{(m,n)}$ as the following labeling of the graph $\Gamma_{(m,n)}$. The horizontal edges are labeled with $\{0, \star\}$, while the vertical edges are labeled $\{0, 1, \{0, 1\}\}$. An example is shown for $P(3, 5)$ in Figure 2.13.

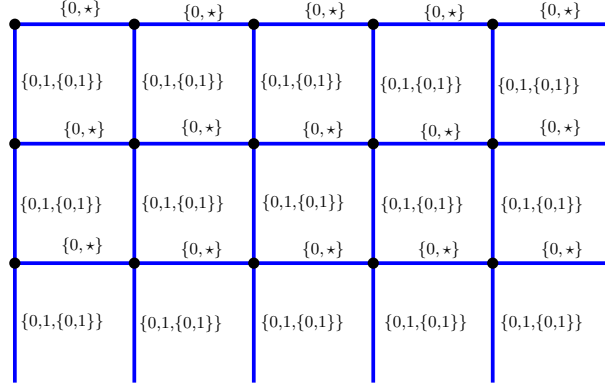


Figure 2.13. The complete partial sum graph $\bar{\Gamma}_{(3,5)}$.

Definition 2.6.2. A *0-dimensional component* of $\bar{\Gamma}_{(m,n)}$ is a labeling of $\Gamma_{(m,n)}$ such that the edge labels are one element subsets of the edge labels of $\bar{\Gamma}_{(m,n)}$ and such that the edge labels come from the partial sums of a sign matrix as follows: Let the edges be labeled as in \hat{M} for some $m \times n$ sign matrix M , with the exception that horizontal edges labeled by nonzero numbers in \hat{M} are now labeled as \star . For any $m \times n$ sign matrix M , let $g(M)$ be the 0-dimensional component of $\bar{\Gamma}_{(m,n)}$ associated to M .

Lemma 2.6.3. *The set of 0-dimensional components of $\bar{\Gamma}_{(m,n)}$ are in bijection with $m \times n$ sign matrices.*

Proof. Recall we may recover a sign matrix M from its column partial sums. Thus, even though we are not keeping the exact values of the row partial sums, we still have enough information to recover a sign matrix M from $g(M)$. Thus, given sign matrices $M_1 \neq M_2$, $g(M_1) \neq g(M_2)$. \square

Definition 2.6.4. Let δ and δ' be labelings of $\Gamma_{(m,n)}$ such that the edge labels are subsets of the corresponding edge label sets in $\bar{\Gamma}_{(m,n)}$. Define the *union* $\delta \cup \delta'$ as the labeling of $\Gamma_{(m,n)}$ such that each edge is labeled by the union of the corresponding labels on δ and δ' , where we consider $0 \cup \star = \star$. Define the *intersection* $\delta \cap \delta'$ to be a labeling of $\Gamma_{(m,n)}$ such that each edge is labeled

by the intersection of the corresponding labels on δ and δ' , where we consider $0 \cap \star = 0$. So the vertical edges will have labels of $\emptyset, 0, 1$, or $\{0, 1\}$ and the horizontal edges will have labels of 0 or \star . In our figures, vertical edges labeled $\{0, 1\}$ and horizontal edges labeled \star will be darkened (blue).

Definition 2.6.5. Let δ be a labeling of $\Gamma_{(m,n)}$ such that the edge labels are subsets of the corresponding edge label sets in $\bar{\Gamma}_{(m,n)}$.

1. δ is a *component* of $\bar{\Gamma}_{(m,n)}$ if it is either the empty labeling of $\Gamma_{(m,n)}$ (we call this the empty component) or if it can be presented as the union of any set of 0-dimensional components.
2. For two components δ and δ' of $\bar{\Gamma}_{(m,n)}$, we say δ is a *component of* δ' if the edge labels of δ are each a subset of the corresponding edge labels of δ' , where we consider 0 to be a subset of \star .

Remark 2.6.6. Note if δ and δ' are components of $\bar{\Gamma}_{(m,n)}$, $\delta \cup \delta'$ is also a component. This is because each of δ and δ' is a union of 0-dimensional components, so $\delta \cup \delta'$ is as well.

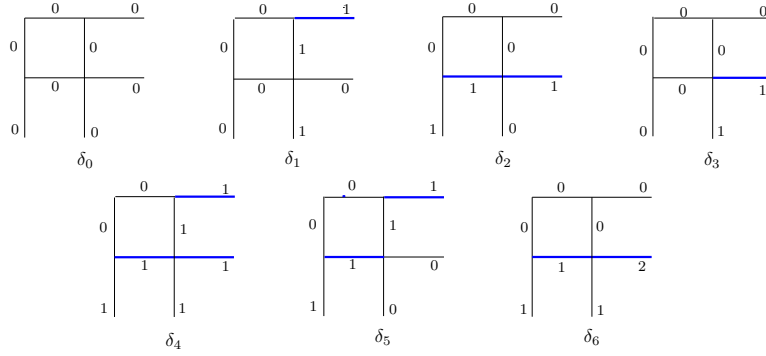
Next, we define a partial order on components of $\bar{\Gamma}_{(m,n)}$.

Definition 2.6.7. Define a partial order $\Lambda_{(m,n)}$ on components of $\bar{\Gamma}_{(m,n)}$ by containment. That is, $\delta \leq \delta'$ in $\Lambda_{(m,n)}$ if and only if δ is a component of δ' . Say δ' *covers* δ , denoted $\delta < \delta'$, if δ is contained in δ' and there is no component δ'' of $\Lambda_{(m,n)}$ such that $\delta < \delta'' < \delta'$.

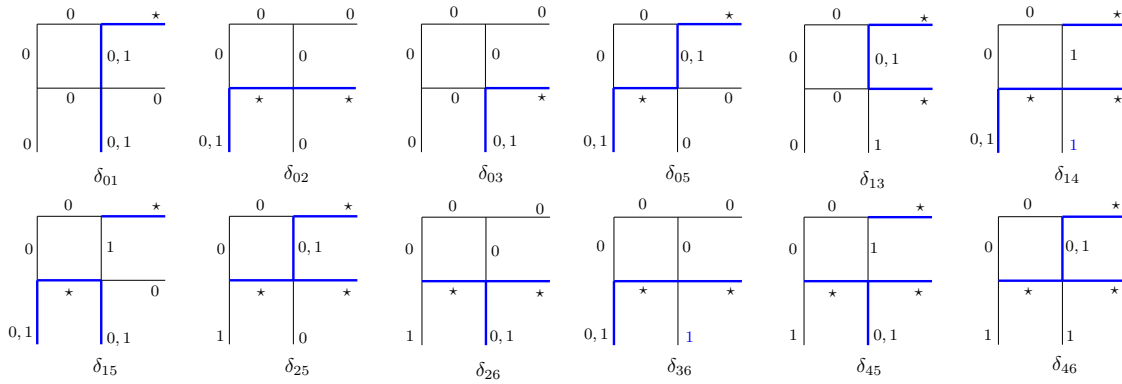
Remark 2.6.8. For components δ and δ' of $\bar{\Gamma}_{(m,n)}$, we may define $\delta \vee \delta' = \delta \cup \delta'$. By Remark 2.6.6, this is itself a component of $\bar{\Gamma}_{(m,n)}$. Also, it is the smallest component containing both δ and δ' as subcomponents, so this is the *join operator* of $\Lambda_{(m,n)}$. Theorems 2.6.14 and 2.6.15 show that $\Lambda_{(m,n)}$ is the face lattice of $P(m, n)$, thus there also exists a well-defined meet operator, since $\Lambda_{(m,n)}$ is a lattice. The meet $\delta \wedge \delta'$ will be the maximal component contained in the intersection $\delta \cap \delta'$; note this could be the empty component.

Remark 2.6.9. Note the maximal component of $\Lambda_{(m,n)}$ is the union of all 0-dimensional components. Thus, it has labels $\{0, 1\}$ on the vertical edges of $\Gamma_{(m,n)}$ and \star on the horizontal edges.

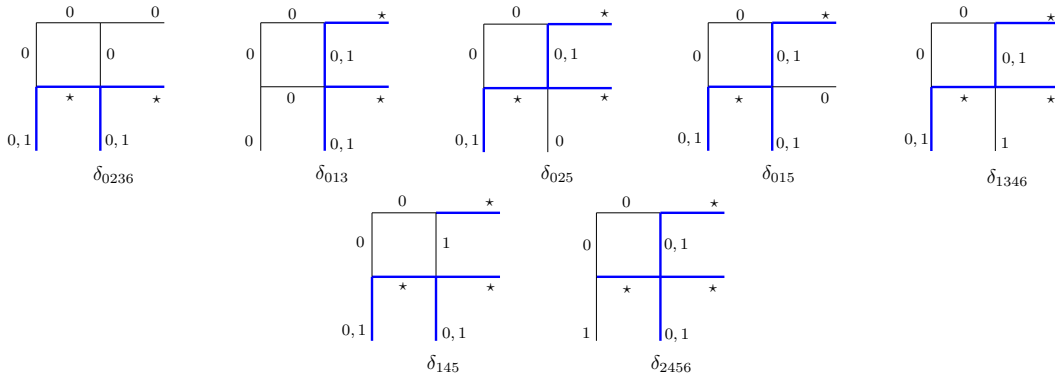
Example 2.6.10. We show examples of several of the above definitions using Figure 2.14 (which by the upcoming Theorems 2.6.14 and 2.6.15 is the face lattice of one of the 3-dimensional faces of $P(2, 2)$).



Seven of the ten $\bar{\Gamma}_{(2,2)}$ 0-dimensional components



Twelve of the 23 $\bar{\Gamma}_{(2,2)}$ 1-dimensional components



Seven of the 21 $\bar{\Gamma}_{(2,2)}$ 2-dimensional components



One of the eight 3-dimensional components

The complete partial sum graph $\bar{\Gamma}_{(2,2)}$

Figure 2.14. A set of components of $\bar{\Gamma}_{(2,2)}$.

- i). We first exhibit a component as a union of 0-dimensional components: $\delta_{025} = \delta_0 \cup \delta_2 \cup \delta_5$.
- ii). We now show how the union of two components can contain more 0-dimensional components than are contained in the original component: $\delta_{14} \cup \delta_{46} = \delta_{0123456}$. Note $\delta_{0123456}$ is the join.
- iii). Next we intersect two components: $\delta_{2456} \cap \delta_{015} = \delta_5$. Note δ_5 is the meet.
- iv). To illustrate containment of components, note the 1-dimensional components δ_{01} , δ_{03} , and δ_{13} are all contained in the 2-dimensional component δ_{013} .

Definition 2.6.11. Given a component $\delta \in \Lambda_{(m,n)}$, consider the planar graph G composed of the darkened edges of δ ; we regard any darkened edges on the right and bottom as meeting at a point in the exterior region. We say a *region* of δ is defined as a planar region of G , excluding the exterior region. Let $\mathcal{R}(\delta)$ denote the number of regions of δ . For consistency we set $\mathcal{R}(\emptyset) = -1$.

See Figure 2.15 for an example of this definition and see Definition 1.6.1 for the definition of a planar graph.

We now state a lemma which shows that moving up in the partial order $\Lambda_{(m,n)}$ increases the number of regions. This lemma is used in the proof of Theorem 2.6.15.

Lemma 2.6.12. *Suppose a component $\delta \in \Lambda_{(m,n)}$ has $\mathcal{R}(\delta) = \omega$. If $\delta \triangleleft \delta'$ then $\mathcal{R}(\delta') \geq \omega + 1$.*

Proof. By convention, the empty component has $\mathcal{R}(\emptyset) = -1$. If λ is a 0-dimensional component, $\mathcal{R}(\lambda) = 0$, as there are no regions in a 0-dimensional component. Suppose a component $\delta \in \Lambda_{(m,n)}$ has $\mathcal{R}(\delta) = \omega$. We wish to show if $\delta \triangleleft \delta'$ then $\mathcal{R}(\delta') \geq \omega + 1$. $\delta \triangleleft \delta'$ implies that the labels of each edge of δ are subsets of the labels of each edge of δ' . Thus all the 0-dimensional components contained in δ are also contained in δ' . δ' must contain at least one more 0-dimensional component than δ , otherwise δ' would equal δ . This 0-dimensional δ' component differs from any other 0-dimensional component in δ by at least one circuit of differing partial sums: consider a 0-dimensional component in δ' that has a partial column sum that differs from the corresponding partial sum in any 0-dimensional component in δ . By Equation (2.9), at least one adjacent row or column partial sum of δ' must also differ from the corresponding partial sum in δ . Thus, δ' has at least one new open or closed circuit of darkened edges, creating at least one new region. So $\mathcal{R}(\delta') \geq \omega + 1$. \square

We now define a map, which we show in Theorem 2.6.14 gives a bijection between faces of $P(m, n)$ and components of $\bar{\Gamma}_{(m, n)}$.

Definition 2.6.13. Given a collection of sign matrices $\mathcal{M} = \{M_1, M_2, \dots, M_q\}$, we define the map $g(\mathcal{M}) = \bigcup_{i=1}^q g(M_i)$.

Theorem 2.6.14. Let F be a face of $P(m, n)$ and $\mathcal{M}(F)$ equal to the set of sign matrices that are vertices of F . The map $\psi : F \mapsto g(\mathcal{M}(F))$ is a bijection between faces of $P(m, n)$ and components of $\bar{\Gamma}_{(m, n)}$.

Proof. Let F be a face of $P(m, n)$. Then $g(\mathcal{M}(F))$ is a component of $\bar{\Gamma}_{(m, n)}$ since $g(\mathcal{M}(F)) = \bigcup_{i=1}^q g(M_i)$ is a union of 0-dimensional components. We now construct the inverse of ψ , call it φ . Given a component ν of $\bar{\Gamma}_{(m, n)}$, let $\varphi(\nu)$ be the face that results as the intersection of the facets corresponding to the not darkened edges of ν .

We wish to show $\psi(\varphi(\nu)) = \nu$. First, we show $\nu \subseteq \psi(\varphi(\nu))$. Let M be a sign matrix such that $g(M)$ is a 0-dimensional component of ν . M is in the intersection of the facets that yields $\varphi(\nu)$, since otherwise $g(M)$ would not be a 0-dimensional component of ν . Thus $g(M)$ is in $\psi(\varphi(\nu))$ as well. So $\nu \subseteq \psi(\varphi(\nu))$, which means the edge labels of ν must be subsets of the edge labels of $\psi(\varphi(\nu))$.

Next, we show $\nu = \psi(\varphi(\nu))$. Suppose not. Then there exists some edge e of $\Gamma_{(m, n)}$ whose label in $\psi(\varphi(\nu))$ strictly contains the label of e in ν . Suppose e is a horizontal edge, then the label of e in ν is 0 and the label of e in $\psi(\varphi(\nu))$ is \star . Then the facet corresponding to the label 0 on e would have been one of the facets intersected to get $\varphi(\nu)$. Therefore the matrix partial row sum corresponding to edge e would be fixed as 0 in each sign matrix in $\varphi(\nu)$. So in the union $\psi(\varphi(\nu))$, this edge label would be the union of the edge labels of all the sign matrices in $\varphi(\nu)$, and this union would be 0. This is a contradiction. Now suppose e is a vertical edge. Then the label of e in ν is 0 or 1 and the label of e in $\psi(\varphi(\nu))$ is $\{0, 1\}$. Let γ denote the label of e in ν . As in the previous case, the facet corresponding to the label γ on e would have been one of the facets intersected to get $\varphi(\nu)$. Therefore the matrix partial column sum corresponding to edge e would be fixed as γ in each sign matrix in $\varphi(\nu)$. So in the union $\psi(\varphi(\nu))$, that edge label would be the union of the edge labels of all the sign matrices in $\varphi(\nu)$, and this union would be γ . This is a contradiction. Thus $\nu = \psi(\varphi(\nu))$. □

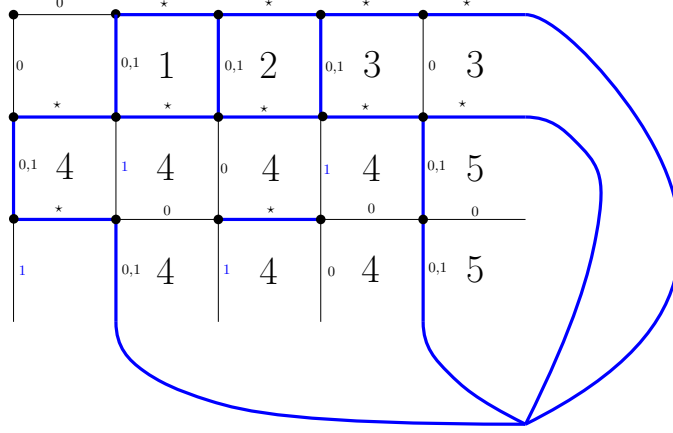


Figure 2.15. A dimension 5 face of $P(3,5)$, where the five regions are numbered.

Theorem 2.6.15. *The map $\psi: \text{Faces of } P(m,n) \rightarrow \text{Components of } \bar{\Gamma}_{(m,n)}$ is a poset isomorphism. Moreover, we have*

$$\dim F = \dim \psi(F)$$

for every face F in $P(m,n)$.

Proof. Let F_1 and F_2 be faces of $P(m,n)$ such that $F_1 \subseteq F_2$. Then F_1 is an intersection of F_2 and some facet hyperplanes. In other words, F_1 is obtained from F_2 by setting one of the inequalities in Theorem 2.4.3 to an equality. We have that $\psi(F_1)$ is obtained from $\psi(F_2)$ by changing at least one darkened edge to a non-darkened edge. Therefore we have $\psi(F_1) \subseteq \psi(F_2)$.

Conversely, suppose that $\psi(F_1) \subseteq \psi(F_2)$. Recall the inverse of ψ is φ , where for any component ν of $\Gamma_{(m,n)}$, $\varphi(\nu)$ is the face of $P(m,n)$ that results as the intersection of the facets corresponding to the not darkened edges of ν . Now if $\psi(F_1) \subseteq \psi(F_2)$, the darkened edges of $\psi(F_1)$ are a subset of the darkened edges of $\psi(F_2)$, so the not darkened edges of $\psi(F_2)$ are a subset of the not darkened edges of $\psi(F_1)$. So $\varphi(\psi(F_1))$ is an intersection of the facets intersected in $\varphi(\psi(F_2))$ and some additional facets (if $F_1 \neq F_2$). Thus $F_1 = \varphi(\psi(F_1)) \subseteq \varphi(\psi(F_2)) = F_2$.

Now, we prove the dimension claim. Recall that $\dim(P(m,n)) = mn$. Since ψ is a poset isomorphism, ψ maps a maximal chain of faces $F_0 \subset F_1 \subset \dots \subset F_{mn}$ to the maximal chain $\psi(F_0) \subset \psi(F_1) \subset \dots \subset \psi(F_{mn})$ in the components of $\bar{\Gamma}_{(m,n)}$. We know that the maximal component

of $\Lambda_{(m,n)}$ has mn regions, thus the result follows by Lemma 2.6.12 and by noting $\nu \subsetneq \nu'$ implies $\dim \nu < \dim \nu'$ for every $\nu, \nu' \in$ the components of $\bar{\Gamma}_{(m,n)}$. \square

We now discuss the face lattice of $P(\lambda, n)$. The main result is restated in this new setting, but since most of the definitions and proofs are exactly analogous, we only note where additional notation or arguments are needed.

Definition 2.6.16. Define the *shape-complete partial sum graph* denoted $\bar{\Gamma}_{(\lambda,n)}$ as the following labeling of the graph $\Gamma_{(\lambda_1,n)}$. The vertical edges are labeled $\{0, 1, \{0, 1\}\}$ as before. The horizontal edges are labeled with the fixed row sum $\{0, \star\}$, except the last horizontal edge in row i is labeled with a_{λ_1-i+1} . An example is shown in Figure 2.16.

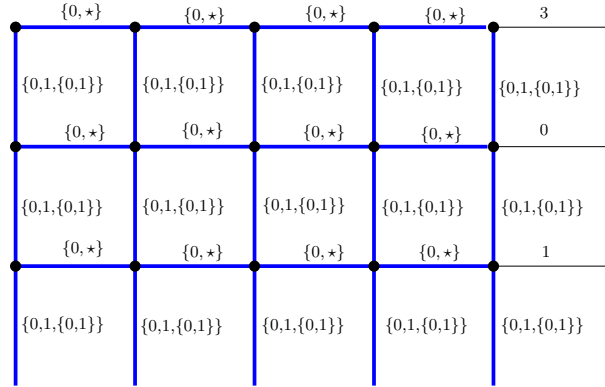


Figure 2.16. The shape-complete partial sum graph of $P([3, 3, 3, 1], 5)$.

Remark 2.6.17. 0-dimensional components, components, containment of components, and regions are defined analogously. Let $\Lambda_{(\lambda,n)}$ denote the partial order on components of $\bar{\Gamma}_{(\lambda,n)}$ by containment.

See Figure 2.17 for an example of a component of $\Lambda_{(\lambda,n)}$.

Remark 2.6.18. Note the maximal component of $\Lambda_{(\lambda,n)}$ is the union of all 0-dimensional components. Thus, it has labels $\{0, 1\}$ on the vertical edges of $\Gamma_{(\lambda_1,n)}$ and \star on the horizontal edges, but with the fixed row sums in the n th column.

Theorem 2.6.19. Let F be a face of $P(\lambda, n)$ and $\mathcal{M}(F)$ equal to the set of sign matrices that are vertices of F . The map $\psi(\mathcal{M}(F))$ is a bijection between faces of $P(\lambda, n)$ and components of $\bar{\Gamma}_{(\lambda,n)}$. Moreover, ψ is a poset isomorphism, and the dimension of F is equal to the dimension of $\psi(F)$.

Proof. The proof is analogous to the proofs of Theorems 2.6.14 and 2.6.15; we need only check that the dimension of the maximal component of $\Lambda_{(\lambda,n)}$ matches the dimension of $P(\lambda,n)$. Recall the dimension of $P(\lambda,n)$ equals $\lambda_1(n-1)$ when $1 \leq k < n$, and $(\lambda_1 - \lambda_n)(n-1)$ when $k = n$. Note that when $1 \leq k < n$, there are $\lambda_1(n-1)$ regions in the maximal component of $\Lambda_{(\lambda,n)}$. When $k = n$ the column partial sums in the last λ_n rows of $\Gamma_{\lambda,n}$ are all fixed to be one, due to the first λ_n columns of the tableau being $1, \dots, n$. Thus there will be no darkened vertical edges in the bottom λ_n rows. This means that there are no open regions in these rows, so there will be $(\lambda_1 - \lambda_n)(n-1)$ regions in the maximal component of $\Lambda_{(\lambda,n)}$. \square

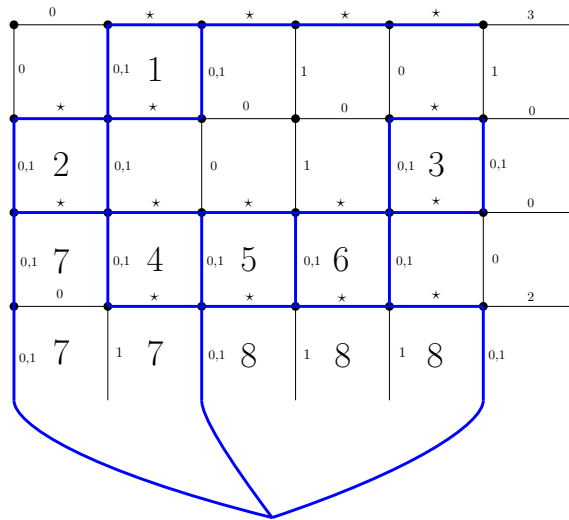


Figure 2.17. An 8-dimensional component of $P([4, 4, 4, 1, 1], 6)$.

2.7. Connections and related polytopes

In this section, we describe connections between sign matrix polytopes and related polytopes. First we describe how $P(\lambda,n)$ and $P(m,n)$ are related.

Lemma 2.7.1. *Suppose $\lambda_1 \leq m$. Then $P(\lambda,n)$ is the intersection of a $\lambda_1(n-1)$ -dimensional subspace of \mathbb{R}^{mn} and $P(m,n)$.*

Proof. The only difference between the inequality descriptions in Theorem 2.4.1 and Theorem 2.4.3 is (2.8), which fixes the row total sums in $P(\lambda,n)$. So $P(\lambda,n)$ is the intersection of $P(m,n)$ and the subspace defined by (2.8). \square

See Figure 2.18 for an example.

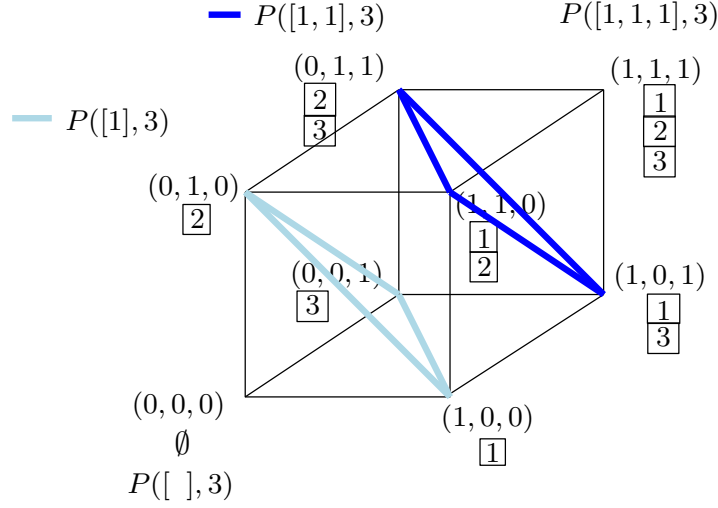


Figure 2.18. The cube above is $P(1,3)$; the $P(\lambda,3)$ polytopes for each partition shape λ in a 1×3 box are also indicated. $P([\],3)$ and $P([1,1,1],3)$ are each a single point, while $P([1],3)$ and $P([1,1],3)$ are the indicated triangles cutting through $P(1,3)$.

The following lemma is implicit in Aval’s paper on sign matrices. Recall from Definition 1.3.39 that $A(n)$ denotes the set of $n \times n$ alternating sign matrices.

Lemma 2.7.2 ([2]). *$A(n)$ is the set of sign matrices $M = (M_{ij})$ in $M([n, n - 1, \dots, 2, 1], n)$ satisfying the additional requirement:*

$$\sum_{j'=1}^j M_{ij'} \in \{0, 1\} \text{ for all } i, j. \tag{2.25}$$

Proof. Let $M \in A(n)$. Then the nonzero entries of M alternate between 1 and -1 across any row or column. The first nonzero entry in a row or column must be a 1, since otherwise that row or column would not sum to 1. Thus (2.1) and (2.2) from Definition 2.1.3 of a sign matrix and (2.25) above are satisfied. Also in an alternating sign matrix, all of the total row sums are 1. Recall from (2.3) that the row sums of a sign matrix equal a_{λ_1-i+1} , so since each row sum of M is 1, M must be in $M([n, n - 1, \dots, 2, 1], n)$.

Now let $M \in M([n, n - 1, \dots, 2, 1], n)$ satisfy (2.25). M is an $n \times n$ matrix whose rows each sum to 1 since $M \in M([n, n - 1, \dots, 2, 1], n)$. By (2.1) and the fact that the sum of all the matrix

entries is n , we have that the columns must each sum to 1. Then (2.1) and (2.25) imply that the nonzero entries of M alternate in sign along each row and column. \square

Remark 2.7.3. It is well-known (see e.g. [23]) that alternating sign matrices are in bijection with *monotone triangles*, which are equivalent to semistandard Young tableau of staircase shape with first column $[1, 2, \dots, n]$ and such that each northeast to southwest diagonal is strictly increasing. This bijection is a specialization of the bijection of Theorem 2.1.5.

Recall from Definition 1.3.41 that ASM_n denotes the n th alternating sign matrix polytope. We see the connection between $P(\lambda, n)$ and ASM_n in the following theorem.

Lemma 2.7.4. $P([n, n-1, \dots, 2, 1], n)$ contains ASM_n .

Proof. Lemma 2.7.2 gives that the set of $n \times n$ alternating sign matrices is a subset of $M([n, n-1, \dots, 2, 1], n)$. So the convex hull of $n \times n$ alternating sign matrices will be contained in the convex hull of $M([n, n-1, \dots, 2, 1], n)$, which is $P([n, n-1, \dots, 2, 1], n)$. \square

Recall from Remark 1.3.38 that the Birkhoff polytope contains no lattice points except the permutation matrices, which are its vertices. We show something similar happens in the case of sign matrices and alternating sign matrices.

Theorem 2.7.5. *There are no lattice points in $P(m, n)$, $P(\lambda, n)$, or ASM_n other than the matrices used to construct them.*

Proof. Let M be an integer-valued matrix inside the polytope $P(m, n)$. Then M fits the inequality description of $P(m, n)$. From the inequalities, all partial column sums are either 0 or 1, thus the entries of M must be in $\{-1, 0, 1\}$. Also, all partial row sums are nonnegative, so M satisfies the definition of an $m \times n$ sign matrix.

By Lemma 2.7.1, $P(\lambda, n)$ is contained in $P(\lambda_1, n)$. By Lemma 2.7.4, ASM_n is contained in $P([n, n-1, \dots, 2, 1], n)$ which by Theorem 2.7.1 is contained in $P(n, n)$. Thus, the results follow. \square

2.8. $P(v, \lambda, n)$ and transportation polytopes

Thus far in this paper, we have defined and studied the sign matrix polytope $P(m, n)$ and the polytope $P(\lambda, n)$ whose vertices are the sign matrices with row sums determined by λ . We may

furthermore restrict to sign matrices with prescribed column sums; we define this polytope below, calling it $P(v, \lambda, n)$. We show in Theorem 2.8.11 that the nonnegative part of this polytope is a transportation polytope.

Definition 2.8.1. Let λ be a partition and v a vector of length k with strictly increasing entries at most n . Let $SSYT(v, \lambda, n)$ denote the set of semistandard Young tableaux of shape λ with entries at most n and first column v .

For example, the tableau of Figure 1.21 is in $SSYT((1, 2, 3, 6), [6, 3, 3, 1], n)$ for any $n \geq 7$.

Remark 2.8.2. We do not know an enumeration for $SSYT(v, \lambda, n)$, although the numbers we have calculated look fairly nice.

Definition 2.8.3. Fix λ and $n \in \mathbb{N}$ and v a vector of length k with strictly increasing entries at most n . Let $M(v, \lambda, n)$ be the set of $M \in M(\lambda, n)$ such that:

$$\sum_{i=1}^{\lambda_1} M_{ij} = 1, \quad \text{if } j \in v \text{ and } 0 \text{ otherwise.} \quad (2.26)$$

Theorem 2.8.4. $M(v, \lambda, n)$ is in explicit bijection with $SSYT(v, \lambda, n)$.

Proof. We know that $M(\lambda, n)$ is in bijection with $SSYT(\lambda, n)$ from Theorem 2.1.5. So we only need to check (2.26). Consider $M \in M(v, \lambda, n)$ and follow the bijection of Theorem 2.1.5 to construct the corresponding $T \in SSYT(\lambda, n)$. Recall that in $M(v, \lambda, n)$, v records which columns of M have a fixed sum of 1. Thus, the numbers in v are the entries of T in the first column of λ , so $T \in SSYT(v, \lambda, n)$.

Now consider $T \in SSYT(v, \lambda, n)$ and its corresponding sign matrix $M \in M(\lambda, n)$. The first column of T is fixed to be the numbers in v . The first column of T gets mapped to the last row of M . That is, for each number in the first column of T , the corresponding column of M will sum to 1. The rest of the columns of M will sum to 0. Thus $M \in M(v, \lambda, n)$. \square

Definition 2.8.5. Let $P(v, \lambda, n)$ be the polytope defined as the convex hull, as vectors in $\mathbb{R}^{\lambda_1 n}$, of all the matrices in $M(v, \lambda, n)$. We say this is the sign matrix polytope with row sums determined by λ and column sums determined by v .

We now prove analogous properties to those proved in the rest of the paper regarding $P(m, n)$ and $P(\lambda, n)$. Since many of these proofs are very similar to proofs we have already discussed, we only note how the proofs differ from those in the other cases.

Proposition 2.8.6. *The dimension of $P(v, \lambda, n)$ is $(\lambda_1 - 1)(n - 1)$ if $1 \leq k < n$. When $k = n$, the dimension is $(\lambda_1 - \lambda_n)(n - 1)$.*

Proof. Since each matrix in $M(v, \lambda, n)$ is $\lambda_1 \times n$, the ambient dimension is $\lambda_1 n$. However, when constructing the sign matrix corresponding to a tableau of shape λ , as in Theorem 2.1.5, the last column is determined by the shape λ via the prescribed row sums (2.3) of Definition 2.1.4. The last row of the matrix is determined by v using (2.26). These are the only restrictions on the dimension when $1 \leq k < n$, reducing the free entries in the matrix by one column and one row. Thus, the dimension is $(\lambda_1 - 1)(n - 1)$. When $k = n$, it must be that $v = (1, 1, \dots, 1)$ and $P(v, \lambda, n)$ equals $P(\lambda, n)$, so we reduce to this case. \square

Theorem 2.8.7. *The vertices of $P(v, \lambda, n)$ are the sign matrices $M(v, \lambda, n)$.*

Proof. The hyperplane constructed in the proof of Theorem 2.2.6 separates a given sign matrix from all other sign matrices in $M(\lambda, n)$, which includes $M(v, \lambda, n)$. \square

Theorem 2.8.8. *$P(v, \lambda, n)$ consists of all $\lambda_1 \times n$ real matrices $X = (X_{ij})$ such that:*

$$0 \leq \sum_{i'=1}^i X_{i'j} \leq 1, \quad \text{for all } 1 \leq i \leq \lambda_1, 1 \leq j \leq n \quad (2.27)$$

$$0 \leq \sum_{j'=1}^j X_{ij'}, \quad \text{for all } 1 \leq j \leq n, 1 \leq i \leq \lambda_1 \quad (2.28)$$

$$\sum_{j'=1}^n X_{ij'} = a_{\lambda_1 - i + 1}, \quad \text{for all } 1 \leq i \leq \lambda_1 \quad (2.29)$$

$$\sum_{i'=1}^{\lambda_1} X_{i'j} = 1, \quad \text{if } j \in v \text{ and } 0 \text{ otherwise.} \quad (2.30)$$

Proof. This proof follows the proof of Theorem 2.4.1, except since both the row and column sums are fixed, only closed circuits are needed. \square

Definition 2.8.9. Define $\bar{\Gamma}_{(v,\lambda,n)}$ as the following labeling of the graph $\Gamma_{(\lambda_1,n)}$. All edges are labeled as in $\bar{\Gamma}_{(\lambda,n)}$, except the last vertical edge in column j is labeled 1 if $j \in v$ and 0 otherwise. 0-dimensional components, components, containment of components, and regions are defined analogously. Let $\Lambda_{(v,\lambda,n)}$ denote the partial order on components of $\bar{\Gamma}_{(v,\lambda,n)}$ by containment.

Theorem 2.8.10. *Let F be a face of $P(v,\lambda,n)$ and $\mathcal{M}(F)$ equal to the set of sign matrices that are vertices of F . The map $\psi(\mathcal{M}(F))$ is a bijection between faces of $P(v,\lambda,n)$ and components of $\bar{\Gamma}_{(v,\lambda,n)}$. Moreover, ψ is a poset isomorphism, and the dimension of F is equal to the dimension of $\psi(F)$.*

Proof. The proof is analogous to the proof of Theorem 2.6.19; we need only check the dimension of the maximal component of $\Lambda_{(v,\lambda,n)}$ matches the dimension of $P(v,\lambda,n)$. Recall the dimension of $P(v,\lambda,n)$ equals $(\lambda_1 - 1)(n - 1)$ when $1 \leq k < n$, and $(\lambda_1 - \lambda_n)(n - 1)$ when $k = n$. Note that when $1 \leq k < n$, there are $(\lambda_1 - 1)(n - 1)$ regions in the maximal component of $\Lambda_{(v,\lambda,n)}$. When $k = n$, the only possible first column of $T \in SSYT(\lambda,n)$ is $v = (1, 2, \dots, n)$, thus $P(v,\lambda,n) = P(\lambda,n)$ and we may use Theorem 2.6.19. \square

Theorem 2.8.11 relates sign matrix polytopes to transportation polytopes. See Definition 1.3.59 for the definition of transportation polytopes.

Theorem 2.8.11. *The nonnegative part of $P(v,\lambda,n)$ is the transportation polytope $P_{(y,z)}$, where $y_i = a_{\lambda_1 - i + 1}$ for all $1 \leq i \leq \lambda_1$ and $z_j = 1$ if $j \in v$ and 0 otherwise.*

Proof. By Theorem 2.8.8, $P(v,\lambda,n)$ is contained in $P_{(y,z)}$, since for these choices of y and z , (1.6) and (1.7) are exactly (2.29) and (2.30). For the reverse inclusion, note in addition that any matrix with nonnegative entries and column sums at most 1 satisfies (2.27) and (2.28). \square

This is analogous to the fact that the non-negative part of the alternating sign matrix polytope is the Birkhoff polytope [3, 31].

3. CATALAN AND ORDER POLYTOPES

In Chapter 2, two polytope families with origins in semistandard Young tableaux were discussed. In this chapter, similar theory and techniques will be used to discuss polytopes that are formed from standard Young tableaux. The focus of the discussion in this chapter will revolve around a special shape of SYT that is a Catalan object and the polytope family made from these SYT . The main theorem, Theorem 3.4.2, states that this new polytope family is in bijection with a specific order polytope. The general class of order polytopes was discussed in Subsection 1.3.8; recall that order polytopes are a unique class of polytopes where volume can be combinatorially interpreted. Other properties of this new polytope family that will be discussed in this chapter include: the enumeration of vertices and facets, the inequality description, and the face lattice description. All of these properties are proved as corollaries of the main theorem.

3.1. Standard Young tableaux and standard sign matrices

A bijection between semistandard Young tableaux and sign matrices was discussed in the previous chapter. This subsection introduces a special type of sign matrices, which will be shown to be in bijection with standard Young tableaux.

Definition 3.1.1. A *standard sign matrix* is an $m \times n$ sign matrix M with the added properties that there is exactly one 1 in each column and if $M_{i,j} = 1$ then $M_{i+1,j} = -1$ for $1 \leq i \leq m - 1$. Standard sign matrix will be denoted as SSM .

In other words, whenever there is an entry of 1 in a SSM , the entry directly below it is a -1 . Thus there is always a -1 below a 1, with the exception of the bottom row, as there is no place for a -1 to be below a 1 in the last row.

Recall from Definition 1.4.3 that a standard Young tableau is defined as a filling of a Young diagram with the numbers 1 through n (where n is the number of boxes). Each of the numbers is used exactly once, and the rows and columns are strictly increasing. Also recall $SYT(\lambda)$ denotes the set of standard Young tableaux of shape λ . This is similar to the notation $SSYT(\lambda, n)$ in Chapter 2.

Definition 3.1.2. Define $SSM(\lambda)$ to be the $\lambda_1 \times n$ standard sign matrices that are formed from standard Young tableaux of shape λ , where λ has n boxes.

Theorem 3.1.3. $SYT(\lambda)$ is in bijection with $SSM(\lambda)$.

Proof. Theorem 2.1.5 gives a bijection between $SSYT(\lambda, n)$ and $M(\lambda, n)$. Since $SYT(\lambda)$ are a special case of $SSYT(\lambda, n)$ and $SSM(\lambda)$ are a special case of $M(\lambda, n)$, all that needs to be proved are the added properties of both SYT and SSM .

Starting with a $T \in SYT(\lambda)$, follow the algorithm of Theorem 2.1.5 to get a sign matrix M . A SYT uses only one of each number so there will be only one 1 in each column of M . In the bijection algorithm, if the number ν is in the $(\lambda_1 - i + 1)$ st column of T when moving from column $\lambda_1 - i + 1$ to $\lambda_1 - i$ in T , there will be a 1 in the i th row and ν th column of M and a -1 in the $(i + 1)$ st row, ν th column. Thus the property of having only one of each number in T implies there must be a -1 in M directly below a 1 that is not in the bottom row. Notice further that if ν is in the first column of T , then there will be a 1 in the λ_1 st row of M without a -1 below it. Therefore we have obtained a SSM .

Now start with $M \in SSM(\lambda)$ and follow the reverse algorithm to get a tableau T . M was a standard sign matrix, so there is only one 1 in each column and a -1 is directly below; thus each number will only appear once in T . Also, the columns of the 1's in the bottom row of M become the first column of T . From the original bijection in Theorem 2.1.5, it is known that the columns of M are strictly increasing and the rows will be weakly increasing. However since there is only one 1 in each column of M , there will be only one of each number to appear in T , therefore the rows of T strictly increase. Thus a standard Young tableau is obtained. \square

An example of this bijection is shown in Figure 3.1.

$$\begin{array}{|c|c|c|c|} \hline 1 & 3 & 4 & 7 \\ \hline 2 & 6 & 9 & \\ \hline 5 & & & \\ \hline 8 & & & \\ \hline \end{array} \iff \begin{bmatrix} 0 & 0 & 0 & 0 & 0 & 0 & 1 & 0 & 0 \\ 0 & 0 & 0 & 1 & 0 & 0 & -1 & 0 & 1 \\ 0 & 0 & 1 & -1 & 0 & 1 & 0 & 0 & -1 \\ 1 & 1 & -1 & 0 & 1 & -1 & 0 & 1 & 0 \end{bmatrix}$$

Figure 3.1. Example of the bijection between $SYT([4, 3, 1, 1])$ and $SSM([4, 3, 1, 1])$.

Two basic shapes of tableaux are rows and columns, since given any single row or column, there is only one *SYT* of that shape. The following is a remark about specifying their standard sign matrices. Notice that there is only one tableau, thus one matrix for each λ . Examples of each item in the remark can be found in Figures 3.2 and 3.3.

Remark 3.1.4. • Let λ be the one row shape $\lambda = [\lambda_1]$. Then $SSM([\lambda_1])$ is the $\lambda_1 \times \lambda_1$ matrix with 1's on the anti-diagonal and -1 's along the subanti-diagonal.

- Let λ be the one column shape $\lambda = [1^n]$. Then $SSM([1^n])$ is the $1 \times n$ matrix filled with all ones.

$$\begin{array}{|c|c|c|c|c|} \hline 1 & 2 & 3 & 4 & 5 \\ \hline \end{array} \iff \begin{bmatrix} 0 & 0 & 0 & 0 & 1 \\ 0 & 0 & 0 & 1 & -1 \\ 0 & 0 & 1 & -1 & 0 \\ 0 & 1 & -1 & 0 & 0 \\ 1 & -1 & 0 & 0 & 0 \end{bmatrix}$$

Figure 3.2. An example of a row tableau and its corresponding standard sign matrix.

$$\begin{array}{|c|} \hline 1 \\ \hline 2 \\ \hline 3 \\ \hline 4 \\ \hline 5 \\ \hline \end{array} \iff [1 \ 1 \ 1 \ 1 \ 1]$$

Figure 3.3. An example of a column tableau and its corresponding standard sign matrix.

The standard sign matrix polytope is defined next.

Definition 3.1.5. Let $SSMP(\lambda)$ be the polytope defined as the convex hull, as vectors in $\mathbb{R}^{\lambda_1 n}$, of all the matrices in $SSMP(\lambda)$. Call this the *standard sign matrix polytope of shape λ* .

There is not much known about $SSMP(\lambda)$ in general, however the rest of this chapter discusses $SSMP(\lambda)$ for specific shapes. The following conjecture is about the polytope made from *SYT* of hook shape and was found using Sage [30].

Conjecture 3.1.6. The number of facets of $SSM([\lambda_1, 1^k])$ is $2k\lambda_1 - 3\lambda_1 - 3k + 6$.

3.2. Catalan sign matrices and polytopes

The previous subsection introduced $SSMP(\lambda)$ and now special SYT of rectangular shape with two rows will be discussed. These special tableaux will be used to make the polytope $SSMP([m, m])$. In Section 1.5 it was noted that SYT of this shape are Catalan objects. Since these SYT are Catalan objects, their corresponding standard sign matrices will be Catalan objects as well.

Definition 3.2.1. Define the set of *Catalan sign matrices*, denoted $CSM(m)$, as $SSM([m, m])$. That is, a Catalan sign matrix is an $m \times 2m$ standard sign matrix $X = (X_{i,j})$ such that:

$$\sum_{j=1}^{2m} X_{1,j} = 2, \tag{3.1}$$

$$\sum_{j=1}^{2m} X_{i,j} = 0, \quad 2 \leq i \leq m. \tag{3.2}$$

Corollary 3.2.2. $CSM(m)$ is in bijection with $SYT([m, m])$.

Proof. This follows from Theorem 3.1.3 by setting $\lambda = [m, m]$. □

The following proposition shows some properties of $CSM(m)$ that result from the bijection with standard Young tableaux.

Proposition 3.2.3. *Given $M \in CSM(m)$, the following hold:*

- $M_{m,1} = 1$ and $M_{1,2m} = 1$.
- $M_{i,j} = 0$ for $1 \leq j \leq m - i$.
- $M_{i,j} = 0$ for $2m - i + 3 \leq j \leq 2m$.
- *The second 1 in each row is determined by the placement of the first 1 in all rows.*

Proof. Recall that each $M \in CSM(m)$ is in bijection with $T \in SYT([m, m])$. In T , when the Young diagram is filled, the 1 is fixed in the upper left and $2m$ is fixed in the lower right. In M , this correlates to $M_{m,1} = 1$ and $M_{1,2m} = 1$.

If the first row of T is $1, 2, \dots, m$, then the corresponding sign matrix is the second example of Figure 3.4. Notice that for every row i in M , there are at least $m - i$ zeros at the beginning, since the $(\lambda_1 - i + 1)$ st column of T corresponds to the i th row in M . Since the largest number that can be in the 1st column of T is $m + 1$, the m th row of M has more than $2m - (m + 1)$ zeros at the end; therefore at least $m - 2$ zeros at the end of the m th row of M . As i gets smaller, there is one less minimal zero per row, thus $M_{i,j} = 0$ for $2m - i + 3 \leq j \leq 2m$.

The last item holds because after the top row of T is decided, the bottom row is fixed. The top row of T corresponds to the first 1 in each row of M and the second 1 in each row of M corresponds to the bottom row of T . Therefore all four items hold for all $M \in CSM(m)$. \square

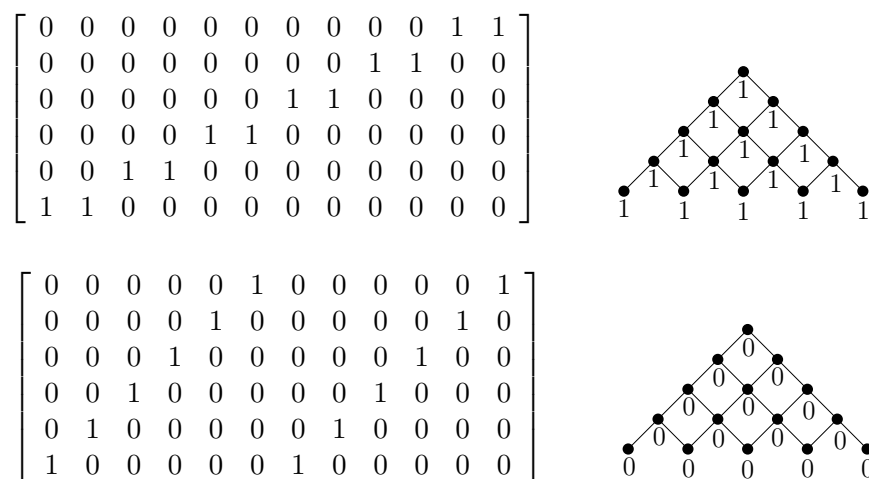


Figure 3.4. Examples of the extreme cases of partial column sum matrices of $CSM(6)$ and their corresponding $f \in \mathcal{O}(Q_6)$.

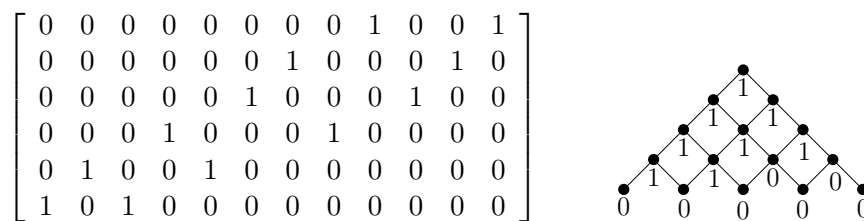


Figure 3.5. Examples of a middle case of a partial column sum matrix of $CSM(6)$ and the corresponding $f \in \mathcal{O}(Q_6)$.

Using the same ideas as in Chapter 2, the polytope that is formed by Catalan sign matrices will be discussed. Since Catalan sign matrices have been shown to be a Catalan object, the Catalan polytope is defined next.

Definition 3.2.4. Let CP_m be the polytope defined as the convex hull, as vectors in \mathbb{R}^{2m^2} , of all Catalan sign matrices. CP_m is called the *Catalan polytope*.

Remark 3.2.5. Note in the notation of Definition 3.1.5, $CP_m = SSMP([m, m])$.

Theorem 3.2.6. *The vertices of CP_m are the Catalan sign matrices $CSM(m)$.*

Proof. Catalan sign matrices are vertices of $P([m, m], 2m)$, so since the hyperplane from that proof separates each sign matrix from all other sign matrices in $M([m, m], 2m)$, it also separates it from all other Catalan sign matrices in $CSM(m)$. The following hyperplane:

$$H_M(X) := \sum_{(i,j) \in C_M} \sum_{i'=1}^i X_{i'j} = |\lambda| - \frac{1}{2}. \quad (3.3)$$

separates an individual sign matrix from all the other sign matrices in CP_m . Thus all Catalan sign matrices $CSM(m)$ are necessarily vertices. \square

The dimension of CP_m will be discussed next.

Theorem 3.2.7. *The dimension of CP_m is $\binom{m}{2} = \frac{m(m-1)}{2}$.*

Proof. The binomial coefficient $\binom{m}{2}$ counts the triangle numbers, $\{1, 3, 6, 10, 15, \dots\}$. This can also be thought of as $1, 1+2, 1+2+3, 1+2+3+4, \dots, \sum_{i=1}^{m-1} i$. Consider $M \in CSM(m)$. Using the bijection to tableaux, the columns of the corresponding *SYT* T will be used. The 1 is fixed to the upper left of T , thus a 1 is fixed in the last row of M ; this is row m . The 2 has two columns of T in which it could be placed (the column next to the 1, or directly below the 1), so there are two rows of M that could have a 1 in the second column. There are three possible columns to put a 3 in T , thus there are three possible rows to put a 1 in the third column of M . This pattern continues until the $(m+1)$ st number, there are only m places left with the possibility of m columns. Now the number decreases with each number as there are less and less places left in T . So the number of places to put a 1 in the matrix is $1+2+3+\dots+m+m+\dots+2+1$. Since the row sums of the

matrix are determined, the dimension decreases by the number of rows, which is $2m$; we subtract $2m$ from this sum to obtain $1 + 2 + \cdots + m - 1 + m - 1 + \cdots + 2 + 1$. However, when filling a two row rectangular *SYT*, once the top row is complete the bottom row is determined. Therefore, only half of the possible spots need to be counted, resulting in $1 + 2 + 3 + \cdots + m - 1 = \binom{m}{2}$. \square

3.3. Building blocks of CP_m and $\mathcal{O}(Q_m)$

The order polytope is a family of polytopes with particular properties, some of which are discussed in Subsection 1.3.8. Theorem 3.4.2 is the main theorem of Chapter 3; this subsection will lay the groundwork for proving the theorem which shows the equivalence between the Catalan polytope and the order polytope of a certain poset. In this subsection, there are two maps given in Definitions 3.3.4 and 3.3.9 which detail how the two polytopes are connected. The graph $\Delta(Q_m)$ is introduced, in Definition 3.3.3, as a means to utilize the poset Q_m . The partial sum matrix $\hat{C}(X)$ from Definition 1.6.4 is recalled to be used with the Catalan sign matrix.

3.3.1. Properties of Q_m and $\mathcal{O}(Q_m)$

This subsection will focus the discussion around a particular poset Q_m that was introduced in Definition 1.3.19 and its corresponding set of order ideals $J(Q_m)$ from Definition 1.3.17. As stated in Proposition 1.3.53, the convex hull of $J(Q_m)$ forms the order polytope $\mathcal{O}(Q_m)$. The function $f \in \mathcal{O}(Q_m)$ is a labeling of the elements of the poset Q_m with values. Figure 3.6 shows one such labeling of the order ideals of Q_4 with the corresponding vector (read from left to right and bottom to top in the poset).

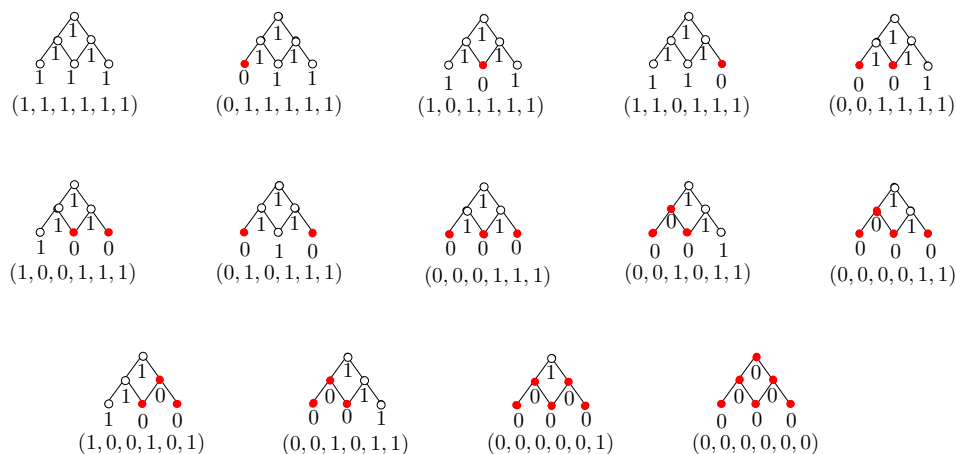


Figure 3.6. The 14 order ideals in $J(Q_4)$ and their corresponding vectors in $\mathcal{O}(Q_m)$.

A labeling f of the poset Q_m can be expressed as an n -tuple in generic terms, so it can be denoted as a vector. Following the order of vectors in $\mathcal{O}(Q_m)$ (left to right and bottom to top), a vector in $\mathcal{O}(Q_3)$ is of the form $(f(a_{2,1}), f(a_{1,1}), f(a_{2,2}))$, in $\mathcal{O}(Q_4)$ is of the form $(f(a_{3,1}), f(a_{2,1}), f(a_{1,1}), f(a_{3,2}), f(a_{2,2}), f(a_{3,3}))$, in $\mathcal{O}(Q_5)$ is of the form $(f(a_{4,1}), f(a_{3,1}), f(a_{2,1}), f(a_{1,1}), f(a_{4,2}), f(a_{3,2}), f(a_{2,2}), f(a_{4,3}), f(a_{3,3}), f(a_{4,4}))$ and so on. Examples of these posets are in Figure 3.7.

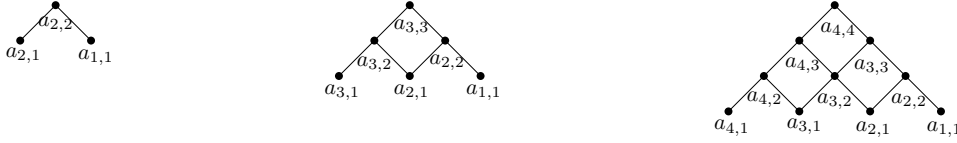


Figure 3.7. Q_m for $m = 3, 4, 5$, respectively.

From Stanley [25] it is known how to construct the polytope inequalities of $\mathcal{O}(Q_m)$ from the cover relations of Q_m . The following is a corollary which states them explicitly for this case.

Theorem 3.3.1 ([25]). $\mathcal{O}(Q_m)$ is defined by the following inequalities:

$$f(a_{s,t-1}) \leq f(a_{s,t}) \quad 1 \leq t \leq s \leq m-1 \quad (3.4)$$

$$f(a_{s-1,t-1}) \leq f(a_{s,t}) \quad 1 \leq t \leq s \leq m-1 \quad (3.5)$$

$$0 \leq f(a_{s,1}) \quad 1 \leq s \leq m-1 \quad (3.6)$$

$$f(a_{m-1,m-1}) \leq 1 \quad (3.7)$$

These inequalities can be seen in Figure 3.8.

In the proofs in this chapter, the following notation is used.

Definition 3.3.2. Given $f \in \mathcal{O}(Q_m)$, set $f(a_{s,t}) := \begin{cases} 1 & s = m \text{ or } t > s \\ 0 & t = 0 \end{cases}$.

The following labeled graph is defined as a way to visualize the proofs.

Definition 3.3.3. Define a labeled graph $\Delta(Q_m)$ to be the Hasse diagram of Q_m with m elements added at the bottom, $a_{s,0}$ for $0 \leq s \leq m-1$, and $m-1$ elements added above the sides of the

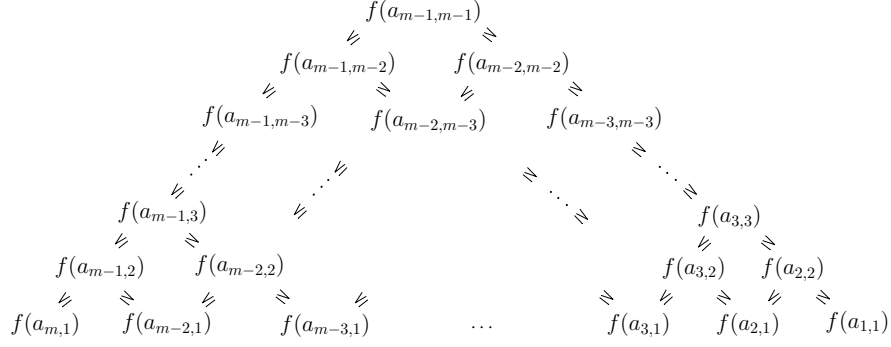


Figure 3.8. An illustration of the inequalities for the order polytope $\mathcal{O}(Q_m)$.

triangular poset: $a_{m,t}$ for $2 \leq t \leq m$ and $a_{s,s+1}$ for $1 \leq s \leq m-1$. The edge set is the cover relations of Q_m with the following edges added when the elements are defined:

$$\text{Additional Edges} := \begin{cases} a_{s,t} \text{ to } a_{s,t+1} & s = t \text{ or } t = 0 \\ a_{s,t} \text{ to } a_{s+1,t+1} & s = m-1 \text{ or } t = 0 \end{cases}$$

An example of $\Delta(Q_6)$ is in Figure 3.9.

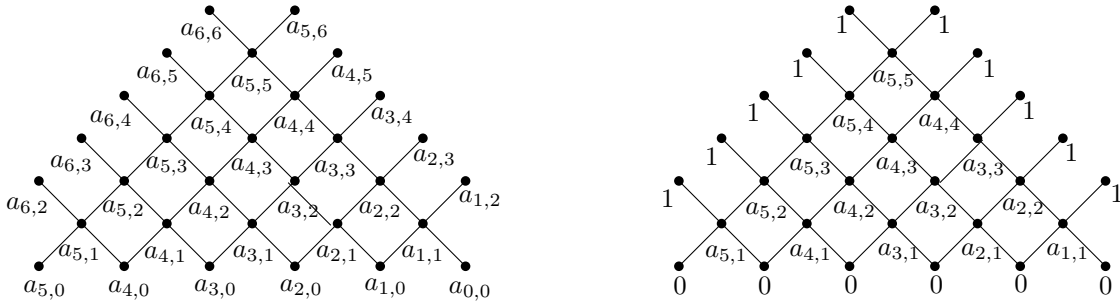


Figure 3.9. The graph $\Delta(Q_6)$ before and after specifying boundary vertex labels as in Definition 3.3.3.

3.3.2. Order polytope to Catalan polytope

In this subsection, a map from the order polytope to $m \times 2m$ matrices will be discussed.

Lemma 3.3.8 will show the image of this map is in CP_m .

Definition 3.3.4. Define a map $\xi : \mathcal{O}(Q_m) \rightarrow \mathbb{R}^{m \times 2m}$ on $f \in \mathcal{O}(Q_m)$. The first step of the map is as follows:

$$c_{i,j} := \begin{cases} 0, & 1 \leq i \leq m, 1 \leq j \leq m - i, \\ 0, & 2 \leq i \leq m, 2m - i + 2 \leq j \leq 2m, \\ 1, & i = m, j = 1 \text{ or } i = 1, j = 2m \\ f(a_{(2m-j-i)+1, (2m-j-2i)+2}) - f(a_{2m-j-i, (2m-j-2i)+1}), & m - i + 1 \leq j \leq 2m - 2i + 1, \\ f(a_{i-1, j-(2m-2i)-1}) - f(a_{i-1, j-(2m-2i)-2}), & 2m - 2i + 2 \leq j \leq 2m - i + 1 \end{cases} .$$

The second step of the map is to apply \hat{C}^{-1} .

In other words, considering $\Delta(Q_m)$ take the difference of the labels for two vertices at a time and the difference of these labels will become the entries in the partial column sum matrix $\hat{C}(X)$ from Definition 1.6.4. Figure 3.10 shows the pattern of these differences and Figure 3.14 shows the resulting general partial column sum matrix for $m = 6$. The top row of the matrix comes from differences starting at the top of the graph and going down the solid black line on the right. The second row of the matrix follows the dashed line, the second line from the top, and so on down the left side. Notice that some paths make a check mark; when the bottom is reached the differences continue up the other side, however, the difference will still be between the bigger (or higher) element and the smaller. The bottom, or m th row, of the matrix follows the gray solid line up the left side of $\Delta(Q_m)$, taking differences of bigger and smaller elements as before. This partial column sum matrix will be an $m \times 2m$ matrix. Recall that any matrix can be recovered uniquely from the corresponding column partial sum matrix of Definition 1.6.6. The map ξ is demonstrated in Example 3.3.5 and in Figure 3.11.

Example 3.3.5. Using the $\Delta(Q_m)$ and matrix in Figure 3.11, examples of some $\hat{C}(X)$ entries for the first step of the map ξ are shown. Figure 3.10 demonstrates the line of differences being followed.

- $c_{2,2} = 0$ since $2 < 6 - 2 = 4$.

The next few entries are the differences following the top, solid black, line of Figure 3.10.

- $c_{1,6} = f(a_{2(6)-6-1+1, 2(6)-6-2(1)+2}) - f(a_{2(6)-6-1, 2(6)-6-2(1)+1}) = f(a_{6,6}) - f(a_{5,5}) = 1 - 0.8 = 0.2$

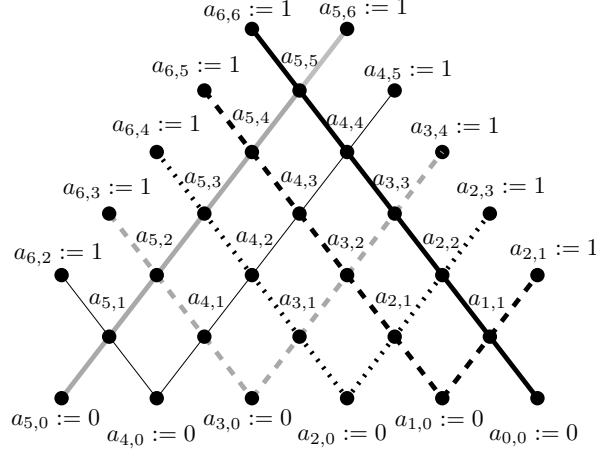


Figure 3.10. A way to visualize Definition 3.3.4, explained in Example 3.3.5.

- $c_{1,7} = f(a_{2(6)-7-1+1,2(6)-7-2(1)+2}) - f(a_{2(6)-7-1,2(6)-7-2(1)+1}) = f(a_{5,5}) - f(a_{4,4}) = 0.8 - 0.8 = 0$
- $c_{1,11} = f(a_{2(6)-11-1+1,2(6)-11-2(1)+2}) - f(a_{2(6)-11-1,2(6)-11-2(1)+1}) = f(a_{1,1}) - f(a_{0,0}) = 0 - 0 = 0$

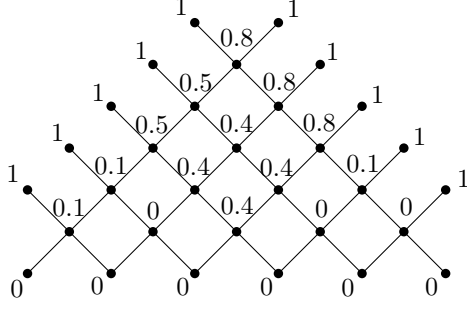
The next few entries are from the middle of $\hat{C}(X)$ in row 3 and follow the line third from the top, which is dotted in Figure 3.10. The first step in the calculation will no longer be shown.

- $c_{3,7} = f(a_{3,1}) - f(a_{2,0}) = 0.4 - 0 = 0.4$
- $c_{3,8} = f(a_{2,1}) - f(a_{2,0}) = 0 - 0 = 0$
- $c_{3,9} = 0.1 - 0 = 0.1$
- $c_{3,10} = f(a_{2,3}) - f(a_{2,2}) = 1 - 0.1 = 0.9$

The last few example entries are from the bottom row of the matrix, $m = 6$, and follow the gray line back up the left side of Figure 3.10.

- $c_{6,1} = c_{m,1} = 1$
- $c_{6,2} = f(a_{5,1}) - f(a_{5,0}) = 0.1 - 0 = 0.1$
- $c_{6,3} = f(a_{5,2}) - f(a_{5,1}) = 0.1 - 0.1 = 0$
- $c_{6,7} = f(a_{5,6}) - f(a_{5,5}) = 1 - 0.8 = 0.2$

It may be helpful to have the map to a matrix X in CP_m directly from $\mathcal{O}(Q_m)$. The following lemma gives this map and shows the linearity of the matrix.



$$\begin{bmatrix} 0 & 0 & 0 & 0 & 0 & .2 & 0 & 0 & .7 & .1 & 0 & 1 \\ 0 & 0 & 0 & 0 & .5 & .1 & 0 & .4 & 0 & 0 & 1 & 0 \\ 0 & 0 & 0 & .5 & .1 & 0 & .4 & 0 & .1 & .9 & 0 & 0 \\ 0 & 0 & .9 & .1 & 0 & .4 & 0 & .4 & .2 & 0 & 0 & 0 \\ 0 & .9 & .1 & 0 & .4 & 0 & .4 & .2 & 0 & 0 & 0 & 0 \\ 1 & .1 & 0 & .4 & 0 & .3 & .2 & 0 & 0 & 0 & 0 & 0 \end{bmatrix}$$

Figure 3.11. Example of the maps between an element of $\Delta(Q_6)$ and a matrix in $\xi(f)$ used in Examples 3.3.5 and 3.3.10.

Lemma 3.3.6. *The map ξ of Definition 3.3.4 can be described in a single step as follows.*

$$X_{i,j} = \begin{cases} 0, & 1 \leq i \leq m, 1 \leq j \leq m - i, \\ 0, & 2 \leq i \leq m, 2m - i + 2 \leq j \leq 2m, \\ 1, & i = m, j = 1 \text{ or } i = 1, j = 2m \\ -1, & i = 2, j = 2m \\ f(a_{2m-j, 2m-j}) - f(a_{2m-j-1, 2m-j-1}) & 1 \leq j \leq 2m - 1 \\ f(a_{2m-j-i+1, 2m-j-2i+2}) - f(a_{2m-j-i, 2m-j-2i+1}) & \\ -f(a_{2m-j-i+2, 2m-j-2i+4}) + f(a_{2m-j-i+1, 2m-j-2i+3}) & 2 \leq i \leq m, \\ & 1 \leq j \leq 2m - 2i + 1 \\ f(a_{i-1, j-2m+2i-1}) - f(a_{i-1, j-2m+2i-2}) & \\ -f(a_{2m-j-i+2, 2m-j-2i+4}) + f(a_{2m-j-i+1, 2m-j-2i+3}) & 2 \leq i \leq m, \\ & 2m - 2i + 2 \leq j \leq 2m - 2i + 3 \\ f(a_{i-1, j-2m+2i-1}) - f(a_{i-1, j-2m+2i-2}) & \\ -f(a_{i-2, j-2m+2i-3}) + f(a_{i-2, j-2m+2i-4}) & 2 \leq i \leq m, \\ & 2m - 2i + 4 \leq j \leq 2m \end{cases}$$

Proof. All calculations follow the map \hat{C}^{-1} in Remark 1.6.6 and use the following two statements from Definition 3.3.4:

I. $c_{i,j} = f(a_{2m-j-i+2,2m-j-2i+2}) - f(a_{2m-j-i+1,2m-j-2i+1})$ for $m-i+1 \leq j \leq 2m-2i+1$

II. $c_{i,j} = f(a_{i-1,j-2m+2i-1}) - f(a_{i-1,j-2m+2i-2})$ for $2m-2i+2 \leq j \leq 2m-i+1$ Notice

that the first three statements follow directly.

- Case 1: $i = 1, 1 \leq j \leq 2m$.

$$X_{i,j} = c_{i,j} = f(a_{2m-j-i+2,2m-j-2i+2}) - f(a_{2m-j-i+1,2m-j-2i+1})$$

- Case 2: $2 \leq i \leq m, 1 \leq j \leq 2m-2i+1$. (This calculation uses equation I.)

$$\begin{aligned} X_{i,j} = c_{i,j} - c_{i-1,j} &= f(a_{2m-j-i+1+1,2m-j-2i+2}) - f(a_{2m-j-i+1,2m-j-2i+1}) \\ &\quad - f(a_{2m-j-i+1+2,2m-j-2i+4}) + f(a_{2m-j-i+2,2m-j-2i+3}) \end{aligned}$$

- Case 3: $2 \leq i \leq m, 2m-2i+2 \leq j \leq 2m-2i+3$. (This calculation uses equations I and II.)

$$\begin{aligned} X_{i,j} = c_{i,j} - c_{i-1,j} &= f(a_{i-1,j-2m+2i-1}) - f(a_{i-1,j-2m+2i-2}) \\ &\quad - f(a_{2m-j-i+3,2m-j-2i+4}) + f(a_{2m-j-i+2,2m-j-2i+3}) \end{aligned}$$

- Case 4: $2 \leq i \leq m, 2m-2i+4 \leq j \leq 2m$. (This calculation uses equation II.)

$$\begin{aligned} X_{i,j} = c_{i,j} - c_{i-1,j} &= f(a_{i-1,j-2m+2i-1}) - f(a_{i-1,j-2m+2i-2}) \\ &\quad - f(a_{i-2,j-2m+2i-3}) + f(a_{i-2,j-2m+2i-4}) \end{aligned}$$

□

From a partial column sum matrix, applying \hat{C}^{-1} recovers the matrix X as just discussed.

Then by applying \hat{R} the partial row sum matrix is obtained. The matrix that results from $\hat{R}(X)$ will be used in the proof of Lemma 3.3.8. The direct map follows:

Lemma 3.3.7. *The composite map $\hat{R} \circ \xi$ can be described as follows to obtain the following partial row sum matrix $\hat{R}(\xi(f))$, (all statements are for $2 \leq i \leq m$ unless stated otherwise.):*

$$r_{i,j} = \begin{cases} 0, & 1 \leq i \leq m, 1 \leq j \leq m-i, \\ 0, & 2m-i+2 \leq j \leq 2m, \\ 1, & i = m, j = 1 \\ 1 - f(a_{2m-j-1,2m-j-1}) & i = 1, 1 \leq j \leq 2m-1 \\ 2 & i = 1, j = 2m \\ f(a_{2m-j-i+1,2m-j-2i+3}) - f(a_{2m-j-i,2m-j-2i+1}) & 1 \leq j \leq 2m-2i+1 \\ 2f(a_{i-1,1}) & j = 2m-2i+2 \\ f(a_{i-1,2i-2m+j-1}) - f(a_{i-2,2i-2m+j-3}) & 2m-2i+3 \leq j \leq 2m-i+1 \end{cases}$$

Proof. All calculations follow the map \hat{R} in Definition 1.6.5 applied to X from Lemma 3.3.6, therefore there are four cases. Notice that the first three statements, and the fifth follow directly.

- Case 1: $i = 1, 1 \leq j \leq 2m - 1$.

$$\begin{aligned}
r_{1,j} &= \sum_{k=1}^j X_{1,k} = \sum_{k=1}^j (f(a_{2m-k,2m-j}) - f(a_{2m-k-1,2m-k-1})) \\
&= (f(a_{2m-1,2m-1}) - f(a_{2m-2,2m-2})) + (f(a_{2m-2,2m-2}) - f(a_{2m-3,2m-3})) + \cdots \\
&\quad + (f(a_{2m-j+1,2m-j+1}) - f(a_{2m-j,2m-j})) + (f(a_{2m-j,2m-j}) - f(a_{2m-j-1,2m-j-1})) \\
&= (f(a_{2m-1,2m-1}) - f(a_{2m-j-1,2m-j-1})) = 1 - f(a_{2m-j,2m-j})
\end{aligned}$$

Notice when $i = 1$ and $j = m$, the calculation is $1 - f(a_{2m-j,2m-j}) + X_{1,2m} = 1 - 0 + 1 = 2$.

- Case 2: $2 \leq i \leq m, 1 \leq j \leq 2m - 2i + 1$.

$$\begin{aligned}
r_{i,j} &= \sum_{k=1}^j X_{i,k} = \sum_{k=1}^j (f(a_{2m-k-i+1,2m-k-2i+2}) - f(a_{2m-k-i,2m-k-2i+1}) + \\
&\quad - f(a_{2m-k-i+2,2m-k-2i+4}) + f(a_{2m-k-i+1,2m-k-2i+3})) \\
&= f(a_{2m-i,2m-2i+1}) - f(a_{2m-i-1,2m-2i}) - f(a_{2m-i+1,2m-2i+3}) + f(a_{2m-i,2m-2i+2}) \\
&\quad + f(a_{2m-i-1,2m-2i}) - f(a_{2m-i-2,2m-2i-1}) + -f(a_{2m-i,2m-2i+2}) + f(a_{2m-i-1,2m-2i+1}) + \cdots \\
&\quad + f(a_{2m-j-i+1,2m-j-2i+2}) - f(a_{2m-j-i,2m-j-2i+1}) \\
&\quad - f(a_{2m-j-i+2,2m-2i+3}) + f(a_{2m-j-i+1,2m-j-2i+3}) \\
&\quad + f(a_{2m-i,2m-2i+1}) - f(a_{2m-i+1,2m-2i+3}) + -f(a_{2m-j-i,2m-j-2i+1}) + f(a_{2m-j-i+1,2m-j-2i+3}) \\
&= 1 - 1 + f(a_{2m-j-i+1,2m-j-2i+3}) - f(a_{2m-j-i,2m-j-2i+1}) \\
&= f(a_{2m-j-i+1,2m-j-2i+3}) - f(a_{2m-j-i,2m-j-2i+1})
\end{aligned}$$

- Case 3: $2 \leq i \leq m$, $j = 2m - 2i + 2$.

$$\begin{aligned}
r_{i,j} &= \sum_{k=1}^j X_{i,k} = \sum_{k=1}^j (f(a_{i-1,k-2m+2i-1}) - f(a_{i-1,k-2m+2i-2}) - f(a_{2m-k-i+2,2m-k-2i+4}) \\
&\quad + f(a_{2m-k-i+1,2m-k-2i+3})) \\
&= f(a_{i-1,2i-2m}) - f(a_{i-1,2i-2m-1}) - f(a_{2m-i+1,2m-2i+3}) + f(a_{2m-i,2m-2i+2}) \\
&\quad + f(a_{i-1,2i-2m}) - f(a_{i-1,2i-2m-1}) - f(a_{2m-i+1,2m-2i+3}) + f(a_{2m-i,2m-2i+2}) \\
&\quad + f(a_{i-1,2i-2m+1}) - f(a_{i-1,2i-2m}) - f(a_{2m-i,2m-2i+2}) + f(a_{2m-i-1,2m-2i+1}) + \cdots \\
&\quad + f(a_{i-1,1}) - f(a_{i-1,0}) - f(a_{i,2}) + f(a_{i-1,1}) \\
&= f(a_{i-1,1}) - f(a_{i-1,2i-2m-1}) + f(a_{i-1,1}) - f(a_{2m-i+1,2m-2i+3}) \\
&= 2f(a_{i-1,1})
\end{aligned}$$

- Case 4: $2 \leq i \leq m$, $2m - 2i + 3 \leq j \leq 2m$.

$$\begin{aligned}
r_{i,j} &= \sum_{k=1}^j X_{i,k} = \sum_{k=1}^j (f(a_{i-1,k-2m+2i-1}) - f(a_{i-1,k-2m+2i-2}) - f(a_{i-2,k-2m+2i-3}) \\
&\quad + f(a_{i-2,k-2m+2i-4})) \\
&= f(a_{i-1,2i-2m}) - f(a_{i-1,2i-2m-1}) - f(a_{i-2,2i-2m-2}) + f(a_{i-2,2i-2m-3}) \\
&\quad + f(a_{i-1,2i-2m+1}) - f(a_{i-1,2i-2m}) - f(a_{i-2,2i-2m-1}) + f(a_{i-2,2i-2m-2}) + \cdots + \\
&\quad + f(a_{i-1,2i-2m+j-2}) - f(a_{i-1,2i-2m+j-3}) - f(a_{i-2,2i-2m+j-4}) + f(a_{i-2,2i-2m+j-5}) \\
&\quad + f(a_{i-1,2i-2m+j-1}) - f(a_{i-1,2i-2m+j-2}) - f(a_{i-2,2i-2m+j-3}) + f(a_{i-2,2i-2m+j-4}) \\
&= f(a_{i-1,2i-2m-3}) - f(a_{i-1,2i-2m-1}) + f(a_{i-1,2i-2m+j-1}) - f(a_{i-2,2i-2m+j-3}) \\
&= 0 - 0 + f(a_{i-1,2i-2m+j-1}) - f(a_{i-2,2i-2m+j-3}) \\
&= f(a_{i-1,2i-2m+j-1}) - f(a_{i-2,2i-2m+j-3})
\end{aligned}$$

Thus the formula is established. □

Each row of the matrix from $\hat{R}(X)$ can be seen as a pattern on $\Delta(Q_m)$ in Figure 3.12. The differences are still top to bottom as in $\hat{C}(X)$. In the figure, three of the paths are shown. The top path, shown in red dashed lines, corresponds to row two of the matrix from $\hat{R}(X)$ which can

be seen in Figure 3.13. The second path, shown in gray lines, corresponds to row three of the matrix from $\hat{R}(X)$. The third path, shown in blue dotted lines, corresponds to the fourth row of the matrix from $\hat{R}(X)$. All paths are not shown. An example of the matrix from $\hat{R}(X)$ for $m = 6$ is shown in Figure 3.13.

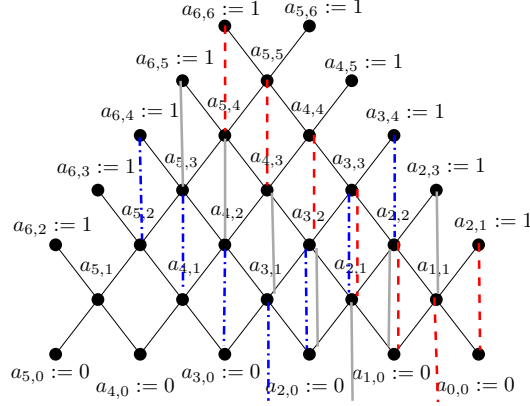


Figure 3.12. Example of the differences between labels of $\Delta(Q_m)$ to get entries of $\hat{R}(X)$.

$$\begin{bmatrix} 0 & 0 & 0 & 0 & 0 & 1 - a_{5,5} & a_{5,5} - a_{4,4} & a_{4,4} - a_{3,3} & a_{3,3} - a_{2,2} & a_{2,2} - a_{1,1} & a_{1,1} & 2 \\ 0 & 0 & 0 & 0 & 1 - a_{5,4} & a_{5,5} - a_{4,3} & a_{4,4} - a_{3,2} & a_{3,3} - a_{2,1} & a_{2,2} - a_{1,0} & 2a_{1,1} & 1 & 0 \\ 0 & 0 & 0 & 1 - a_{5,3} & a_{5,4} - a_{4,2} & a_{4,3} - a_{3,1} & a_{3,2} - a_{2,0} & 2a_{2,1} & a_{2,2} - a_{1,0} & 1 - a_{1,1} & 0 & 0 \\ 0 & 0 & 1 - a_{5,2} & a_{5,3} - a_{4,1} & a_{4,2} - a_{3,0} & 2a_{1,1} & a_{3,2} - a_{2,0} & a_{3,3} - a_{2,1} & 1 - a_{2,2} & 0 & 0 & 0 \\ 0 & 1 - a_{5,1} & a_{5,2} - a_{4,0} & 2a_{4,1} & a_{4,2} - a_{3,0} & a_{4,3} - a_{3,1} & a_{4,4} - a_{3,2} & 1 - a_{3,3} & 0 & 0 & 0 & 0 \\ 1 & 2a_{5,1} & a_{5,2} - a_{4,0} & a_{3,3} - a_{4,1} & a_{5,4} - a_{4,2} & a_{5,5} - a_{4,3} & 1 - a_{4,4} & 0 & 0 & 0 & 0 & 0 \end{bmatrix}$$

Figure 3.13. The general version of $\hat{R}(X)$ for $m = 6$ using $f(a_{i,j})$ values, written without the f due to space constraints.

The next lemma considers a vertex of $\mathcal{O}(Q_m)$, $f \in J(Q_m)$, then applies the map ξ . The resulting $\xi(f)$ is shown to be a Catalan sign matrix. The process is then extended to show that for any f in $\mathcal{O}(Q_m)$, $\xi(f)$ results in a matrix in CP_m .

Lemma 3.3.8. *Let $f \in \mathcal{O}(Q_m)$. Then $\xi(f) = X$ where $X \in CP_m$.*

Proof. First it will be shown that ξ maps the order polytope vertices $J(Q_m)$ to $CSM(m)$. Then the proof will be given that ξ maps $\mathcal{O}(Q_m)$ into CP_m .

Let $f \in \mathcal{O}(Q_m)$ such that $f(a_{s,t}) \in \{0, 1\}$ for all s, t . So $f \in J(\mathcal{O}(P))$. Let $M = \xi(f)$. It is necessary to show $M \in CSM(m)$. Recall that a matrix is a sign matrix if two conditions are satisfied: The partial column sums are between 0 and 1 (2.1) and the partial row sums are nonnegative (2.2). A Catalan sign matrix requires that the total row sum for the top row is 2 (3.1) and the other rows sum to 0 (3.2). It is also necessary to show that there is exactly one 1 in each column of M and below each 1 there is a -1 .

Apply the first step of ξ to obtain a matrix $\hat{C}(M)$. Notice that all entries in $\hat{C}(M)$ are nonnegative, since all f in the order polytope are positive and the differences in Definition 3.3.4 are of the form $f(a_{x,y}) - f(a_{x-1,y-1})$ or $f(a_{x,y}) - f(a_{x,y-1})$. These are nonnegative since $f \in \mathcal{O}(Q_m)$ so that $f(a_{x-1,y-1}) \leq f(a_{x,y})$ since $a_{x-1,y-1} \leq a_{x,y}$, and $f(a_{x,y-1}) \leq f(a_{x,y})$ since $a_{x,y-1} \leq a_{x,y}$. Further notice that since all values of $f(a_{s,t})$ are 0 and 1 and follow the form just noted, the differences are not just nonnegative, they are either 1 or 0. The total column sum is $c_{m,j}$ for all j ; this is also between 0 and 1, so (2.2) is satisfied. For (2.1), refer to $\hat{R}(M)$ in Lemma 3.3.7 and notice that all entries are either differences of $f(a_{s,t})$ that are defined to be nonnegative or a single nonnegative value, thus all partial row sums of M are nonnegative.

To see (3.1), consider the top row of $\hat{C}(M)$. In row 1 the partial column sums are the same as the entries in M . Thus each matrix entry in the top row of M is nonnegative and the total sum of the top row is:

$$\begin{aligned}
\sum_{j=1}^{2m} x_{1,j} &= \sum_{j=1}^{2m} c_{1,j} = \sum_{j=1}^{m-1} c_{1,j} + \sum_{j=m}^{2m-1} c_{1,j} + c_{1,2m} = 0 + \sum_{j=m}^{2m-1} c_{1,j} + 1 \\
&= 0 + \sum_{j=m}^{2m-1} (f(a_{2m-j,2m-j}) - f(a_{2m-j-1,2m-j-1})) + 1 \\
&= 0 + (f(a_{m,m}) - f(a_{m-1,m-1})) + (f(a_{m-1,m-1}) - f(a_{m-2,m-2})) \\
&\quad + (f(a_{m-2,m-2}) - f(a_{m-3,m-3})) + \cdots \\
&\quad + (f(a_{3,3}) - f(a_{2,2})) + (f(a_{2,2}) - f(a_{1,1})) + (f(a_{1,1}) - f(a_{0,0})) + 1 \\
&= 0 + (f(a_{m,m}) - f(a_{0,0})) + 1 = 0 + (1 - 0) + 1 = 2
\end{aligned}$$

as needed. Thus (3.1) is satisfied.

For (3.2), again consider $\hat{R}(M)$. Notice that for each row in $2 \leq i \leq m$ of M there are $m - i$ zeros at the beginning and $i - 1$ zeros at the end of the row, thus only the entries in between need to be in the summation. First consider when $2 \leq i \leq m - 1$ and $j \leq 2m - i + 2$, the calculation is as follows:

$$\begin{aligned} r_{i,2m-i+2} &= f(a_{i-1,2i-2m+2m-i+2-1}) - f(a_{i-2,2i-2m+2m-i+2-3}) \\ &= f(a_{i-1,i+1}) - f(a_{i-2,i-1}) \\ &= 1 - 1 = 0. \end{aligned}$$

Now consider when $i = m$ then need $j = m + 2$, the calculation is:

$$r_{m,m+2} = f(a_{m-1,m+2-2m+2m-1}) - f(a_{m-1,m+2-2m+2m-2}) = a_{m-1,m+1} - a_{m-1,m} = 1 - 1 = 0.$$

Recall that if $s < t$ then $f(a_{s,t}) = 0$ and $2m - 1 > m - 1$ and $2m - 3 > m - 2$ for $m > 0$ and $m > 1$ respectively. Therefore condition (3.2) is satisfied.

Now it is left to show that there is exactly one 1 in each column of M and that below each 1 there is a -1 . This condition translates to the following: if $c_{i,j} = 1$ then $c_{i+1,j} = 0$. Use Proposition 3.2.3 as a reference. Figures 3.4 and 3.5 show examples.

Let $f_v \in J(Q_m)$ be a vertex in $\mathcal{O}(Q_m)$ and consider $\xi(f_v)$. Now let $c_{i,j} = 1$; it needs to be shown that $c_{i+1,j} = 0$. Notice for $2 \leq i \leq m - 1$ the row of the matrix $\hat{C}(M)$ is divided into three parts based on the map (in Figure 3.10 it is the left side of the check mark, the bottom of the checkmark and the right side). Row $i = m$ will not need to be considered as there is no row below it. The fourth expression of Definition 3.3.4 corresponds the the beginning of the row and will be considered first.

- Case 1: $1 \leq i \leq m$ and $j \leq m - 2i + 1$.

$$\begin{aligned} c_{i,j} &= f_v(a_{2m-j-i+1,2m-j-2i+2}) - f_v(a_{2m-j-i,2m-j-2i+1}) \\ c_{i+1,j} &= f_v(a_{2m-j-i,2m-j-2i}) - f_v(a_{2m-j-i-1,2m-j-2i-1}). \end{aligned}$$

The only way a difference can be 1 is of the form $1 - 0 = 1$ since all entries of f_v are either 1 or 0. Therefore $f_v(a_{2m-j-i+1,2m-j-2i+2}) = 1$ and $f_v(a_{2m-j-i,2m-j-2i+1}) = 0$. Notice that in Q_m , $a_{2m-j-i,2m-j-2i+1}$ covers both $a_{2m-j-i,2m-j-2i}$ and $a_{2m-j-i-1,2m-j-2i-1}$ thus

$f_v(a_{2m-j-i, 2m-j-2i+1}) = 0 = f_v(a_{2m-j-i, 2m-j-2i}) = f_v(a_{2m-j-i-1, 2m-j-2i-1})$. Therefore if $c_{i,j} = 1$ then $c_{i+1,j} = 0$ for all $c_{i,j}$.

- Case 2: $1 \leq i \leq m-1$ and $2m-2i+1 \leq j \leq 2m-2i+2$.

The middle of the checkmark results from one entry in the fourth expression and one entry in the fifth expression, but when looking at row $i+1$, both entries are a result of expression five only.

- Case 2a: $j = 2m-2i+1$

$$\begin{aligned} c_{i, 2m-2i+1} &= f_v(a_{2m-(2m-2i+1)-i+1, 2m-(2m-2i+1)-2i+2}) \\ &\quad - f_v(a_{2m-(2m-2i+1)-i, 2m-(2m-2i+1)-2i+2}) = f_v(a_{i,1}) - f_v(a_{i-1,0}) = f_v(a_{i,1}) \\ c_{i+1, 2m-2i+1} &= f_v(a_{i+1-1, 2m-2i+1-2m+2(i+1)-1}) - f_v(a_{i+1-1, 2m-2i+1-2m+2(i+1)-2}) \\ &= f_v(a_{i,2}) - f_v(a_{i,1}) \end{aligned}$$

Let $c_{i, 2m-2i+1} = f_v(a_{i,1}) = 1$. If $f_v(a_{i,1}) = 1$, then $f_v(a_{i,2}) = 1$ also. Therefore if

$$c_{i, 2m-2i+1} = f_v(a_{i,1}) = 1 \text{ then } c_{i+1, 2m-2i+1} = f_v(a_{i,2}) - f_v(a_{i,1}) = 1 - 1 = 0.$$

- Case 2b: $j = 2m-2i+2$

$$\begin{aligned} c_{i, 2m-2i+2} &= f_v(a_{i-1, 2m-2i+2-2m+2i-1}) - f_v(a_{i-1, 2m-2i+2-2m+2i-2}) \\ &= f_v(a_{i-1,1}) - f_v(a_{i-1,0}) = f_v(a_{i-1,1}) \\ c_{i+1, 2m-2i+2} &= f_v(a_{i+1-1, 2m-2i+2-2m+2(i+1)-1}) - f_v(a_{i+1-1, 2m-2i+2-2m+2(i+1)-2}) \\ &= f_v(a_{i,3}) - f_v(a_{i,2}) \end{aligned}$$

Let $c_{i, 2m-2i+1} = f_v(a_{i-1,1}) = 1$, then notice that

$$1 \geq f_v(a_{i,3}) \geq f_v(a_{i,2}) \geq a_{i-1,1} = 1 \text{ therefore } f_v(a_{i,2}) = f_v(a_{i,3}) = 1.$$

Thus if $c_{i, 2m-2i+1} = f_v(a_{i-1,1}) = 1$ then $c_{i+1, 2m-2i+2} = 1 - 1 = 0$.

- Case 3: $1 \leq i \leq m-1$ and $2m-2i+2 \leq j \leq 2m-i+1$

For this case the entries are to the right of the checkmark and thus only expression five is used. Notice that when $j > 2m-i+1$ the rest of the row is zeros and does not apply.

$$c_{i,j} = f_v(a_{i-1, j-2m+2i-1}) - f_v(a_{i-1, j-2m+2i-2})$$

$$c_{i+1,j} = f_v(a_{i+1-1, j-2m+2(i+1)-1}) - f_v(a_{i+1-1, j-2m+2(i+1)-2})$$

$= f_v(a_{i, j-2m+2i+1}) - f_v(a_{i, j-2m+2i})$. Let $c_{i,j} = f_v(a_{i-1, j-2m+2i-1}) - f_v(a_{i-1, j-2m+2i-2}) = 1$. Since $f_v(a_{i-1, j-2m+2i-1}) \geq f_v(a_{i-1, j-2m+2i-2})$, the only way the difference is 1 is if $f_v(a_{i-1, j-2m+2i-1}) = 1$ and $f_v(a_{i-1, j-2m+2i-2}) = 0$. Now notice that $1 = f_v(a_{i-1, j-2m+2i-1}) \leq f_v(a_{i, j-2m+2i}) \leq f_v(a_{i, j-2m+2i+1})$. Therefore all three entries are 1. Thus if $c_{i,j} = f_v(a_{i-1, j-2m+2i-1})$

$$-f_v(a_{i-1, j-2m+2i-2}) = 1, \text{ then } c_{i+1,j} = f_v(a_{i, j-2m+2i+1}) - f_v(a_{i, j-2m+2i}) = 1 - 1 = 0.$$

Consequently, no matter where there is a 1 in $\hat{C}(M)$, there is a 0 directly below it. Therefore in X , where there is a 1, directly below it is a -1 .

It is now established that for any $f \in J(Q_m)$, $\xi(f(a_{s,t})) = M$ is in CSM . Now consider any $f \in \mathcal{O}(Q_m)$. Each f can be written as a convex combination of the vertices $\{f_{v_1}, f_{v_2}, \dots, f_{v_d}\}$ where $f_v \in J(Q_m)$. Since the convex combination is a summation, this result can be shown by linearity.

$$\begin{aligned} \xi(f) &= \xi(\mu_1 f_{v_1} + \mu_2 f_{v_2} + \dots + \mu_d f_{v_d}) \\ &= \xi(\mu_1 f_{v_1}) + \xi(\mu_2 f_{v_2}) + \dots + \xi(\mu_d f_{v_d}) \\ &= \mu_1 \xi(f_{v_1}) + \mu_2 \xi(f_{v_2}) + \dots + \mu_d \xi(f_{v_d}) \\ &= \mu_1(M_1) + \mu_2(M_2) + \dots + \mu_d(M_d) \end{aligned}$$

This is the convex combination of vertices of CP_m , completing the proof. \square

3.3.3. Catalan polytope to order polytope

In this subsection, a map from the Catalan polytope to the order polytope will be explored. Lemma 3.3.11 will show the image of this map is in $\mathcal{O}(Q_m)$.

Definition 3.3.9. Define a map $\hat{\xi} : CP_m \rightarrow \mathbb{R}^{\binom{m}{2}}$ on $X \in CP_m$. The first step of the map is to apply \hat{C} . The second step is as follows:

$$f(a_{s,t}) = \sum_{k=2m-2s+t}^{2m-2s+2t-1} c_{(s-t)+1,k} \quad \text{for } 1 \leq t \leq s \leq m-1. \quad (3.8)$$

Notice in Figure 3.14 of $C(\hat{X})$ each row i is a pair of differences where the difference between s and t values of $f(a_{s,t})$ are constant. In Figure 3.10 notice that on each checkmark, the same differences of s and t appear, with $s-t=0$ as the rightmost diagonal, $s-t=1$ the next checkmark to the left, etc.. Thus each of these diagonals equates to one row of the matrix $\hat{C}(X)$ where $s-t+1=i$. The map uses the summation of the rows starting at $c_{i,j} = f(a_{i,1})$ and summing left until the desired value is reached.

Example 3.3.10. The graph and matrix in Figure 3.11 are used to show examples of the map $\hat{\xi}$ from Definition 3.3.9.

$$\begin{bmatrix} 0 & 0 & 0 & 0 & 0 & 1 - a_{5,5} & a_{5,5} - a_{4,4} & a_{4,4} - a_{3,3} & a_{3,3} - a_{2,2} & a_{2,2} - a_{1,1} & a_{1,1} & 1 \\ 0 & 0 & 0 & 0 & 1 - a_{5,4} & a_{5,4} - a_{4,3} & a_{4,3} - a_{3,2} & a_{3,2} - a_{2,1} & a_{2,1} & a_{1,1} & 1 - a_{1,1} & 0 \\ 0 & 0 & 0 & 1 - a_{5,3} & a_{5,3} - a_{4,2} & a_{4,2} - a_{3,1} & a_{3,1} & a_{2,1} & a_{2,2} - a_{2,1} & 1 - a_{2,2} & 0 & 0 \\ 0 & 0 & 1 - a_{5,2} & a_{5,2} - a_{4,1} & a_{4,1} & a_{3,1} & a_{3,2} - a_{3,1} & a_{3,3} - a_{3,2} & 1 - a_{3,3} & 0 & 0 & 0 \\ 0 & 1 - a_{5,1} & a_{5,1} & a_{4,1} & a_{4,2} - a_{4,1} & a_{4,3} - a_{4,2} & a_{4,4} - a_{4,3} & 1 - a_{4,4} & 0 & 0 & 0 & 0 \\ 1 & a_{5,1} & a_{5,2} - a_{5,1} & a_{5,3} - a_{5,2} & a_{5,4} - a_{5,3} & a_{5,5} - a_{5,4} & 1 - a_{5,5} & 0 & 0 & 0 & 0 & 0 \end{bmatrix}$$

Figure 3.14. The general version of $\hat{C}(X)$ for $m = 6$ using $f(a_{i,j})$ values, written without the f due to space constraints.

The first calculations give $s - t = 0$ values of $f(a_{s,t})$ which come from row $i = 1$ of the matrix. The full calculation will be shown for the first few only.

$$\bullet f(a_{1,1}) = \sum_{k=2(6)-2(1)+1}^{2(6)-2(1)+2(1)-1} c_{(1-1)+1,k} = \sum_{k=11}^{11} c_{1,k} = c_{1,11} = 0$$

$$\bullet f(a_{2,2}) = \sum_{k=2(6)-2(2)+1}^{2(6)-2(2)+2(2)-1} c_{(2-2)+1,k} = \sum_{k=10}^{11} c_{1,k} = c_{1,10} + c_{1,11} = 0 + 0.1 = 0.1$$

$$\bullet f(a_{3,3}) = \sum_{k=2(6)-2(3)+1}^{2(6)-2(3)+2(3)-1} c_{(3-3)+1,k} = \sum_{k=9}^{11} c_{1,k} = c_{1,9} + c_{1,10} + c_{1,11} = .7 + 0 + 0.1 = 0.8$$

$$\bullet f(a_{4,4}) = \sum_{k=8}^{11} c_{1,k} = c_{1,8} + c_{1,9} + c_{1,10} + c_{1,11} = 0 + .7 + 0 + 0.1 = 0.8$$

$$\bullet f(a_{5,5}) = \sum_{k=7}^{11} c_{1,k} = c_{1,7} + c_{1,8} + c_{1,9} + c_{1,10} + c_{1,11} = 0 + 0 + .7 + 0 + 0.1 = 0.8$$

The next calculations give $s - t = 1$ which come from row $i = 2$ of the matrix.

$$\bullet f(a_{2,1}) = \sum_{9}^9 c_{2,k} = c_{2,9} = 0$$

$$\bullet f(a_{3,2}) = \sum_{8}^9 c_{2,k} = c_{2,8} + c_{2,9} = 0.4 + 0 = 0.4$$

$$\bullet f(a_{4,3}) = \sum_{7}^9 c_{2,k} = c_{2,7} + c_{2,8} + c_{2,9} = 0.4$$

$$\bullet f(a_{5,4}) = c_{2,6} + c_{2,7} + c_{2,8} + c_{2,9} = 0.5$$

The next calculations give $s - t = 2$ values which come from row $i = 3$ of the matrix.

- $f(a_{3,1}) = \sum_{k=7}^7 c_{3,k} = c_{3,7} = 0.4$
- $f(a_{4,2}) = c_{3,6} + c_{3,7} = 0.4$
- $f(a_{5,3}) = c_{3,5} + c_{3,6} + c_{3,7} = 0.5$

The next calculations give $s - t = 3$ values which come from row $i = 4$ of the matrix.

- $f(a_{4,1}) = \sum_{k=5}^5 c_{4,k} = c_{4,5} = 0$
- $f(a_{5,2}) = c_{4,4} + c_{4,5} = 0.1$

The last calculation gives $s - t = 4$ values which come from row $i = 5$ of the matrix.

- $f(a_{5,1}) = \sum_{k=3}^3 c_{5,k} = c_{5,3} = 0.1$

It remains to be shown that the resulting f is actually in $\mathcal{O}(Q_m)$.

Lemma 3.3.11. *Let $X \in CP_m$. Then $\hat{\xi}(X) = f$ where $f \in \mathcal{O}(Q_m)$.*

Proof. It needs to be shown that if $\hat{\xi}(X) = f$ then f fits the inequality description for $\mathcal{O}(Q_m)$. First this will be shown for $M \in CSM(m)$, then for all $X \in CP_m$. $f(a_{s,t})$ in Definition 3.3.9 will be shown to fit each inequality in Theorem 3.3.1. There are four cases, as the definition of $f(a_{i,j})$ needs to fit in the inequalities of (3.4), (3.5), (3.6), and (3.7).

- Case (3.4): $f(a_{s,t-1}) \leq f(a_{s,t})$.

$$f(a_{s,t-1}) = \sum_{k=2m-2s+t-1}^{2m-2s+2t-3} c_{s-t+2,k} \quad \text{and} \quad f(a_{s,t}) = \sum_{k=2m-2s+t}^{2m-2s+2t-1} c_{s-t+1,k}.$$

First notice that the row sums of these two cases are in adjacent rows of $\hat{C}(M)$; the top row from $f(a_{s,t})$ will be called A and bottom row from $f(a_{s,t-1})$ will be called B . Figure 3.15 shows this relationship, using boxes to help visualize. In row A there are a total of t boxes, while in row B there are $t - 1$ boxes. Notice if $t = 1$, $a_{s,t-1} = a_{s,0} = 0$, thus the inequality is trivial. Therefore assume $t \geq 2$. Notice row A extends two more boxes to the right than row B and row B extends

one more box to the left than A . So the length of the overlap in the boxes is $t - 2$, where there would be no overlap if $t = 2$.

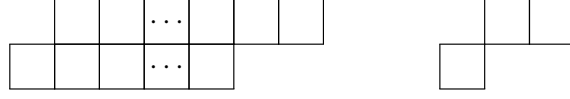


Figure 3.15. The visual representation of rows A and B for a large t and $t = 2$ in the proof of Lemma 3.3.11.

Consider the two $CSM(6)$ matrices in Figure 3.4; the top one shows the farthest right the first 1 in every row can occur and the bottom one shows the farthest left the first 1 in every row can occur. These are the extreme cases as they correspond to the empty order ideal and the entire order ideal (this can also be seen in the SYT ; if the top row is $1, \dots, m$ this corresponds to the entire order ideal and if the top row of tableau is all odd numbers, this corresponds to the empty order ideal). For the extreme cases in general, the 1's in row i occur at $j = 2m - 2i + 1 = 2m - 2(s - t + 1) + 1 = 2m - 2s + 2t - 1$ and $j = 2m - 2i + 2 = 2m - 2(s - t + 1) + 2 = 2m - 2s + 2t$ for the full order ideal case (pictured on top in Figure 3.4 for $m = 6$), while in the empty order ideal case there is one 1 which occurs at $m - i + 1 = m - s + t$ and the second 1 at $2m - i + 1 = 2m - s + t$. Therefore in all other $M \in CSM(m)$ the first 1 will occur between these values. An example of a Catalan sign matrix between the extremes is shown in Figure 3.5.

Now consider the equation from Definition 3.3.9 for $f(a_{s,t})$. The summation ends at $j = 2m - 2s + 2t - 1$, which is where there is the first 1 in the first extreme case. Thus the boxes in A are guaranteed to have a summation of 1 in this case, as the second 1 in the row is to the right. Next notice in the second extreme case that both 1's in every row are outside the bounds on both $f(a_{s,t-1})$ and $f(a_{s,t})$. Now consider the equation for $f(a_{s,t-1})$ which is row B ; the summation ends at $2m - 2s + 2t - 3 = 2m - 2i - 1$, which is two to the left of A . Therefore, the only way that a 1 can be in this box is if at least the columns to the left follow the first extreme case and this would be the second 1. In that case $f(a_{s,t}) = 1$ also since this is the next column to the right in A after the second 1 in row B . If the pattern follows the top extreme case in columns of M until this point in B , but not after, notice that the only option for the next 1 is $c_{i-1,j+1}$, which is in A . Any other case results in row B as all zeros. Therefore it is always the case that $f(a_{s,t-1}) \leq f(a_{s,t})$.

- Case (3.5): $f(a_{s-1,t-1}) \leq f(a_{s,t})$

$$\begin{aligned}
f(a_{s-1,t-1}) &= \sum_{k=2m-2s+t+1}^{2m-2s+2t-1} c_{s-t+1,k} \\
f(a_{s,t}) - f(a_{s-1,t-1}) &= \sum_{k=2m-2s+t}^{2m-2s+2t-1} c_{s-t+1,k} - \sum_{k=2m-2s+t+1}^{2m-2s+2t-1} c_{s-t+1,k} \\
&= c_{s-t+1,2m-2s+t} \geq 0
\end{aligned}$$

Since all $0 \leq c_{i,j} \leq 1$ for all i, j , $f(a_{s-1,t-1}) \leq f(a_{s,t})$.

- Case (3.6): $0 \leq f(a_{s,1})$

$$f(a_{s,1}) = \sum_{k=2m-2s+1}^{2m-2s+1} c_{s,k} = c_{s,2m-2s+1} \geq 0.$$

Therefore $0 \leq f(a_{s,1})$.

- Case (3.7): $f(a_{m-1,m-1}) \leq 1$

$$f(a_{m-1,m-1}) = \sum_{k=m+1}^{2m-1} c_{1,k} \leq \sum_{k=1}^{2m-1} c_{1,k} = 1.$$

Therefore $f(a_{m-1,m-1}) \leq 1$.

It is now established that for any $M \in CSM$, $\hat{\xi}(M) = f$ is in $\mathcal{O}(Q_m)$. Now consider any $X \in CP_m$. Each X can be written as a convex combination of $M_i \in CSM(m)$ such that $X = \mu_1 M_1 + \mu_2 M_2 + \cdots + \mu_d M_d$ where $\sum_{i=1}^d \mu_i = 1$ and $\mu_i \geq 0$ for all i . Since the convex combination is a summation, this result can be shown by linearity.

$$\begin{aligned}
\hat{\xi}(X) &= \hat{\xi}(\mu_1 M_1 + \mu_2 M_2 + \cdots + \mu_d M_d) \\
&= \hat{\xi}(\mu_1 M_1) + \hat{\xi}(\mu_2 M_2) + \cdots + \hat{\xi}(\mu_d M_d) \\
&= \mu_1 \hat{\xi}(M_1) + \mu_2 \hat{\xi}(M_2) + \cdots + \mu_d \hat{\xi}(M_d) \\
&= \mu_1 (f_1(a_{s,t})) + \mu_2 (f_2(a_{s,t})) + \cdots + \mu_d (f_d(a_{s,t}))
\end{aligned}$$

Therefore the result is the convex combination of vertices of $\mathcal{O}(Q_m)$, completing the proof. \square

3.4. The Catalan polytope and order polytope connection

This section contains the main theorem. The previous sections defined the maps and tools needed to prove that the Catalan polytope is integrally equivalent to $\mathcal{O}(Q_m)$, which ensures equivalent volume of the polytopes.

Definition 3.4.1 ([29]). Two integral polytopes \mathcal{P} in \mathbb{R}^d and \mathcal{Q} in \mathbb{R}^m are *integrally equivalent*, if there is a transformation $\psi : \mathbb{R}^d \rightarrow \mathbb{R}^m$ whose restriction to \mathcal{P} is a bijection $\psi : \mathcal{P} \rightarrow \mathcal{Q}$ that preserves the lattice.

Note: It can be shown that two integral polytopes are integrally equivalent if the determinant of the reduced transformation matrix is 1 or -1 .

Theorem 3.4.2. *The Catalan polytope CP_m is integrally equivalent to the order polytope $\mathcal{O}(Q_m)$.*

Proof. To show the bijection between the polytopes, an invertible map between $\mathcal{O}(Q_m)$ and CP_m needs to be established. The proof proceeds by showing the maps ξ and $\hat{\xi}$ are inverses.

Start with $f \in \mathcal{O}(Q_m)$. It needs to be shown that for any $a_{s,t} \in (Q_m)$, $\hat{\xi}(\xi(f(a_{s,t}))) = f(a_{s,t})$.

Now consider an individual $f(a_{s,t})$; there are two possible cases to address in Definition 3.3.4. Consider the bounds of the fourth statement; the upper bound is $j \leq 2m - 2i + 1$. Notice the maximum j in the summation defining $\hat{\xi}$ is $j = 2m - 2s + 2t - 1 = 2m - 2(s - t + 1) + 1 = 2m - 2i + 1$, thus only statement four needs to be shown. The calculation is as follows:

$$\begin{aligned}
\hat{\xi}\xi(f(a_{s,t})) &= \hat{\xi}\left(\sum_{k=2m-2s+t}^{2m-2s+2t-1} c_{s-t+1,k}\right) \\
&= \sum_{k=2m-2s+t}^{2m-2s+2t-1} (f(a_{2m-k-(s-t+1)+1, 2m-k-2(s-t+1)+2}) - f(a_{2m-k-(s-t+1), 2m-k-2(s-t+1)+1})) \\
&= \sum_{k=2m-2s+t}^{2m-2s+2t-1} (f(a_{2m-s+t-k, 2m-2s+2t-k} - a_{2m-s+t-k-1, 2m-2s+2t-k-1})) \\
&= (f(a_{s,t}) - f(a_{s-1,t-1}) + (f(a_{s-1,t-1}) - f(a_{s-2,t-2}))) + \cdots \\
&\quad + (f(a_{s-t+2,2}) - f(a_{s-t+1,1})) + (f(a_{s-t+1,1}) - f(a_{s-t,0})) = f(a_{s,t}).
\end{aligned}$$

Therefore, $\hat{\xi}(\xi(f(a_{s,t}))) = f(a_{s,t})$ for all $f \in \mathcal{O}(Q_m)$.

Now it will be shown that $\xi(\hat{\xi}(c_{i,j})) = c_{i,j}$ for all $c_{i,j} \in \hat{C}(M)$ for all $M \in CP_m$. The calculation is as follows:

$$\begin{aligned}
\xi(\hat{\xi}(c_{i,j})) &= \xi(f(a_{2m-j-i+1, 2m-j-2i+2}) - f(a_{2m-j-i, 2m-j-2i+1})) \\
&= \sum_{k=2m-2(2m-j-i+1)+2m-j-2i+2}^{2m-2(2m-j-i+1)+2(2m-j-2i+2)-1} c_{(2m-j-i+1)-(2m-j-2i+2)+1, k} \\
&\quad - \sum_{k=2m-2(2m-j-i)+2m-j-2i+1}^{2m-2(2m-j-i)+2(2m-j-2i+1)-1} c_{i, k} = \sum_{k=j}^{2m-2i+1} c_{i, k} - \sum_{k=j+1}^{2m-2i+1} c_{i, k} = c_{i, j}
\end{aligned}$$

Therefore, since $\hat{\xi}(\xi(f(a_{s,t}))) = f(a_{s,t})$ and $\xi(\hat{\xi}(c_{i,j})) = c_{i,j}$, the maps ξ and $\hat{\xi}$ are inverses.

It remains to be shown that CP_m and $\mathcal{O}(Q_m)$ are integrally equivalent.

The map ξ considers one row of a matrix $X \in CP_m$ at a time. Since X to $\hat{C}(X)$ could be thought of as a series of row operations that would not change a determinant, therefore the matrix $\hat{C}(X)$ will be used. Notice that each row of $\hat{C}(X)$ is determined by the value of $s-t$. Notice further that for every $X_{i,j}$, $i = s-t+1$. The proof proceeds by considering the first row of $\hat{C}(X)$, then considering a row in general, to make a transformation matrix of the $f(a_{s,t})$ coefficients. The first row of $\hat{C}(X)$ will be considered first where $s = t$. Notice that ignoring zeros, the top row of $\hat{C}(X)$ is the following:

$$\begin{array}{ccccccc}
1 - a_{m-1, m-1} & a_{m-1, m-1} - a_{m-2, m-2} & a_{m-2, m-2} - a_{m-3, m-3} & & & & \\
\cdots & a_{3, 3} - a_{2, 2} & a_{2, 2} - a_{1, 1} & a_{1, 1} & 1 & &
\end{array}$$

When this row of $\hat{C}(X)$ is put into a transformation matrix, the last entry will be all zeros and one 1 to represent the 1, as shown in the matrix below. The second to the last entry will be all zeros and one 1 to represent the $a_{1,1}$. The transformation matrix for the first row is as follows (the labels above show which coefficients are represented by that column):

$$\begin{pmatrix}
a_{m-1,m-1} & a_{m-2,m-2} & a_{m-3,m-3} & \cdots & a_{3,3} & a_{2,2} & a_{1,1} & 1 \\
-1 & 0 & 0 & 0 & 0 & 0 & \cdots & 0 & 0 & 1 \\
1 & -1 & 0 & 0 & 0 & \cdots & 0 & 0 & 0 & 0 \\
0 & 1 & -1 & 0 & 0 & \cdots & 0 & 0 & 0 & 0 \\
\vdots & \vdots & \vdots & \cdots & \cdots & \cdots & \vdots & \vdots & \vdots & \vdots \\
0 & 0 & 0 & \cdots & 0 & 1 & -1 & 0 & 0 & 0 \\
0 & 0 & 0 & \cdots & 0 & 0 & 1 & -1 & 0 & 0 \\
0 & 0 & 0 & \cdots & 0 & 0 & 0 & 1 & -1 & 0 \\
0 & 0 & 0 & \cdots & 0 & 0 & 0 & 0 & 1 & 0 \\
0 & 0 & 0 & \cdots & 0 & 0 & 0 & 0 & 0 & 1
\end{pmatrix}$$

Notice this is a $m + 1 \times m + 1$ matrix. Notice further that if row reducing from the bottom, all row reduction proceeds by adding rows, which does not change the determinant. In this fashion, the determinant of this matrix is ± 1 (the ± 1 is due to possible row swaps). Notice that there are none of the same entries in row two that were also in row one. Thus each row of $\hat{C}(X)$ can be considered as an independent block in the transformation matrix. The completed transformation matrix will have a square block for each row of $\hat{C}(X)$, and zeros to fill in the upper right and lower left. Therefore the determinant of the entire matrix is the product of the determinants of the smaller blocks, as the matrix will be block diagonal. Row one was discussed above; the blocks for the rest of $\hat{C}(X)$ are now discussed.

Consider a row in $2 \leq i \leq m - 1$, and notice all entries of row m have been in previous rows, thus row m of $\hat{C}(X)$ is a linear combination of rows in previous blocks of the final transition matrix. A typical row in $2 \leq i \leq m - 1$, ignoring zeros looks like the following:

$$\begin{array}{cccccccc}
1 - a_{m-1,m-1-(s-t)} & a_{m-1,m-1-(s-t)} - a_{m-2,m-2-(s-t)} & a_{m-2,m-2-(s-t)} - a_{m-3,m-3-(s-t)} & & & & & \\
\cdots & a_{s-t+1,2} - a_{s-t,1} & a_{s-t,1} & a_{s-t-1,1} & a_{s-t-1,s-t-1} - a_{s-t-1,1} & a_{s-t-1,s-t} - a_{s-t-1,s-t-1} & & \\
\cdots & a_{s-t-1,s-t-2} - a_{s-t-1,s-t-3} & a_{s-t-1,s-t-1} - a_{s-t-1,s-t-2} & 1 - a_{s-t-1,s-t-1} & & & &
\end{array}$$

Notice that in the middle there are two entries $a_{s-t,1}$ and $a_{s-t-1,1}$. These entries equate to rows of all zeros and one 1 in the transformation matrix for this block. As with the row one

case, there is a telescopic effect with row reduction to reduce the transformation matrix to be a $(m+2) \times (m+2)$ square. Notice that again after row reduction, all rows will be all zeros with one 1, therefore the determinant is ± 1 .

Since each block gives a determinant of ± 1 , the entire determinant is also ± 1 . Therefore CP_m and $\mathcal{O}(Q_m)$ are integrally equivalent. \square

The following is a corollary of Theorem 3.4.2 and Theorem 1.3.56.

Corollary 3.4.3. *The facets of CP_m are enumerated by the formula $(m-1)^2 + 1 = m^2 - 2m + 2$.*

Proof. From Stanley [25], it is known that for an order polytope, the number of facets equals the number of cover relations plus the number of minimal elements plus the number of maximal elements in the poset, as discussed in Theorem 1.3.56. Consider the triangle poset Q_m . The cover relations can be counted from the top down: $2 + 4 + 6 + 8 + \dots + 2(m-2) = 2(1 + 2 + 3 + 4 + \dots + m-2) = 2\binom{m-1}{2} = (m-1)(m-2) = m^2 - 3m + 2$. The number of minimal elements is $m-1$ and there is one maximal element. Therefore the number of facets is $m^2 - 3m + 2 + m - 1 + 1 = m^2 - 2m + 2$ as needed. \square

3.5. Inequality description of CP_m .

When the inequality description of the order polytope is converted via ξ to the Catalan polytope, these inequalities are converted to $\hat{C}(X)$ and the following inequalities are obtained for CP_m .

Theorem 3.5.1. *CP_m consists of all $m \times 2m$ real matrices $X = (X_{i,j})$ such that the entries of the partial column sum matrix $\hat{C}(X)$ satisfy:*

$$\sum_{k=2m-2s+t-1}^{2m-2s+2t-3} c_{s-t+2,k} \leq \sum_{k=2m-2s+t}^{2m-2s+2t-1} c_{s-t+1,k}, \quad 2 \leq t \leq s \leq m-1, \quad (3.9)$$

$$0 \leq c_{s-t+1, 2m-2s+t}, \quad 2 \leq t \leq s \leq m-1, \quad (3.10)$$

$$0 \leq c_{s, 2m-2s+1}, \quad 1 \leq s \leq m-1, \quad (3.11)$$

$$\sum_{k=m+1}^{2m-1} c_{1,k} \leq 1. \quad (3.12)$$

Proof. The calculations for these inequalities are shown in the proof of Lemma 3.3.11. It remains to be shown that they are a minimal set. It is known from Corollary 3.4.3 that the number of facets is given by $m^2 - 2m + 2$. Thus the same number of inequalities needs to be established to have a minimal set of inequalities. Notice that for the top two inequalities there are $m - 1$ elements between 2 and $m - 1$ for both s and t to pick, thus there are $\binom{m-1}{2} = (m-1)(m-2) = m^2 - 3m + 2$ choices for each inequality. The third inequality has $m - 1$ choices and the last is a single inequality. Together there are $m^2 - 3m + 2 + m - 1 + 1 = m^2 - 2m + 2$ choices of inequalities to change to an equality and obtain a facet. \square

3.6. Face lattice of CP_m

In the last section it was shown that CP_m is integrally equivalent to an order polytope. Using the properties of order polytopes, the face lattice of CP_m is now presented. This discussion will follow Stanley [25].

Every face is an intersection of facets, therefore a face F_π of $\mathcal{O}(P)$ corresponds to a certain partition of \hat{P} . Recall from Definition 1.3.54 that \hat{P} is obtained from P by adjoining a $\hat{1}$ element above the poset and adjoining a $\hat{0}$ element below the poset.

Definition 3.6.1. $\pi = \{B_1, B_2, \dots, B_k\}$ is a *partition* of \hat{P} if the blocks B_i are all nonempty and pairwise disjoint, and $B_1 \cup B_2 \cup \dots \cup B_k = \hat{P}$.

Definition 3.6.2. Let a partition of \hat{P} be called *connected* if every block B of π is connected as an (induced) subposet of \hat{P} .

Definition 3.6.3. Define a binary relation \leq_π on π by setting $B_i \leq B_j$ if $x \leq y$ for some $x \in B_i$ and $y \in B_j$. Call π *compatible* if the transitive closure of \leq_π is a partial order.

The following theorem gives a description of the face lattice of $\mathcal{O}(P)$.

Theorem 3.6.4 ([25]). *The lattice of faces of $\mathcal{O}(P)$ is isomorphic to the lattice of connected compatible partitions of \hat{P} , ordered by reverse refinement. (In particular, the partition π into a single block \hat{P} yields the empty set $F_\pi = \emptyset$, which is regarded as a face.)*

Now a corollary of this theorem and Theorem 3.4.2 is given.

Corollary 3.6.5. *The face lattice of CP_m is isomorphic to the lattice of connected compatible partitions of \hat{Q}_m , ordered by reverse refinement.*

An example of the face lattice of CP_3 can be seen in Figures 3.16 and 3.17.

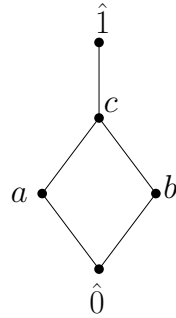


Figure 3.16. The poset Q_3 with added $\hat{1}$ and $\hat{0}$ to obtain \hat{Q}_3 .

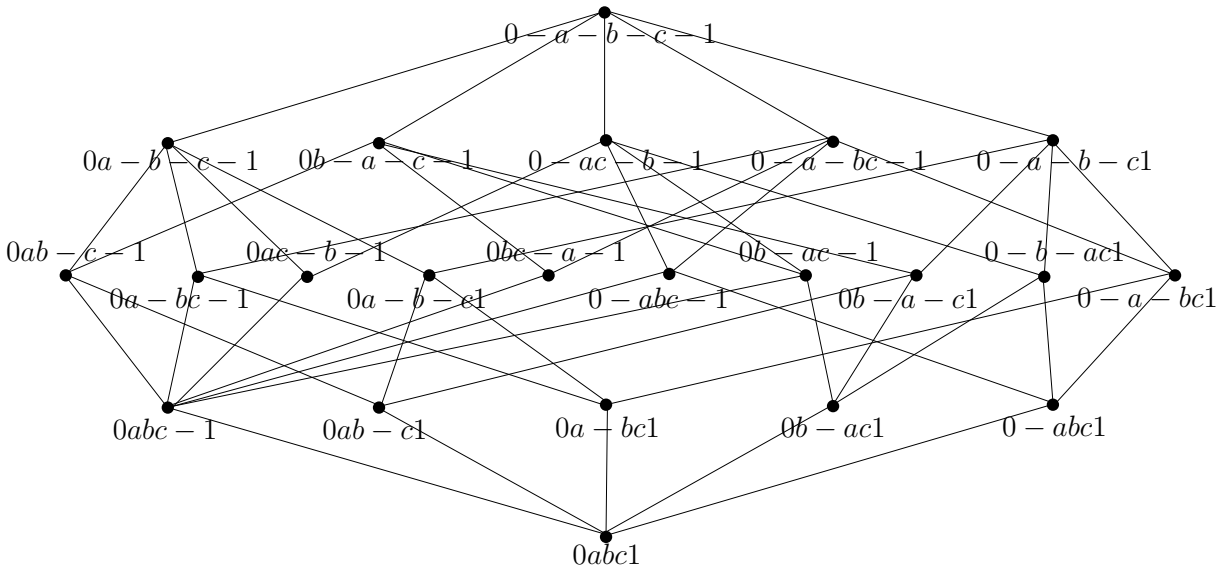


Figure 3.17. The face lattice for the poset in Figure 3.16.

3.7. Ehrhart polynomial and volume

The following corollaries are obtained from Stanley's theory of order polytopes [25] and Theorem 3.4.2.

Corollary 3.7.1. *The Ehrhart polynomial of CP_m is $\Omega(Q_m, t + 1)$.*

Corollary 3.7.2. *The normalized volume of CP_m is $e(Q_m)$, where $e(Q_m)$ is the number of linear extensions of Q_m .*

Remark 3.7.3. Notice that $e(Q_m)$ is equal to the number of *SYT* of staircase shape $[m-1, \dots, 2, 1]$. Recall that *SYT* are counted by the hook-length formula introduced in Definition 1.4.6. Thus

$$\text{vol}\mathcal{O}(Q_m) = \text{vol}CP_m = e(Q_m) = \frac{\binom{m}{2}!}{1^{m-1}3^{m-2}\dots(2m-3)^1}$$

Notice that since the poset Q_m has $m-1$ minimal elements, this does not contradict what was calculated in Subsection 1.4.3. In that example, *SYT* of staircase shape $[m, m-1, \dots, 2, 1]$ was used.

4. FUTURE WORK

The following chapter is a discussion of possible future work.

4.1. Tableaux polytopes

This study of sign matrices is the beginning of research of polytopes from tableaux. Further exploration of sign matrix polytopes from semistandard and standard Young tableaux is possible. Other shapes of tableaux or types such as increasing tableau, defined next, are of interest.

Definition 4.1.1. An *increasing tableau* is a filling of a Young diagram with positive integers such that the rows are strictly increasing and the columns are strictly increasing.

Recall that standard Young tableaux have a similar definition. However, for a *SYT*, each number can only be used once, and the maximum entry is the number of boxes in the Young diagram. An increasing tableau can leave out numbers, or repeat numbers, just not in the same row like *SSYT*. Figure 4.1 shows the eight tableaux in $SSYT([2, 1], 3)$. The set $\{C, D, E, F, H\}$ is the set of all increasing tableau, and the set $\{D, E\}$ is $SYT([2, 1])$.

$$\begin{array}{cccc}
 A = \begin{array}{|c|c|} \hline 1 & 1 \\ \hline 2 & \\ \hline \end{array} & B = \begin{array}{|c|c|} \hline 1 & 1 \\ \hline 3 & \\ \hline \end{array} & C = \begin{array}{|c|c|} \hline 1 & 2 \\ \hline 2 & \\ \hline \end{array} & D = \begin{array}{|c|c|} \hline 1 & 2 \\ \hline 3 & \\ \hline \end{array} \\
 \\
 E = \begin{array}{|c|c|} \hline 1 & 3 \\ \hline 2 & \\ \hline \end{array} & F = \begin{array}{|c|c|} \hline 1 & 3 \\ \hline 3 & \\ \hline \end{array} & G = \begin{array}{|c|c|} \hline 2 & 2 \\ \hline 3 & \\ \hline \end{array} & H = \begin{array}{|c|c|} \hline 2 & 3 \\ \hline 3 & \\ \hline \end{array}
 \end{array}$$

Figure 4.1. The 8 tableaux in $SSYT([2, 1], 3)$.

Polytopes from increasing tableaux could be a stepping stone to learn more about by polytopes from standard Young tableaux, using techniques from research on $SSYT(\lambda, n)$.

4.2. Sign matrices

Another area of possible future work is with sign matrices. Since sign matrices are in bijection with SSYT, they could be further bijected to the *row or column word* of a SSYT. The column word of a SSYT is formed by the numbers in a semistandard Young tableau by reading the words from the bottom to top and left to right across a tableau. Thus the exploration of research

on words can be now studied using sign matrices. *Robinson-Schensted-Knuth (RSK) insertion* is an operation on words of particular interest. It would be intriguing to study the effect of RSK on a sign matrix.

Permutations of words would be interesting to study on sign matrices, specifically pattern avoidance cases. Pattern avoidance in a permutation is the study of all permutations that do not contain a certain pattern. It is possible there is a way to see these patterns on sign matrices.

4.3. Connection to Gelfand-Tsetlin polytopes

The Gelfand-Tsetlin polytope is another polytope that may have connections to the sign matrix polytopes from this research. Gelfand-Tsetlin polytopes have been studied in [12, 16, 18].

Definition 4.3.1 ([26, p. 313]). A *Gelfand-Tsetlin pattern* is a triangular configuration of nonnegative integers where the entries must satisfy the conditions $x_{i+1,j} \geq x_{ij}$ and $x_{ij} \geq x_{i+1,j+1}$ for all values of i, j where $1 \leq i \leq n$ and $1 \leq j \leq i$.

An example of a Gelfand-Tsetlin pattern and its inequalities are shown in Figure 4.2. The *Gelfand-Tsetlin polytope* is formed as the convex hull of all Gelfand-Tsetlin patterns satisfying certain properties (e.g. entries at most n or with prescribed top row). The inequalities in the figure are the inequalities that describe such a polytope. It is worth mentioning that, in general, not all Gelfand-Tsetlin patterns included in the convex hull are vertices of this polytope.

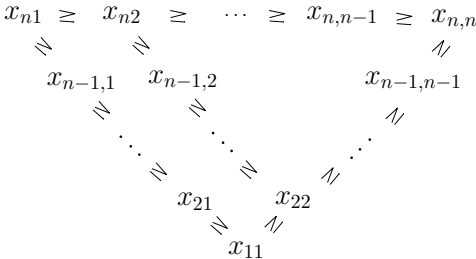


Figure 4.2. The inequalities of the Gelfand-Tsetlin pattern are shown.

It is well known that $SSYT(\lambda, n)$ are in bijection with Gelfand-Tsetlin patterns [26, p. 314]. Since Gelfand-Tsetlin patterns are in bijection with $SSYT$, it is likely that there is a connection between their respective polytopes. It is also possible that $SSYT(\lambda, n)$ projects onto the Gelfand-Tsetlin polytope.

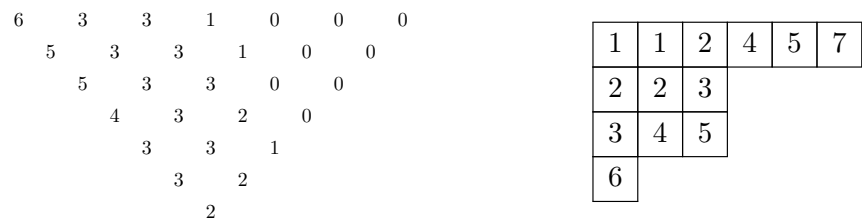


Figure 4.3. Example of the bijection between the Gelfand-Tsetlin pattern on the left and the *SSYT* on the right.

REFERENCES

- [1] Byung Hee An, Yunhyung Cho, and Jang Soo Kim. On the f -vectors of Gelfand-Cetlin polytopes. *European J. Combin.*, 67:61–77, 2018.
- [2] Jean-Christophe Aval. Keys and alternating sign matrices. *Sém. Lothar. Combin.*, 59:Art. B59f, 13, 2007/10.
- [3] Roger E. Behrend and Vincent A. Knight. Higher spin alternating sign matrices. *Electron. J. Combin.*, 14(1):Research Paper 83, 38, 2007.
- [4] Louis J. Billera and A. Sarangarajan. All 0-1 polytopes are traveling salesman polytopes. *Combinatorica*, 16(2):175–188, 1996.
- [5] Garrett Birkhoff. Three observations on linear algebra. *Univ. Nac. Tucumán. Revista A.*, 5:147–151, 1946.
- [6] R.G. Brown, J.W. Jurgensen, and R.C. Jurgensen. *Geometry*. McDougal Littell, Houghton Mifflin Company, 1997.
- [7] Richard A. Brualdi and Peter M. Gibson. Convex polyhedra of doubly stochastic matrices. IV. *Linear Algebra and Appl.*, 15(2):153–172, 1976.
- [8] Daniel Bump and Anne Schilling. *Crystal bases*. World Scientific Publishing Co. Pte. Ltd., Hackensack, NJ, 2017. Representations and combinatorics.
- [9] Gary Chartrand, Linda Lesniak, and Ping Zhang. *Graphs & digraphs*. CRC Press, Boca Raton, FL, fifth edition, 2011.
- [10] O. Cheong. *The Ipe extensible drawing editor (Version 7)*, 2016. <http://ipe.otfried.org/>.
- [11] Jesús A. De Loera and Edward D. Kim. Combinatorics and geometry of transportation polytopes: an update. In *Discrete geometry and algebraic combinatorics*, volume 625 of *Contemp. Math.*, pages 37–76. Amer. Math. Soc., Providence, RI, 2014.

- [12] Jesús A. De Loera and Tyrrell B. McAllister. Vertices of Gelfand-Tsetlin polytopes. *Discrete Comput. Geom.*, 32(4):459–470, 2004.
- [13] David S. Dummit and Richard M. Foote. *Abstract algebra*. John Wiley & Sons, Inc., Hoboken, NJ, third edition, 2004.
- [14] J. S. Frame, G. de B. Robinson, and R. M. Thrall. The hook graphs of the symmetric groups. *Canadian J. Math.*, 6:316–324, 1954.
- [15] William Fulton. *Young tableaux: With applications to representation theory and geometry*. London Mathematical Society Student Texts. Cambridge University Press, Cambridge, 1997.
- [16] Yibo Gao, Benjamin Krakoff, and Lisa Yang. *Diameter and Automorphisms of Gelfand-Tsetlin Polytopes*, 2016. <https://arxiv.org/abs/1611.06983>.
- [17] Basil Gordon. A proof of the Bender-Knuth conjecture. *Pacific J. Math.*, 108(1):99–113, 1983.
- [18] Pavel Gusev, Valentina Kiritchenko, and Vladlen Timorin. Counting vertices in Gelfand-Zetlin polytopes. *J. Combin. Theory Ser. A*, 120(4):960–969, 2013.
- [19] SageMath Inc. *CoCalc Collaborative Computation Online*, 2016. <https://cocalc.com/>.
- [20] Anatol N. Kirillov, Anne Schilling, and Mark Shimozono. A bijection between Littlewood-Richardson tableaux and rigged configurations. *Selecta Math. (N.S.)*, 8(1):67–135, 2002.
- [21] Greg Kuperberg. Another proof of the alternating-sign matrix conjecture. *Internat. Math. Res. Notices*, (3):139–150, 1996.
- [22] Karola Mészáros, Alejandro H. Morales, and Jessica Striker. *On flow polytopes, order polytopes, and certain faces of the alternating sign matrix polytope*, 2015. <https://arxiv.org/abs/1510.03357>.
- [23] W. H. Mills, David P. Robbins, and Howard Rumsey, Jr. Alternating sign matrices and descending plane partitions. *J. Combin. Theory Ser. A*, 34(3):340–359, 1983.
- [24] Sara Solhjem and Jessica Striker. *Sign matrix polytopes from Young tableaux*, 2018. <https://arxiv.org/abs/1805.11647>.

- [25] Richard P. Stanley. Two poset polytopes. *Discrete Comput. Geom.*, 1(1):9–23, 1986.
- [26] Richard P. Stanley. *Enumerative combinatorics. Volume 2.* Cambridge Studies in Advanced Mathematics. Cambridge University Press, Cambridge, 1999.
- [27] Richard P. Stanley. *Enumerative combinatorics. Volume 1.* Cambridge Studies in Advanced Mathematics. Cambridge University Press, Cambridge, Second edition, 2012.
- [28] Richard P. Stanley. *Catalan numbers.* Cambridge University Press, New York, 2015.
- [29] Richard P. Stanley and Jim Pitman. A polytope related to empirical distributions, plane trees, parking functions, and the associahedron. *Discrete Comput. Geom.*, 27(4):603–634, 2002.
- [30] W. A. Stein et al. *Sage Mathematics Software (Version 7.3).* The Sage Development Team, 2016. <http://www.sagemath.org>.
- [31] Jessica Striker. The alternating sign matrix polytope. *Electron. J. Combin.*, 16(1):Research Paper 41, 15, 2009.
- [32] John von Neumann. A certain zero-sum two-person game equivalent to the optimal assignment problem. In *Contributions to the theory of games, Vol. 2*, Annals of Mathematics Studies, no. 28, pages 5–12. Princeton University Press, Princeton, N. J., 1953.
- [33] Doron Zeilberger. Proof of the alternating sign matrix conjecture. *Electron. J. Combin.*, 3(2):Research Paper 13, 1996. The Foata Festschrift.
- [34] Günter M. Ziegler. *Lectures on polytopes.* Graduate Texts in Mathematics. Springer-Verlag, New York, 1995.